universität wien

DIPLOMARBEIT

Insights into the developmental cycle of *Protochlamydia amoebophila* UWE25, an endosymbiont of free-living amoebae

angestrebter akademischer Grad

Magistra der Naturwissenschaften (Mag. rer. nat.)

an der Fakultät für Lebenswissenschaften der Universität Wien

Verfasserin:	Lena König
Matrikel-Nummer:	0003059
Studienrichtung /Studienzweig:	A 441 Diplomstudium Genetik - Mikrobiologie
Betreuerin / Betreuer:	Matthias Horn

Wien, am 10.02.2009

“I think it was very informative, but a lot still needs to be done.”

Pablo Neruda

Table of Contents

1 Introduction

1.1 Interactions between *Chlamydiae* and host cells

1.1.1 The symbiosis

According to the definition of symbiosis by Anton de Bary in the mid-nineteenth century, the term generally refers to an intimate association between two dissimilar organisms (de Bary, 1879), thereby including mutualism, commensalism, competition, neutralism as well as parasitism. Since the interaction between members of the bacterial phylum *Chlamydiae* and their eukaryotic host cells is obligate in the sense that chlamydial growth is dependent on an intracellular environment, *Chlamydiae* can broadly be referred to as obligate endosymbionts.

The phylum comprises the well-established animal and human pathogens belonging to the family of *Chlamydiaceae* on the one hand, but also includes the just recently discovered and phylogenetically diverse *Chlamydia*-like organisms on the other hand (Table 1). Members of the latter group were found to exist in numerous different eukaryotic hosts such as terrestrial isopods, insects, the marine worm-like *Xenoturbella*, salmonid fish, cattle, Australian marsupials as well as free-living amoebae (Amann *et al*., 1997; Bodetti *et al*., 2003; Corsaro *et al*., 2007; Draghi *et al*., 2004; Fritsche *et al*., 2000; Horn *et al*., 2000; Israelsson, 2007; Karlsen *et al*., 2008; Kostanjšek *et al*., 2004; Michel *et al*., 2000; Rurangirwa *et al*., 1999; Thao *et al*., 2003). Besides, novel *Chlamydia*-like organisms as well as yet uncultured chlamydiae could be identified in various clinical and environmental samples (Collingro *et al*., 2005a; Collingro *et al*., 2005b; Corsaro and Venditti, 2006; Horn and Wagner, 2001; Kahane *et al*., 1993; Thomas *et al*., 2006), whereby identification of the original host could not be accomplished. Currently, *Chlamydia*-like bacteria fall into seven families (Horn, 2008) although the variety of both hosts and chlamydial 16S rDNA sequences retrieved from different environments suggests an even higher chlamydial diversity.

While members of the *Chlamydiaceae* are clearly perceived to be parasites for humans and a number of animals, the type of symbiosis between *Chlamydia*-like organisms and their hosts remains to be clarified. Some members of the so far best-characterized *Parachlamydiaceae*, for example, seem to be only harmful under certain conditions or have minor adverse effects on free-living amoebae, their natural hosts, so that a stable interaction can possibly be maintained. On the other hand, these organisms are considered to be emerging human pathogens, since invasion and multiplication within human cells (Collingro *et al*., 2005b; Greub *et al*., 2003a), as well as a rare association with respiratory tract infections could be observed (Birtles *et al*., 1997; Casson *et al*., 2008).

Table 1. Described *Chlamydiaceae*-related bacteria[1]

Family	Organism[2]	Natural host	Location[3]	Comments[4]	Reference[5]
Piscichlamydiaceae	"*Cand.* Piscichlamydia salmonis"	Atlantic salmon	Gill	Associated with epitheliocystis	Draghi *et al.*, 2004
Clavochlamydiaceae	"*Cand.* Clavochlamydia salmonicola"	Atlantic salmon	Gill	Associated with epitheliocystis	Karlsen *et al.*, 2008
Rhabdochlamydiaceae	"*Cand.* Rhabdochlamydia porcellionis"	Terrestrial isopod (*Porcellio scaber*)	Digestive glands	Infected cell were damaged	Drobne *et al.*, 1999* Kostanjšek *et al.*, 2004
	"*Cand.* Rhabdochlamydia crassificans"	Cockroach (*Blatta orientalis*)	Fat bodies, ovaries	Causes swelling of abdomen	Corsaro *et al.*, 2007
Simkaniaceae	*Simkania negevensis*	Unknown		Discovered as a contaminant in cell cultures	Kahane *et al.*, 1993* Kahane *et al.*, 1999
	symbiont of *Xenoturbella*	Marine bilaterian (*Xenoturbella bocki*)	Gastrodermis	No cytopathological effects could be observed	Israelsson, 2007*
	"*Cand.* Fritschea eriococci"	Scale insect (*Eriococcus spurious*)	Unknown		Thao *et al.*, 2003
	"*Cand.* Fritschea bemisiae"	White fly (*Bemisia tabaci*)	Bacteriocytes	Vertically transmitted to oocytes	Costa *et al.*, 1995* Thao *et al.*, 2003
Waddliaceae	*Waddlia malaysiensis*	Fruit bat (*Eonycteris spelaea*)	Urine	Can grow in a wide range of human and animal cell types	Chua *et al.*, 2005
	Waddlia chondrophila	Cattle	Aborted foetus	Associated with bovine abortion	Dilbeck *et al.*, 1990* Rurangirwa *et al.*, 1999
Criblamydiaceae	*Criblamydia sequanensis*	Unknown		Isolated from river water by amoebal co-cultivation, able to survive in A549 cells	Thomas *et al.*, 2006
Parachlamydiaceae	*Parachlamydia acanthamobeae* UV-7	Unknown		Isolated from activated sludge by amoebal co-cultivation, cytophatic effect on Vero, NCI and HeLa cells	Collingro *et al.*, 2005a

Table 1 (continued)

Family	Organism[2]	Natural host	Location[3]	Comments[4]	Reference[5]
Parachlamydiaceae	*Parachlamydia acanthamobeae* OEW1	Free-living amoeba (*Acanthamoeba* sp. OEW1)		One of two co-occuring symbionts	Heinz *et al.*, 2007
	Parachlamydia acanthamobeae Hall's coc.	Free-living amoeba (*Acanthamoeba* sp.)		Pneumonia patients sera reacted with organism	Birtles *et al.*, 1997
	Parachlamydia acanthamobeae	Free-living amoeba (*Acanthamoeba* sp. Bn_9)		Unfavorable environmental conditions caused killing of infected host *Acanthamoeba castellanii*	Michel *et al.*, 1994* Amann *et al.*, 1997
	Protochlamydia neagleriophila	Free-living amoeba (*Naegleria* sp.)		Can infect various amoebal genera, possibly associated with pneumonia	Michel *et al.*, 2000* Casson *et al.*, 2008
	Protochlamydia amoebophila UWE25	Free-living amoeba (*Acanthamoeba* sp.)		Can multiply in various *Acanthamoeba* hosts and in *D. discoideum*, complete genome is sequenced	Fritsche *et al.*, 1993* Collingro *et al.*, 2005b
	symbiont of *Acanthamoeba* sp. UWE1	Free-living amoeba (*Acanthamoeba* sp. UWE1			Fritsche *et al.*, 2000*
	Neochlamydia hartmannellae	Free-living amoeba (*Hartmannella vermiformis*)		Blocks cyst formation, infection results in host-cell lysis, infects *D. discoideum* but no other amoebal species tested	Horn *et al.*, 2000
	symbiont of *Acanthamoeba* sp. TUME1	Free-living amoeba (*Acanthamoeba* sp. TUME1)			Fritsche *et al.*, 2000*

[1] The phylogenetic classification is adopted from Horn (2008).
[2] The category "*Candidatus*" (*Cand.*) indicates that the respective bacterial taxon is not yet isolated or cultivated *in vitro*.
[3] Free fields indicate no specification of location due to an unknown natural or unicellular host.
[4] *D. discoideum*, *Dictyostelium discoideum* (social amoebae).
[5] Unless otherwise noted publications that first identified the organisms are listed. Marked references (*) refer to publications that first mentioned the organism.

More precisely, *Acanthamoeba* sp. infected with *Protochlamydia amoebophila* UWE25 (hereafter named *P. amoebophila*) can easily proliferate and recover from starvation (unpublished observation), although the growth rate of infected amoeba was shown to be impaired (Collingro *et al*., 2004). The 16S rRNA gene of the same organism was just recently found to be present in a small proportion of patients with community-acquired pneumonia (Haider *et al*., 2008).

Similar findings were demonstrated for another representative of *Chlamydia*-like bacteria. *Simkania negevensis* is able to grow within free-living amoebae (Kahane *et al*., 2001) and human cells, causing cytopathic effects in the latter case (Kahane *et al*., 2008). In addition, this organism is thought to be a potential pathogen for humans (Friedman *et al*., 2003).

Therefore, at least some *Chlamydia*-like bacteria can be considered as commensalistic to parasitic organisms. They may use the ubiquitous free-living amoebae as environmental reservoirs without being harmful to their protozoan hosts, and additionally could be able to survive within human and animal hosts thereby causing disease (Harb *et al*., 2000). Thus, their interactions would depend on the type of host as well as the host's health status.

1.1.2 Metabolic interactions

Due to the inability to perform genetic manipulations of these obligate intracellular organisms, whole-genome sequence analysis notably contributes to the understanding of chlamydial biology and their interactions with host cells. The reduced numbers of genes that enable biosynthesis of essential amino acids, cofactors and nucleotides accounts for the obligate endosymbiotic relationship, since lacking precursors are captured from the host using numerous compensatory transporter systems. According to genome analysis however, *P. amoebophila* – the so far only *Chlamydia*-like organism sequenced – seems to have a few metabolic capabilities that have not been identified in *Chlamydiaceae*, thereby possibly reflecting the varying environmental conditions in its amoebal host (Table 2) (Horn *et al*., 2004; McClarty, 1999).

In particular, the presence of a rare ATP/ADP exchange system in pathogenic chlamydiae as well as in the sequenced *Chlamydia*-like representative accounts for the closely linked endosymbiont-host metabolism. The import of ATP in exchange for ADP (Trentmann *et al*., 2007) and the evidence for ATP/ADP translocase expression during the developmental cycle of *P. amoebophila* (Schmitz-Esser *et al*., 2004) strongly suggests utilization of the host's ATP pool, and therefore explains the commonly used term of "energy parasites" for chlamydiae. Due to the presence of functional energy-producing enzymes however, chlamydial production of ATP seems to be possible (Iliffe-Lee and McClarty, 1999).

Table 2. Summery of biosynthetic pathways and transporters, cell envelope components and (potential) virulence factors of *Chlamydiaceae* vs. the *Chlamydia*-like representative *P. amoebophila*[1]

	P. amoebophila	*Chlamydiaceae*[2]	Comments
Glucokinase	yes	no	*Chlamydiaceae* are dependend on host-derived P-sugars
Hexophosphate transporter	yes	yes	Import of glucose-6-P from the host
PTS system	partly	partly	Phosphoenolpyruvate:phosphotransferase system; commonly used for sugar transport and phosphorylation
EMP pathway	yes	yes	Glycolysis; untypical phosphofructokinase uses inorganic pyrophosphate as P donor (reversible reaction!)
Pentose phosphate pathway	yes	yes	Production of pentose phosphates and erythrose-4-P (precursor metabolites); generation of NADPH
TCA	yes	partly	Lack of *gltA*, *acnB* and *icd* in *Chlamydiaceae* → acetyl-CoA cannot enter the TCA cycle
Gluconeogenesis	yes	yes	Formation of glucose via untypical phosphofructokinase (*pfkA*) and phosphoenolpyruvate carboxykinase (*pckA*)
Dicarboxylate transporter	no	yes	Supply of dicarboxylic acids (e.g. 2-oxoglutarate) to the TCA cycle
Glycogen metabolism	yes	yes	
Glutamate transporter	yes	yes	
Glutamate/leucine dehydrogenase (*gdhA*)	no	yes	
Glutamate dehydrogenase (*gdhB*)	yes	no	Synthesis of glutamine, proline and serine/glycine; similar to eukaryotic NAD^+-specific glutamate dehydrogenase
Tryptophan biosynthesis (*trp*-operon)	no	partly	*trpABCR* present in *C. trachomatis; trpABFCDR* present in *C. caviae*; absent in *C. pneumoniae* and *C. muridarum*
Tyrosine/tryptophan transporters	yes	yes	Compensation for incapacity for de novo synthesis of most amino acids; amino acid pathways that are present are frequently truncated (aromatic amino acids pathway) and give rise to end products that are used as intermediates for other biosynthetic pathways; transporters exhibit a broad substrate specificity; *P. amoebophila* can generate glycine, serine, glutamine, glutamate, aspartate and proline
Arginine transporter (*artJ*)	no	yes	
Methionine transporter	yes	yes	
Alanine transporters	yes	yes	
Proline transporter	yes	yes	
General amino acid transporters	yes	yes	
Amino acid antiporter	no	yes	
Oligo-peptide ABC transporters	yes	yes	
PRPP synthase	yes	no	Phosphoribosylpyrophosphate synthesis is needed for tryptophan and nucleotide biosynthesis; present in *C. caviae*
Nucleotide transporter	yes	yes	*Pam*NTT1: ATP/ADP exchange, *Pam*NTT2: ribonucleotide exchange (ATP, GTP, UTP, CTP), *Pam*NTT3: H^+ driven UTP uptake, *Pam*NTT4: NAD^+/ADP exchange, *Pam*NTT5: H^+ driven GTP, GDP, ATP uptake; *Ct*NTT1: ATP/ADP exchange, *Ct*NTT2: H^+ driven uptake of ATP, GTP, UTP, CTP (Haferkamp *et al.*, 2006)
Purine and pyrimidine pathways	partly	partly	
CTP synthase	yes	yes	Synthesis of CTP from UTP
Ribonucleotide reductase	yes	yes	Reduction of ribonucleotides to dNTPs (but no dTTP production)
Thymidylate synthase complementing protein (*thyX*)	yes	yes	dTMP formation out of dUTP and methylenetetrahydrofolate
Monophosphate kinases	yes	yes	Reutilization of (d)NMPs and (d)NDPs generated from nucleic acid turnover and as by-products of energy-requiring reactions
Nucleoside diphosphate kinase	yes	yes	

Table 2 (continued)

	P. amoebophila	*Chlamydiaceae*[2]	Comments
Minimal respiratory chain	yes	yes	Includes a V-type ATPase that can possibly synthesize ATP using a Na^+ and/or H^+ gradient
NADH oxidoreductase	yes	yes	Na^+ translocation
NADH oxidoreductase (*nuoA-N*)	yes	no	H^+ translocation
Cytochrome C	yes	no	
Cytochrome C oxidase	yes	no	
ATPase (*atpA-H*)	yes	no	F-type ATPase (ATP synthesis)
Menaquinone pathway	yes	no	
Riboflavin biosynthesis	yes	yes	
Heme biosynthesis	yes	yes	
Folate biosynthesis	yes	partly	
Lipoate biosynthesis	yes	yes	
Pyridine nucleotide biosynthesis	no	no	
Pantothenic acid biosynthesis	no	no	
Coenzyme A biosynthesis	no	no	
Biotin biosynthesis	no	partly	*C. pneumoniae*: complete biotin pathway
Biotin transporter	yes	yes	
Panthothenate transporter	yes	yes	
Iron/manganese transporter	yes	yes	
Zinc transporter	yes	yes	
Sulfonate/nitrate/taurine transporter	yes	yes	
Spermidine/putrescine transporter	yes	no	
Pht protein	yes	no	Protein (PC0544) is similar (33%) to members of the phagosomal nutrient transporter family found in *L. pneumophila* (Chen *et al.*, 2008)
Peptidoglycan synthesis	yes	yes	Minimal gene set present but no detection of peptidoglycan
LPS	yes	yes	Similar to LPS of enteric bacteria but 100-fold less immunostimulatory
D-alanine racemase	yes	no	Independent assembly of the interpeptide bridge during peptidoglycan synthesis; conversion of L-glutamate and L-alanine into their D isomers
D-glutamate racemase	yes	no	
Outer membrane complex A and B	yes	yes	
Disulfide bond isomerase	yes	yes	Catalysation of the rearrangement of -S-S- bonds in proteins; potentially involved in attachment and infectivity (Conant & Stephens, 2007)
Major outer membrane protein (*ompA*)	no	yes	Porin with low conservation among *Chlamydiaceae*

Table 2 (continued)

	P. amoebophila	*Chlamydiaceae*[2]	Comments
Polymorphic outer membrane proteins	no	yes	Autotransporters; role in attachment and entry
Outer membrane protein B (*porB*)	no	yes	
Fatty acid biosynthesis	yes	yes	
Type III secretion system	yes	yes	Untypical distribution of genes (several clusters are scattered on the chromosome)
MIP-like protein	yes	yes	Macrophage infectivity potentiator; lipoprotein; present at the surface of *C. trachomatis* EBs (Neff *et al.*, 2007)
Tarp	no	yes	Translocated actin-recruiting phophoprotein; export through T3SS; involvement in invasion of host cells
CopN, D, B	no	yes	T3SS effectors (Ho & Starnbach, 2005)
Inclusion proteins (*inc*)	yes	yes	Located in the host-derived membrane surrounding the chlamydial cells (inclusion membrane)
Protease-like activity factor (CPAF)	yes	yes	Secreted by pathogenic chlamydiae; able to degrade keratine 8 and human transcription factors required for MHC expression
CADD	no	yes	Chlamydial protein associating with death domains
CT847	no	yes	*C. trachomatis* T3SS effector; interaction with mammalian GCIP (Chellas-Géry *et al.*, 2007)
PC0373, PC0374	yes	yes	T3SS secretion by *Chlamydiacae* is suggested (Subtil *et al.*, 2005); secretion by *P. amoebophila* could be demonstrated (I. Kolarov, unpublished)
Pkn5	yes	yes	Putative *C. trachomatis* T3SS effector (Ho & Starnbach, 2005); similar to PC1401 (36% protein identity)
Lda3	yes	yes	Lipid droplets-associated protein 3 (CT473); might mediate recognition of host-derived lipids at the inclusion surface (Cocchiaro *et al.*, 2008); similar to PC1368 (46% protein identity)
Lda1, 2	no	yes	Lipid droplets-associated proteins 1 and 2 (CT156, CT163); only found in *C. trachomatis* (Kumar *et al.*, 2006)
Clostridium-like cytotoxins	no	yes	
Cysteine protease	no	yes	
Polymorphic membrane protein D	no	yes	Autotransported protein
Hemolysin III	yes	no	Integral membrane protein
Leucine rich repeat proteins	yes	no	
Type IV secretion system	yes	no	Protein export or DNA transfer

[1] Unless otherwise noted, table content is based on results from whole genome analysis published by Horn (2004) and McClarty (1999). The presence of homologous proteins or biosynthetic pathways is indicated by "yes" or if partly present by "partly", the absence by "no". Gene names are mentioned occasionally in order to clarify gene identity.
[2] This clinically significant family comprises two genera and nine species: *Chlamydia muridarum*, *Chlamydia suis*, *Chlamydia trachomatis*, *Chlamydophila pecorum*, *Chlamydophila pneumoniae*, *Chlamydophila psittaci*, *Chlamydophila abortus*, *Chlamydophila caviae*, *Chlamydophila felis* (Everett *et al.*, 1999).

Moreover, usage of host ATP seems to depend on the stage of chlamydial development (Belland *et al*., 2003b; Gérard *et al*., 2002).

1.1.3 *P. amoebophila-Acanthamoeba* sp. relationship

P. amoebophila has been found as an obligate symbiont of an *Acanthamoeba* sp. soil isolate (Fritsche *et al*., 1993), and is able to multiply within various *Acanthamoeba* sp. isolates (Fritsche *et al*., 1998) as well as within *Acanthamoeba castellanii* Neff, a widely used strain isolated from soil more than 50 years ago (Neff, 1957) (Fig. 1).

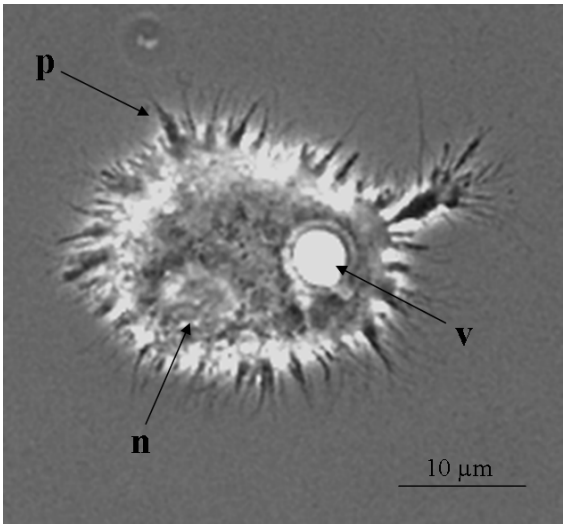

Figure 1. The uninfected *P. amoebophila* host *Acanthamoeba castellanii* strain Neff trophozoite as observed by phase-contrast microscopy. Evident structures comprise the nucleus (n), the spine-like pseudopodia (p), and a contractile vacuole (v).

Ultrastructural analysis of these coccoid, gram-negative bacteria demonstrated their dispersal throughout the amoebal cytoplasm, each cell being surrounded by a membrane termed inclusion membrane (Collingro *et al*., 2005a; Fritsche *et al*., 2000). These single cell inclusions are not only in contrast to inclusion morphology of the more distantly related *Chlamydiaceae*, but differ also from inclusions of other members of the *Parachlamydiaceae*, which either form several large inclusions (Amann *et al*., 1997) or do not reside within vacuoles at all (Horn *et al*., 2000). The host *Acanthamoeba* sp., a widely distributed free-living amoeba, has been recognized to be an opportunistic human pathogen causing keratitis and granulomatous encephalitis (Jager and Stamm, 1972; Naginton *et al*., 1974). Stable infection with several bacterial endosymbionts including *P. amoebophila* could be shown to enhance in vitro cytopathogenicity of their hosts (Fritsche *et al*., 1998) thereby suggesting clinical relevance of this protozoa-chlamydiae relationship.

The capability of multiple different bacterial species to simultaneously survive and multiply within acanthamoebae, as for example various environmental isolates (Pagnier *et al*., 2008) and the facultative intracellular bacteria *L. pneumophila* (Harb *et al*., 2000) and also the observation of chlamydial as well as non-chlamydial obligate bacterial endosymbionts in acanthamoebae (Horn and Wagner, 2004), is another aspect of this symbiosis, since a potential physical encounter theoretically allows for lateral gene transfer between intracellular bacteria.

In support of this, analysis of the *P. amoebophila* genome revealed a genomic island encoding for a type IV secretion system (T4SS) similar to F-like conjugative systems, indicating a recent lateral gene transfer that potentially occurred within an amoebal vacuole (Greub *et al*., 2004; Horn *et al*., 2004). Also, an involvement of the T4SS in DNA transfer between internalized bacteria was suggested (Greub *et al*., 2004).

Furthermore, genome analysis of the arthropod associated obligate intracellular *Rickettsia bellii* strongly indicates lateral gene transfer of several T4SS components between *Rickettsia* ancestors and *P. amoebophila* which could have happened within co-infected amoebae, since *R. bellii* is able to survive in acanthamoebae, and co-infection of amoebae was reported (Ogata *et al*., 2006). Therefore, despite its isolated lifestyle, genetic exchange between *P. amoebophila* and other intracellular bacteria seems to be possible, and might facilitate adaptation to the intracellular environment of eukaryotic cells.

In addition to the already mentioned ATP/ADP translocase (see chapter 1.1.2) the type three secretion system (T3SS) present in all so far sequenced chlamydiae accounts for the host-symbiont interaction, since it is known for many Gram-negative pathogens to inject proteins into target cells thereby interfering with many different host cellular processes (Hueck, 1998). Little is known about effector proteins and therefore functions provided by T3 secretion of *Chlamydia*-like bacteria. However, evidence for secretion of a family of inclusion membrane-localized proteins termed Incs through the T3SS of *C. trachomatis* (Fields *et al*., 2003) allows for speculation about secretion of the *P. amoebophila* homologues by the same mechanism. Also, numerous putative F-box containing proteins (FBPs) considered to be T3/T4SS substrates exploiting the host ubiquitin proteasome system have been identified in *P. amoebophila* but not in *Chlamydiaceae*, suggesting a function of FBPs in basic symbiotic interaction rather than in virulence (Angot *et al*., 2007). However, the presence of a complete type III secretion system as well as genes predicted to encode for other virulence-associated factors in *P. amoebophila* (see table 2) may provide a genetic basis for a potential pathogenicity of *Chlamydia*-like organisms.

1.2 The chlamydial developmental cycle

1.2.1 The paradigm of a biphasic cycle

Bacteria belonging to the phylum *Chlamydiae* share an obligate intracellular lifestyle within eukaryotic cells. In contrast to other obligate intracellular bacteria, like members of the order *Rickettsiales*, chlamydial growth is associated with a unique developmental cycle that generally takes place within non-lysosomal vacuoles termed inclusions. During an active infection the cycle is characterized by an alternate switching between two morphologically and functionally distinct forms (Fig. 2). While metabolically inert elementary bodies (EBs) can enter host cells by endocytosis, metabolically active reticulate bodies (RBs) are generally considered to be non-infectious, although infectivity might be not to be restricted to EBs in the case of *Simkania negevensis* (Kahane *et al*., 2002). Uptake of EBs is followed by differentiation to RBs and a period of binary fission. Finally, redifferentiation to EBs and release of progeny takes place. Whereas exit of bacteria via induction of host cell lysis is a well-established mode of release for

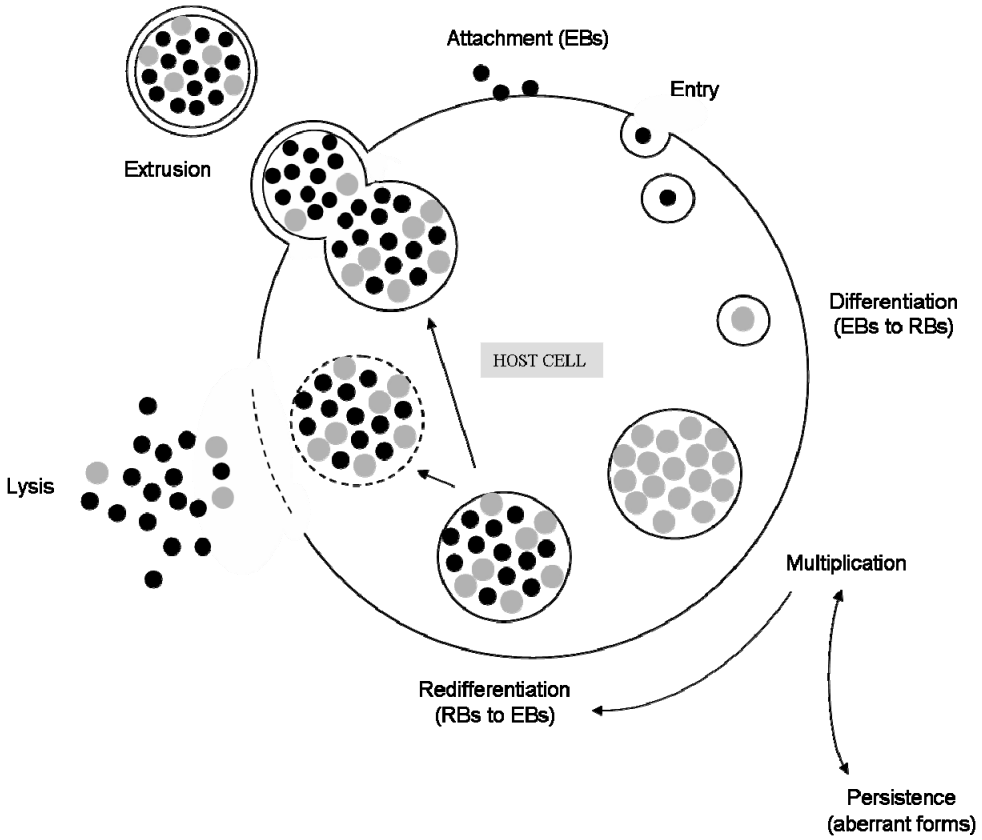

Figure 2. General schematic representation of the chlamydial developmental cycle. Internalization of EBs is followed by differentiation to RBs that undergo binary fission. Redifferentiation to EBs and subsequent release by either host cell lysis or extrusion (Hybiske and Stephens, 2007) allows for another round of infection through EBs. Various stress conditions induce persistence *in vitro*. Note that the entire cycle takes place within a vacuole termed inclusion. Developmental cycles of phylogenetically different *Chlamydiae* vary in length of cycles, number and morphology of inclusions, morphology of EBs and RBs, and mode of release. Dashed lines indicate rupture of membranes.

at least *Chlamydiaceae in vitro* (Neeper *et al*., 1990), extrusion, meaning packaged release of a portion of the chlamydial inclusion by a membranous protrusion leaving an intact host cell and residual inclusion behind, just recently has been suggested to be another chlamydial release pathway (Hybiske and Stephens, 2007).

The course of infection as well as the length of the complete cycle, as studied *in vitro*, differs depending on the infecting species and strain, the type of host cell and environmental conditions. A remarkable difference between *Simkania negevensis* and other chlamydiae concerns the length of the cycle. While the time from entry to release of chlamydial particles usually does not exceed 4-5 days, *S. negevensis* could be demonstrated to require 12 days or longer for lysis of Vero cells (Kahane *et al*., 2002).

The cycle has been phenotypically characterized for members of *Chlamydiaceae* as well as for a few members of *Chlamydia*-like bacteria (Table 3), but presently information about molecular and genetic events during the cycle is mainly available for *C. trachomatis* (AbdelRahman and Belland, 2005). However, due to the larger genome size of the *Chlamydia*-like representative *P. amoebophila* and the presence of certain factors that are thought to play a role in establishment of a replicative niche within the host (e.g. Tarp) exclusively in their pathogenic counterparts, the study of the developmental cycle of *Chlamydia*-like organisms could yield interesting new findings.

The *in vitro* observation for *Chlamydiaceae* to be able to exist as an atypical third form different from EBs and RBs – a phenomenon described as persistence – suggests an alternative life cycle, thereby expanding our view about the chlamydial developmental cycle (Fig. 2) (Hogan *et al*., 2004).

1.2.2 The persistent infection

Persistence has been described for *Chlamydiaceae* to be a reversible aberrant state of infection in which these bacteria are viable but non-culturable, meaning the absence of growth and the reduction of infectious forms (Beatty *et al*., 1994). While the presence of persistent chlamydial forms is well-established *in vitro*, persistence has not yet been proven conclusively to occur *in vivo*. *Chlamydiaceae*-associated chronic diseases however, may be explained by unresolved and temporarily latent chlamydial infections resulting from persistence in an altered form (Hogan *et al*., 2004).

In vitro persistence is triggered by antibiotic treatment (Lambden *et al*., 2006; Matsumoto and Manire, 1970), depletion of amino acids, glucose and iron (Harper *et al*., 2000; Raulston, 1997), cytokine (IFN-γ) exposure (Pantoja *et al*., 2001), infection of monocytes (Koehler *et al*., 1997),

infection by bacteriophages (Salim *et al*., 2008) and heat shock (Kahane and Friedman, 1992). Additionally, aberrant chlamydial forms have been observed to occur spontaneously in long-term infections (Kutlin *et al*., 2001). Different persistence systems that take the type of inducer, the infecting chlamydial species or strain and the origin of host cells into account produce different phenotypic chlamydial changes, but generally cause altered size and shape of RBs (Hogan *et al*., 2004).

In accordance with phenotypic differences of persistent *Chlamydiaceae,* gene expression studies provide mixed results in experiments using different infection models and triggers. While for example some studies describe the down-regulation of transcripts coding for proteins involved in cell division (*fts*K, *fts*W) to provide genetic evidence for the commonly observed inhibition of cell division (Byrne *et al*., 2001; Gérard *et al*., 2001), data derived from other persistence systems show different transcription patterns for the genes mentioned above (Belland *et al*., 2003a; Hogan *et al*., 2004). The down-regulation of chlamydial genes that function in RB-to-EB differentiation however, might be a common characteristic of persistence, thereby accounting for the observed failure to generate infectious particles as long as the inducer is present (Hogan *et al*., 2004).

The supposed persistent phase of these intracellular pathogens might function as a survival response to environmental stress as a result of either a controlled, stimulon-mediated change in gene expression (Belland *et al*., 2003a), or an arrest in transcriptional regulation causing uncontrolled gene expression profiles (Mäurer *et al*., 2007).

Table 3. The phentotypic *in vitro* developmental cycles of different *Chlamydiae* and hosts*

Endosymbiont	Host	MOI	Phenotypic characteristics of developmental cycle	Reference
Parachlamydia acanthamoeba				
strain Hall's coccus	Human macrophages	10	8 hpi: single EBs and RBs within vacuoles 20 hpi: extracellular CBs and dividing RBs, vacuoles with more than six bacteria present, macrophage undergoes early apoptosis 24 hpi: apoptosis of infected cells 0-96 hpi: increase of infected cells Doubling time of two days	Greub *et al.*, 2003
strain Bn9, strain Hall's coccus	*Acanthamoeba polyphaga*	2	Infection by EBs or CBs 0-8 hpi: differentiation of EBs/CBs to RBs, RBs can invade the amoebal cytoplasm Division of RBs and re-differentiation to EBs/CBs occurs mainly in the vacuoles Vacuoles and cytoplasm size increases during multiplication of RBs Release occurs through amoebal lysis (144 hpi) or expelled vesicles Bacteria cannot be observed in cysts, encystment is decreased by infection	Greub & Raoult, 2002
strain UV-7	*Acanthamoeba* sp. UWC1	n.d.	Bacteria are residing in large vacuoles, crescent-shaped stage is observed very rarely (even at 7 days pi)	Collingro *et al.*, 2005a
	Different mammalian cell lines	1	1-2 days pi: small inclusion vacuoles detectable, mostly aberrant RBs are present 2-3 days pi: increase in infected cells, cytopathic effect is visible 4-5 days pi: most host cells are destroyed, many EBs are present extracellularly	
strain Hall's coccus	Pneumocytes and lung fibroblasts	10	0-7 days pi: number of bacteria increases 3- to 7-fold in fibroblasts and pneumocytes, number of infected cells increases, viability of host cells is not impaired, bacteria remain viable for 21 (in pneumocytes) and 14 (in fibroblasts) days	Casson *et al.*, 2006
Protochlamydia amoebophila				
strain UWE25	*Acanthamoeba* sp.	n.d.	Infection does not prevent encystation, bacteria are present in trophozoites and cysts and reside within small inclusions	Collingro *et al.*, 2005b
Neochlamydia hartmannellae				
	Hartmannella vermiformis	n.d.	Infection blocks cyst formation, bacteria are not surrounded by vacuoles 3-5 days pi: high amounts of mature EBs within cells, subsequent lysis/rupture of amoebal cells	Horn *et al.*, 2000
Protochlamydia neagleriophila				
strain KNic	*Naegleria* sp.	n.d.	Bacteria occur as single cells or in small groups at the beginning of infection, crescent-shaped bacteria are present outside the amoebae (possibly an artefact), amoebal nucleus is located at the marginal cytoplasm when numerous bacteria are present at a late stage of infection, infection blocks cyst formation but not transformation to flagellate stage, heavily infected amoebae lyse or rupture, moderately infected amoebae continuously release bacteria	Michel *et al.*, 2000

Table 3 (continued)

Endosymbiont	Host	MOI	Phenotypic characteristics of developmental cycle	Reference
Waddlia chondrophila				
strain 2032/99	*Hartmannella vermiformis*	n.d.	5 days pi: bacteria are present within the amoebal cytoplasm or vacuoles, division is observed	Michel *et al.*, 2004
strain 2032/99	Several free-living amoebae	n.d.	Infection causes block of cyst formation (except for *Vahlkampfia ovis*), cycle ends with lysis of amoebae	Michel *et al.*, 2004
strain ATCC VR-1470	Human macrophages	1-50 (est.)	0-8 hpi: entry of bacteria 4-36 hpi: bacterial growth in vacuoles 36 hpi: host lysis/release begins 72-96 hpi: 100% cells infected Doubling time of 2.8 hours	Goy *et al.*, 2008
Waddlia malaysiensis				
	HEK cells (human embryonic kidney cells)	n.d.	72 hpi: large inclusions with EBs and RBs Presence of a collection of mitochondria close to inclusions	Chua *et al.*, 2005
Criblamydia sequanensis				
strain CRIB-18, T	*Acanthamoeba castellanii*	n.d.	Bacteria are present in trophozoites but not in cysts, viable after 21 days of being extracellular 48 hpi: only few bacteria/cell, 1-10 vacuoles full of bacteria/cell, or completely filled amoebal cells	Thomas *et al.*, 2006
Simkania negevensis				
strain ATCC VR-1471^T	*Acanthamoeba polyphaga*	1	Loss of infectivity but survival when amoebae were infected with bacteria purified from Vero cells Dilution of infected amoebae allowed for growth of bacteria: inclusions contain one or more EBs and RBs, at 24 hpi EBs and dividing RBs are present Encystation: bacteria can be found between cyst walls, in amoebal cytoplasm or in amoebae but without cytoplasm	Kahane *et al.*, 2001
strain ATCC VR-1471^T	Vero cells (simian epithelial cell line)	0.005 -2.8	Cycle takes 12-15 days, many small inclusions in late infection 2-4 days pi: exponential growth of bacteria followed by a long plateau stage Lack of spread of infection/bacteria are not released Electron-dense area in bacteria starts appearing at 3 days pi High amount of infectious particles from day 2-3 pi to day 13 RBs are thought to be infectious Different MOIs give similar results	Kahane *et al.*, 2002

Table 3 (continued)

Endosymbiont	Host	MOI	Phenotypic characteristics of developmental cycle	Reference
strain ATCC VR-1471 Z	Several free-living amoebae	n.d.	*Acanthamoeba* sp. HLA, *Hartmannella vermiformis*, *Balamuthia mandrillaris*: infection prevents encystation *B. mandrillaris*: release of EBs 3-5 days pi *Acanthamoeba* sp. HLA: heavily infected cells, different stages present within vacuoles at 6 days pi	Michel *et al.*, 2005
Chlamydia trachomatis				
serovar K	Human monocytes	1	Single or multiple inclusions close to nuclei throughout 10 days 5-7 days pi: normal and aberrant chlamydial forms detectable 7-10 days pi: aberrant forms dominate in all monocyte inclusions 3-10 days pi: bacteria are non-infectious but viable and metabolically active, and morphologically resemble intermediate forms (condensed structure in the center of bacterial cell)	Koehler *et al.*, 1997
serovar L2	L929 cells (mouse fibroblasts)	1	12 hpi: binary fission of RBs observable 18-24 hpi: peak in RB number, re-differentiation into EBs starts 24 hpi: inclusion is large and contains mostly RBs 48-72 hpi: lysis of host cells;	Nicholson *et al.*, 2003
Chlamydia caviae				
	Drosophila SL2 cells (phagocytic)	5	48 hpi: 20-30% of cells show a large inclusion mainly containing RBs and IBs, some EBs 24-72 hpi: perinuclear inclusion increases 96 hpi: heterogeneous size of inclusions, disrupted inclusions suggesting completion of cycle Re-infection between 72 and 96 hpi	Derré *et al.*, 2007
Chlamydophila pneumoniae				
strain TW 183	*Acanthamoeba castellanii*	1	4 hpi: phagocytosis of EBs 12 hpi: 10-20% amoebae contain small inclusions 3 days pi: single large inclusions can be observed 7-14 days pi: viable and infective bacteria present, all chlamydial stages present including atypical EBs, amoebal viability decreases Restricted chlamydial growth	Essig *et al.*, 1997
strain AR-39	HeLa 229 cells	1	8 hpi: differentiation into RBs starts 12 hpi: typical RBs present 19-36 hpi: multiplication is detecable, no EBs present, densly packed inclusions contain RBs 48 hpi: redifferentiation into EBs starts, cycle becomes asynchronous, intermediate forms are present 60-72 hpi: still RBs present, increasing proportion of EBs 84 hpi: lysis of host cell, release of progeny Inclusions do not fuse	Wolf *et al.*, 2000

Table 3 (continued)

Endosymbiont	Host	MOI	Phenotypic characteristics of developmental cycle	Reference
Chlamydophila psittaci				
strain meningopneumonitis	L cells (mouse fibroblasts)	10-20	4-12 hpi: transition from EBs to RBs 8 hpi: mature RB appears 12 hpi: binary fission of RBs 15-30 hpi: rise in infectious particles, multiple large bacteria containing vacuoles per cell 30 hpi: cytopathic effects, all developmental stages are present (RBs, EBs, IBs) 40 hpi: lysis of host cells	Friis, 1972
strain 6BC	Human monocytes	1	48 hpi: large inclusions 72-96 hpi: rise in number of EBs 96-120 hpi: number of EBs remains steady	Manor & Sarov, 1986
serovar guinea pig inclusion conjunctivitis	Mouse macrophages	1-2	Infection results in apoptosis after 24 hpi	Ojcius *et al.*, 1998
strain Cal 10 meningopneumonitis	Mouse macrophages	1	Lower MOIs are optimal for growth and development of live EBs, highest yield 96 hpi	Wyrick & Brownridge, 1978
		100	Growth reduced, degradation of bacteria 2-6 hpi (macrophage cytotoxicity)	

* Abbrevations: Hpi, hours post infection. IB, intermediate body. CB, crescent body. MOI, multiplicity of infection. DC, dendritic cell. n.d., not determined. est., estimation.

1.3 Aim of diploma thesis

The work in the course of my diploma thesis was aimed at elucidating the developmental cycle of the obligate intracellular *Chlamydia*-like organism *P. amoebophila* within its amoebal host. This work was conducted as a basis for follow-up studies such as gene and protein expression studies as well as ultrastructural analysis, and also to improve knowledge about the developmental cycle of the increasingly diverse *Chlamydiae* (Table 3). The major goal was the description of phenotypic events during the cycle, and in particular the determination of crucial time points in the cycle. Two strategies were pursued: First, the cycle was visualized by fluorescence *in situ* hybridization (FISH), assuming that FISH oligonucleotide probes, unlike the general nuclei acid dye DAPI, cannot detect the metabolically inactive spore-like EBs. Second, numbers of intracellular and extracellular infectious forms during the cycle were determined in order to be able to specify and confirm important developmental events, such as the release of infectious particles from the host cell.

In addition, first steps to clarify whether persistent forms of *P. amoebophila* as a representative of *Chlamydia*-like bacteria exist when introducing a selected environmental stress were performed. Namely, iron depletion of synchronously infected amoebae was selected to search for altered morphological forms. Eventually, my work should contribute to the understanding of mechanisms of symbiosis between the unique *Chlamydiae* and their diverse hosts.

2 Materials and Methods

All chemicals used in this study were purchased in p.a. quality, if not stated otherwise. All buffers, media and solutions were produced utilizing double distilled and filtered water (hereafter named $_{dd}H_2O$) (Water purification system MILLI-Q® biocel, Millipore GmbH, Vienna, Austria). Sodium hydroxide (NaOH) and hydrochloric acid (HCl) were used to adjust the pH.

2.1 Software

Table 4. Software used

Software	Manufacturer/Source
AxioVision 4	Carl Zeiss MicroImaging GmbH, Jena, Germany
Basic Local Alignment Search Tool (Blast)	http://www.ncbi.nlm.nih.gov/BLAST/
FinchTV 1.4.0	Geospiza, Seattle, WA, USA
GraphPad Prism 5.01	GraphPad Software Inc., La Jolla, CA, USA
LSM Image Browser	Carl Zeiss MicroImaging GmbH, Jena, Germany
Microsoft Office 2002	Microsoft Corporation, Redmond, WA, USA

2.2 Technical equipment

Table 5. Technical equipment used

Equipment	Manufacturer
ABI 3130*xl* DNA Sequencer	Applied Biosystems Inc., Foster City, CA, USA
Accu-jet® pro pipette aid	Brand GmbH+Co KG, Wertheim, Germany
CCD camera AxioCam HRc	Carl Zeiss MicroImaging GmbH, Jena, Germany
Centrifuges	
Optima™ L-100 XP ultracentrifuge	Beckman Coulter, Inc., Palo Alto, CA, USA
Centrifuge 5804 R	Eppendorf AG, Hamburg, Germany
Mikro 20 benchtop centrifuge	Andreas Hettich GmbH & Co KG, Tuttlingen, Germany
Filter devices	
Vacuum pump 220 V/50 Hz	Millipore GmbH, Vienna, Austria
Filtering flask 100 ml, glass	Schott Austria GmbH, Vienna, Austria
Fritted glass base (2.5 cm diameter) + silicone stopper	Millipore GmbH, Vienna, Austria
Glass funnel 15 ml, glass	Millipore GmbH, Vienna, Austria
spring clamp, aluminium	Millipore GmbH, Vienna, Austria
Gasprofi 1 SCS micro	Carl Roth GmbH & Co KG, Karlsruhe, Germany
Gelelectrophoresis devices	
Electrophoresis cell (Sub-Cell GT)	Bio-Rad Laboratories GmbH, Munich, Germany
Electrophoresis power supply (PowerPac Basic)	Bio-Rad Laboratories GmbH, Munich, Germany
Sub-Cell GT UV-Transparent Gel Tray (15 x 15)	Bio-Rad Laboratories GmbH, Munich, Germany

Table 5 (continued)

Standard combs	Bio-Rad Laboratories GmbH, Munich, Germany
UV transilluminator	Biostep GmbH, Jahnsdorf, Germany
icycler Thermal cycler	Bio-Rad Laboratories GmbH, Munich, Germany
Incubators	
Microbiological incubator KB 115	Binder GmbH, Tuttlingen, Germany
Hybridization oven UE 500	Memmert GmbH & Co KG, Schwabach, Germany
Laminar flow hood, model 1.8	Holten, Jouan Nordic, Allerød, Denmark
Magnetic stirrer RCT basic	IKA® Werke GmbH & Co KG, Staufen, Germany
Microscopes	
Epifluorescence microscope Axioplan 2 imaging	Carl Zeiss MicroImaging GmbH, Jena, Germany
Inverse microscope Axiovert 25	Carl Zeiss MicroImaging GmbH, Jena, Germany
Confocal Laser Scanning Microscope LSM 510 Meta	Carl Zeiss MicroImaging GmbH, Jena, Germany
NanoDrop® ND-1000 UV/Vis spectrophotometer	NanoDrop Technologies Inc., Wilmington, DE, USA
Neubauer counting chamber	Paul Marienfeld GmbH & Co KG, Lauda-Königshofen, Germany
pH meter inoLab pH Level 1	Wissenschaftlich-Technische Werkstätten GmbH, Weilheim, Germany
PocketBloc® Thermomixer	Biozym Scientific GmbH, Hessisch Oldendorf, Germany
Scales	
OHAUS® Analytical Plus balance	Ohaus Corporation, Pine Brook, NJ, USA
Sartorius BL 3100	Sartorius AG, Göttingen, Germany
UV sterilizing PCR workstation	PeqLab Biotechnologie GmbH, Erlangen, Germany
Vortex-Genie 2	Scientific Industries Inc., Bohemia,NY, USA
Water baths	
Haake DC10-P5/U Heating circulator bath	Thermo Fisher Scientific Inc., Waltham, MA, USA
Incubation bath GFL 1004	Gesellschaft für Labortechnik GmbH, Burgwedel, Germany
Water purification system MILLI-Q® biocel	Millipore GmbH, Vienna, Austria
Watervapour high pressure autoclaves	
Varioclav® 135 S H+P	H+P Labortechnik GmbH, Oberschleißheim, Germany
Varioclav® 25 T H+P	H+P Labortechnik GmbH, Oberschleißheim, Germany

2.3 Disposable items

Table 6. Disposable items used

Disposable item	Manufacturer
25cm2 Tissue culture flasks	Asahi Techno Glass Corporation, Iwaki Glass Co., Ltd., Funabashi-City, Japan
500cm2 Tissue culture flasks	Nunc, Roskilde, Denmark
Cellulose acetate membrane filters (0.45 µm pore size, 25 mm diameter)	Sartorius Stedim Biotech GmbH, Göttingen, Germany
Cover glasses (24 x 50 mm, 24 x 60 mm)	Paul Marienfeld GmbH & Co KG, Lauda-Königshofen, Germany

Table 6 (continued)

Coverslips (12 mm)	Carl Roth GmbH & Co KG, Karlsruhe, Germany
Glass beads (0.75-1.0 mm)	Carl Roth GmbH & Co KG, Karlsruhe, Germany
Greiner tubes (15 ml, 50 ml)	Greiner Bio-One GmbH, Frickenhausen, Germany
Isopore™ polycarbonate membrane filters (0.22 µm pore size, 25 mm diameter, black)	Millipore GmbH, Vienna, Austria
Lab-Tek™ Chamber Slides, glass (16 wells)	Nunc, Roskilde, Denmark
Lab-Tek™ Chambered Coverglass, glass (4 wells, 8 wells)	Nunc, Roskilde, Denmark
Microscope slides (76 x 26 mm)	Carl Roth GmbH & Co KG, Karlsruhe, Germany
Microscope slides, 10 wells	Paul Marienfeld GmbH & Co KG, Lauda-Königshofen, Germany
Multiwell dishes, polystyrene (6 wells, 24 wells)	Nunc, Roskilde, Denmark
Needles Sterican® (Ø 0.45 x 25 mm, Ø 0.90 x 40 mm)	B. Braun Melsungen AG, Melsungen, Germany
Parafilm® M laboratory film	American National Can Company, Chicago, IL, USA
PCR tubes (0.2 ml)	Biozym Scientific GmbH, Hessisch Oldendorf, Germany
plastic pipettes (2 ml, 10 ml)	Barloworld Scientific Ltd., Staffordshire, UK
Plastic tips (various sizes)	Carl Roth GmbH & Co KG, Karlsruhe, Germany
Reaction tube 1.5 ml	Greiner Bio-One GmbH, Frickenhausen, Germany
Reaction tube 2 ml	Greiner Bio-One GmbH, Frickenhausen, Germany
SafeSeal-Tips® Premium (various sizes)	Biozym Scientific GmbH, Hessisch Oldendorf, Germany
Syringe filter, cellulose acetate (0.2 µm)	Asahi Techno Glass Corporation, Iwaki Glass Co., Ltd., Funabashi-City, Japan
Syringe Injekt®-F 1 ml	B. Braun Melsungen AG, Melsungen, Germany
Syringe Omnifix® 50 ml	B. Braun Melsungen AG, Melsungen, Germany
Ultracentrifuge tubes	Beckman Coulter, Inc., Palo Alto, CA, USA

2.4 Chemicals and enzymes

Table 7. Chemicals used

Chemical product	Manufacturer
4',6-Diamidino-2-phenylindole (DAPI)	Lactan Chemikalien und Laborgeräte GmbH, Graz, Austria
Agarose	Biozym Scientific GmbH, Hessisch Oldendorf, Germany
Ammonium chloride (NH_4Cl)	Carl Roth GmbH & Co KG, Karlsruhe, Germany
Ammonium formate (NH_4 formate)	Fluka Chemie AG, Buchs, Switzerland
Ammonium molybdate tetrahydrate ($NH_4Mo_7O_{24}$*4 H_2O)	Carl Roth GmbH & Co KG, Karlsruhe, Germany
Boric acid (H_3BO_3)	Carl Roth GmbH & Co KG, Karlsruhe, Germany
Bovine serum albumin (BSA)	Carl Roth GmbH & Co KG, Karlsruhe, Germany
Bromphenol blue	Sigma-Aldrich Chemie GmbH, Steinheim, Germany
Calcium chloride dihydrate ($CaCl_2$*2 H_2O)	Carl Roth GmbH & Co KG, Karlsruhe, Germany
Citifluor AF1	Agar Scientific Ltd., Stansted, UK
Cobalt(II) chloride hexahydrate ($CoCl_2$)	Fluka Chemie AG, Buchs, Switzerland

Table 7 (continued)

Copper(II) sulphate pentahydrate ($CuSO_4$)	Fluka Chemie AG, Buchs, Switzerland
D(+)-Biotin	Carl Roth GmbH & Co KG, Karlsruhe, Germany
Deferoxamine mesylate (DAM)	Sigma-Aldrich Chemie GmbH, Steinheim, Germany
di-Sodiumhydrogen phosphate dihydrate (Na_2HPO_4*2 H_2O)	Carl Roth GmbH & Co KG, Karlsruhe, Germany
DL-Phenylalanine	Merck GmbH, Vienna, Austria
Ethanol absolute ($EtOH_{abs.}$)	AustrAlco Österreichische Alkoholhandels GmbH, Spillern, Austria
Ethidium bromide solution	Fluka Chemie AG, Buchs, Switzerland
Ethylenediamine-tetraaceticacid (EDTA)	Carl Roth GmbH & Co KG, Karlsruhe, Germany
Ferrous ammonium sulfate hexahydrate ($Fe(NH_4)_2(SO_4)_2$*6 H_2O)	Sigma-Aldrich Chemie GmbH, Steinheim, Germany
Ficoll® 400	Sigma-Aldrich Chemie GmbH, Steinheim, Germany
Folic acid	Sigma-Aldrich Chemie GmbH, Steinheim, Germany
Formaldehyde 37% (w/w) Rotipuran®	Carl Roth GmbH & Co KG, Karlsruhe, Germany
Formamide deionized	Carl Roth GmbH & Co KG, Karlsruhe, Germany
Glycerol Rotipuran®	Carl Roth GmbH & Co KG, Karlsruhe, Germany
Glycine	Carl Roth GmbH & Co KG, Karlsruhe, Germany
Hydrochloric acid 37% (w/w) (HCl)	Carl Roth GmbH & Co KG, Karlsruhe, Germany
Iron(II) sulfate heptahydrate ($FeSO_4$*7 H_2O)	Carl Roth GmbH & Co KG, Karlsruhe, Germany
L(+)-Ascorbic acid	Sigma-Aldrich Chemie GmbH, Steinheim, Germany
L-Alanine	Carl Roth GmbH & Co KG, Karlsruhe, Germany
L-Arginine hydrochloride (L-arginine-HCl)	Carl Roth GmbH & Co KG, Karlsruhe, Germany
L-Asparagine anhydrous	Fluka Chemie AG, Buchs, Switzerland
L-Aspartic acid	Fluka Chemie AG, Buchs, Switzerland
L-Cysteine	Carl Roth GmbH & Co KG, Karlsruhe, Germany
L-Cystine	Sigma-Aldrich Chemie GmbH, Steinheim, Germany
L-Glutamic acid	Sigma-Aldrich Chemie GmbH, Steinheim, Germany
L-Glutamine	Carl Roth GmbH & Co KG, Karlsruhe, Germany
L-Histidine hydrochloride (L-histidine-HCl)	Fluka Chemie AG, Buchs, Switzerland
L-Isoleucine	Carl Roth GmbH & Co KG, Karlsruhe, Germany
L-Leucine	Carl Roth GmbH & Co KG, Karlsruhe, Germany
L-Lysine hydrochloride (L-lysine-HCl)	Sigma-Aldrich Chemie GmbH, Steinheim, Germany
L-Methionine	Carl Roth GmbH & Co KG, Karlsruhe, Germany
L-Proline	Carl Roth GmbH & Co KG, Karlsruhe, Germany
L-Serine	Fluka Chemie AG, Buchs, Switzerland
L-Threonine	Carl Roth GmbH & Co KG, Karlsruhe, Germany
L-Tryptophan	Carl Roth GmbH & Co KG, Karlsruhe, Germany
L-Tyrosine	Carl Roth GmbH & Co KG, Karlsruhe, Germany
L-Valine	Carl Roth GmbH & Co KG, Karlsruhe, Germany
Magnesium chloride hexahydrate ($MgCl_2$)	Carl Roth GmbH & Co KG, Karlsruhe, Germany
Magnesium sulfate heptahydrate ($MgSO_4$*7 H_2O)	Merck GmbH, Vienna, Austria

Table 7 (continued)

Manganese(II) chloride tetrahydrate ($MnCl_2$*4 H_2O)	Carl Roth GmbH & Co KG, Karlsruhe, Germany
Methanol	Carl Roth GmbH & Co KG, Karlsruhe, Germany
Mowiol 4-88	Sigma-Aldrich Chemie GmbH, Steinheim, Germany
Potassium dihydrogen phosphate (KH_2PO_4)	Mallinckrodt Baker B.V., Deventer, Holland
Propidium iodide (PI)	Invitrogen Molecular Probes Inc., Eugene, OR, USA
Proteose peptone	Oxoid Ltd., Hampshire, England
Riboflavin	Carl Roth GmbH & Co KG, Karlsruhe, Germany
Sodium acetate (Na acetate)	Carl Roth GmbH & Co KG, Karlsruhe, Germany
Sodium chloride (NaCl)	Carl Roth GmbH & Co KG, Karlsruhe, Germany
Sodium dihydrogen phosphate (NaH_2PO_4)	Mallinckrodt Baker B.V., Deventer, Holland
Sodium dodecyl sulfate (SDS)	Carl Roth GmbH & Co KG, Karlsruhe, Germany
Sodium hydrogen carbonate ($NaHCO_3$)	Carl Roth GmbH & Co KG, Karlsruhe, Germany
Sodium hydroxide (NaOH)	Carl Roth GmbH & Co KG, Karlsruhe, Germany
Sucrose	Merck GmbH, Vienna, Austria
Sulfuric acid Rotipuran® (H_2SO_4)	Carl Roth GmbH & Co KG, Karlsruhe, Germany
Thiamine hydrochloride (Vitamin B_1)	Carl Roth GmbH & Co KG, Karlsruhe, Germany
Tris Pufferan®	Carl Roth GmbH & Co KG, Karlsruhe, Germany
tri-Sodium citrate-dihydrate	Carl Roth GmbH & Co KG, Karlsruhe, Germany
Trypticase Soy Broth	Oxoid Ltd., Hampshire, England
Tween® 20	Sigma-Aldrich Chemie GmbH, Steinheim, Germany
Vitamin B_{12}	Carl Roth GmbH & Co KG, Karlsruhe, Germany
Xylene cyanole FF	Sigma-Aldrich Chemie GmbH, Steinheim, Germany
Yeast Extract	Oxoid Ltd., Hampshire, England
Zinc sulphate heptahydrate ($ZnSO_4$*7 H_2O)	Carl Roth GmbH & Co KG, Karlsruhe, Germany
α-D(+)-Glucose monohydrate	Carl Roth GmbH & Co KG, Karlsruhe, Germany
α-Lipoic acid	Sigma-Aldrich Chemie GmbH, Steinheim, Germany
Enzymes	**Manufacturer**
Lysozyme	Sigma-Aldrich Chemie GmbH, Steinheim, Germany
Ribonuclease A	Carl Roth GmbH & Co KG, Karlsruhe, Germany
*Vsp*I restriction enzyme + buffer O	Fermentas Inc., Hanover, MD, USA

2.5 Kits and ready-to-use solutions

Table 8. Kits and ready-to-use solutions used

Kit/Solution	Manufacturer
DNeasy blood & tissue kit	Qiagen Vertriebs GmbH, Vienna, Austria
Gene Ruler™ 1kb DNA ladder	Fermentas Inc., Hanover, MD, USA
GeneRuler™ 100 bp DANN ladder	Fermentas Inc., Hanover, MD, USA
QIAquick PCR purification kit	Qiagen Vertriebs GmbH, Vienna, Austria

Table 8 (continued)

VECTASHIELD® HardSet™ Mounting Medium with DAPI	Vector Laboratories Ltd., Burlingame, CA, USA

2.6 Primers, probes and antibodies

Table 9. Primers, oligonucleotide probes and antibodies used

Name	Manufacturer	Sequence (5'-3')[1]	Target molecule[2]	Specificity	Comment[3]	Reference[5]
PanR	Thermo Fisher Scientific GmbH, Ulm, Germany	GTCATCRGCCYYACCTTVSRCRYYTCT	16S rRNA gene	*Chlamydiales*	Ta: 65°C	Corsaro *et al.*, 2002
PanF		CGTGGATGAGGCATGCRAGTCG				
SigR2		TCAGTCCCARTGTTGGC	16S rRNA gene	*Chlamydiales*	Ta: 61°C	Haider *et al.*, 2008
SigF2		CRGCGTGGATGAGGCAT				
PcR		TTNNGGATTTGCTTCVCC	16S rRNA gene	*Parachlamydiaceae Waddliaceae*	Ta: 58°C	Horn and Wagner, 2001
PcF		TCAGATTGAATGCTGAC				
1492R		GGYTACCTTGTTACGACTT	16S rRNA gene	*Bacteria* (incl. mitochondria) but not *Chlamydiales*	Ta: 52°C	Lane, 1991
27F (616V)		AGAGTTTGATYMTGGC				
Chls-0523	Thermo Fisher Scientific GmbH, Ulm, Germany	CCTCCGTATTACCGCAGC	16S rRNA	*Chlamydiales*	Cy3-labelled	Poppert *et al.*, 2002
E25-454		GGATGTTAGCCAGCTC	16S rRNA	*P. amoebophila* UWE25	Cy3-labelled	Amann *et al.*, 1990
Acanth412a		ACTCTTATCGAGCGCCTG	18S rRNA	*Acanthamoeba* sp.	FLUOS-labelled	In prep.
EUK516		ACCAGACTTGCCCTCC	18S rRNA	Eukarya	FLUOS-labelled	In prep.
EUB338[4]		GCTGCCTCCCGTAGGAGT	16S rRNA	most Bacteria	FLUOS-labelled	Amann *et al.*, 1997
EUB338 II[4]		GCAGCCACCCGTAGGTGT	16S rRNA	*Planctomycetales*	FLUOS-labelled	Daims *et al.*, 1999
EUB338 III[4]		GCTGCCACCCGTAGGTGT	16S rRNA	*Verrucomicrobiales*	FLUOS-labelled	Daims *et al.*, 1999
Anti-hsp60	Oregon State University, Seattle, WA, USA	——	Hsp60 (cytosolic protein)	*Chlamydiales*	Generated in guinea pig	Yuan *et al.*, 1992
Anti-E25	Eurogentec S.A., Seraing, Belgium	——	Outer membrane components	*P. amoebophila* UWE25	Generated in rabbit and chicken	In prep.
Anti-chicken IgG	Dianova GmbH, Hamburg, Germany	——	IgG (H+L)	Chicken	Generated in donkey, Cy3-conjugated	——
Anti-rabbit IgG		——	IgG (H+L)	Rabbit	Generated in goat, FITC-conjugated	——

Table 9 (continued)

Anti-guinea pig IgG	Dianova GmbH, Hamburg, Germany	____	IgG (heavy chains)	Guinea pig	Generated in goat, Cy3-conjugated	____

[1] According to the NC-IUB the unspecified bases are represented as follows: R=G or A, Y=T or C, M=A or C, V=G or C or A, S=G or C, N=G or C or A or T;
[2] IgG: Immunoglobulin G, H+L: heavy and light chain;
[3] Ta: annealing temperature, Cy3: Indocarbocyanin, FITC: Fluorescein isothiocyanate, FLUOS: Fluorescein N-hydroxysuccinimidester;
[4] These probes were used as an equimolar mixture (50 ng/µl of each probe).
[5] In prep.: publication in preparation;

Primer and probe solutions were stored at -20°C until use. Use required temporary storage on ice. Dilution of stock solutions was carried out with $_{dd}H_2O$. Working solutions were prepared in small volumes (< 100 µl). Antibody solutions were kept in small aliquots at -20°C before and at 4°C after first usage in order to minimize damage due to repeated freezing and thawing. The light-sensitive probes and antibodies were kept in the dark during all phases of an experiment.

2.7 Organisms

To provide sterility of the cultures and experiments, and additionally protection of the worker and the environment, all vessels and flasks involving organisms were only opened within a class II safety cabinet. Also, multi-well plates and chambered slides containing organisms were sealed with parafilm before removing them from the safety cabinet. Fluid waste containing organism was disposed according to the biosafety guidelines for L2 laboratories, since both *Acanthamoeba* sp. and *P. amoebophila* are classified as L2 organisms.

Table 10. Organisms used

Host	Endosymbiont	Source	Reference
Acanthmoeba sp. UWC1[1]	Endosymbiont-free	University of Washington, Seattle, USA	Fritsche *et al*., 1998
Acanthmoeba sp. UWC1	*P. amoebophila* UWE25	University of Washington, Seattle, USA	Fritsche *et al*., 1993; Fritsche *et al*., 1998
Acanthamoeba castellanii Neff[2]	Endosymbiont-free	American Type Culture Collection (ATCC), Manassas, VA, USA	Neff, 1957
Acanthamoeba castellanii Neff	*P. amoebophila* UWE25	Our laboratory	In preparation

[1] This strain has been isolated from the cornea of a human patient (Fritsche *et al*., 1998).
2 Whole genome sequencing of this strain (ATCC 30010) is ongoing. It has been isolated from soil (Neff, 1957).

2.8 General media, buffers and solutions

All buffers and general media were sterilized for 20 minutes at 121°C and 1.013 x 10^5 Pa pressure using a watervapour high pressure autoclave, and were stored at room temperature prior to usage if not stated otherwise.

Table 11. General media

TSY	Trypticase Soy Broth	30 g	**PYG**	Peptone	20 g
	Yeast extract	10 g		Glucose	18 g
	$_{dd}H_2O$	ad 1000 ml		Yeast extract	2 g
				Sodium citrate	1 g
	pH 7.3			$MgSO_4$*7 H_2O	980 mg
				Na_2HPO_4*7 H_2O	355 mg
				KH_2PO_4	340 g
				$Fe(NH_4)_2(SO_4)_2$*6 H_2O	20 mg
				$_{dd}H_2O$	ad 1000 ml
				pH 6.5	

Table 12. General buffers and solutions

10x PAS*	NaCl	1.2 g	**PBS**	NaH_2PO_4	35.6 g (200 mM)
(Page's amoebic	$MgSO_4$*7 H_2O	40 mg	**stock solution**	Na_2HPO_4	27.6 g (200 mM)
saline)	$CaCl_2$*2 H_2O	40 mg	(20x)	$_{dd}H_2O$	ad 1000 ml
	Na_2HPO_4	1.42 g			
	KH_2PO_4	1.36 g		The pH of the NaH_2PO_4-solution is adjusted to 7.2-7.4 using the Na_2HPO_4-solution.	
	$_{dd}H_2O$	ad 1000 ml			
1x PBS	NaCl	7.6 g	**SPG**	sucrose	75 g
	PBS stock	50 ml	(sucrose-phosphate-	KH_2PO_4	520 mg
	$_{dd}H_2O$	ad 1000 ml	glutamate buffer)	Na_2HPO_4*2 H_2O	1.53 g
				Glutamic acid	720 mg
	pH 7.2-7.4			$_{dd}H_2O$	ad 1000 ml
				pH 7.2	
				The buffer was stored in 100 ml aliquots.	
10x TBE*	Tris	162 g	**4% PFA**	Formaldehyde 37%	1:9.25 dilution
(electrophoresis)	Boric acid	27.5 g	(fixative)	$_{dd}H_2O$	
	EDTA	9.3 g			
	$_{dd}H_2O$	ad 1000 ml		This solution was stored in aliquots at	

Table 12 (continued)

10x TBE* (continued)	pH 8.3-8.7		**4% PFA (continued)**	-20°C.	
Loading buffer (electrophoresis)	Ficoll	25% (w/v)	**Ethidium bromide solution** (gelelectrophoresis)	10 mg/ml Ethidium bromide solution	1:10000 dilution
	Bromphenol blue	0.5% (w/v)		$_{dd}H_2O$	
	Xylencyanol	0.5% (w/v)			
	EDTA	50mM			
	pH 8.0				
DAPI solution (DNA dye)	1 mg/ml DAPI stock solution	1:10000 or 1:1000 dilution	**Mowiol** (mounting medium)	Mowiol 4-88	2.4 g
	$_{dd}H_2O$			Glycerol	6 g
				$_{dd}H_2O$	6 ml
				0.2 M Tris-HCl, pH 8.5	12 ml
	This solution was stored at 4°C.			Mowiol was mixed with glycerol and $_{dd}H_2O$, Tris-HCl was added, solution was stirred at 50-60°C to dissolve Mowiol and centrifuged at 7700 rcf for 15 minutes at RT to remove air bubbles. Supernatant was stored in small aliquots at -20°C.	

* These buffers were diluted 1:10 using $_{dd}H_2O$ before usage in order to generate 1x concentrated buffers.

2.9 Specific media and solutions

Table 13. Specific media and solutions

DGM-21A defined medium for *Acanthamoeba* sp. (Schuster, 2002)	**Solution 1**: Amino acids and salts, 1x stock		**Comments**
	L-Alanine	0.2 g	Amounts smaller than or equal to 1 mg (*) were added to the respective solutions as follows: A random but small amount was weighed in and dissolved in 1 ml $_{dd}H_2O$. The volume containing the proper amount was calculated and added to the solution.
	L-Asparagine	0.5 g	
	L-Aspartic acid	0.3 g	
	L-Arginine-HCl	1.0 g	
	L-Cysteine	0.2 g	
	L-Cystine	0.1 g	
	L-Glutamic acid	0.5 g	
	L-Glutamine	0.5 g	
	Glycine	1.5 g	
	L-Histidine-HCl	0.2 g	
	L-Isoleucine	0.6 g	
	L-Leucine	0.9 g	
	L-Lysine-HCl	1.0 g	
	L-Methionine	0.3 g	
	DL-Phenylalanine	0.9 g	

Solutions 1-4 were prepared separately, sterilized and combined as follows: 10 ml of the 10x stock solution 2 (vitamins), 100 ml of the 10x stock solution 3 (trace elements) and 90 ml of the 1x solution 4 (other components) were added to the 1x solution 1 (amino acids and salts). Individual solutions and the mixture were stored at 4°C, the mixture was warmed up to room temperature before usage.

Solution 1 and 3 were autoclaved, solutions 2 and 4 were filter sterilized

Table 13 (continued)

DGM-21A defined medium (continued)	L-Proline	0.8 g	using a 0.2 µm filter before usage.
	L-Serine	0.2 g	
	L-Threonine	0.5 g	pH before autoclaving was adjusted to 6.5.
	L-Tryptophan	0.2 g	
	L-Tyrosine	0.2 g	In order to avoid precipitation of solution 3 components, Na_2EDTA was first dissolved in a small volume of $_{dd}H_2O$ followed by the addition of four drops of concentrated H_2SO_4.
	L-Valine	0.7 g	
	$CaCl_2$*2 H_2O	0.0074 g	
	$MgSO_4$*7 H_2O	0.25 g	
	KH_2PO_4	0.27 g	
	NH_4Cl	0.0005 g *	
	NH_4 formate	0.0006 g *	
	$FeSO_4$*7 H_2O	0.009 g	
	$_{dd}H_2O$	ad 800 ml	
	Solution 2: Vitamins, 10x stock		
	Biotin	3 mg	
	Folic acid	2 mg	
	Ascorbic acid	20 mg	
	Riboflavin	10 mg	
	Thiamine-HCl	0.1 mg *	
	Thioctic (lipoic) acid	4 mg	
	Vitamin B12	0.1 mg *	
	$_{dd}H_2O$	ad 100 ml	
	Solution 3: Trace elements, 10x stock		
	$ZnSO_4$*7 H_2O	10 mg	
	$MnCl_2$*4 H_2O	23 mg	
	$(NH_4)Mo_7O_{24}$*4 H_2O	4 mg	
	$CoCl_2$	0.17 mg *	
	$CuSO_4$	0.033 mg *	
	H_3BO_3	1 mg *	
	Na_2EDTA	0.1 mg *	
	$_{dd}H_2O$	ad 1000 ml	
	Solution 4: Other components, 1x stock		
	$NaHCO_3$	0.25 g	
	Glucose	15 g	
	Na acetate	2.5 g	
	$EtOH_{abs.}$	0.5 g/633 µl	
	$_{dd}H_2O$	ad 90 ml	

Table 13 (continued)

PYG modified	Peptone	20 g	pH 6,5
	Glucose	18 g	The absence of $Fe(NH_4)_2(SO_4)_2$*6 H_2O is the only difference from regular PYG (table 11).
	Yeast extract	2 g	
	Sodium citrate	1 g	
	$MgSO_4$*7 H_2O	980 mg	
	Na_2HPO_4*7 H_2O	355 mg	
	KH_2PO_4	340 g	
	$_{dd}H_2O$	ad 1000 ml	
DAM solution (deferoxamine mesylate, iron chelator)	DAM	10 mg	This solution was prepared freshly immediately before each experiment.
	$_{dd}H_2O$ (sterile)	1 ml	
PI solution (propidium iodide, nucleic acid stain)	1 mg/ml PI stock solution	1:1000 dilution	Stock and working solution were protected from light and stored at 4°C. Temperature of PI working solution was adjusted to RT before use.
	1x PBS		
Mg-Ethanol solution	$MgCl_2$	305 mg	
	$EtOH_{abs.}$	25 ml	
	$_{dd}H_2O$	ad 100 ml	
RNase A solution	Ribonuclease A (90 u/mg)	1 mg	
	$_{dd}H_2O$	1 ml	

2.10 Cultivation of amoebae and *P. amoebophila*

Acanthamoeba sp. UWC1 and *Acanthamoeba castellanii* Neff (*A. castellanii* Neff) as well as the respective asynchronously *P. amoebophila*-infected amoebae were routinely cultivated at 20°C in sterile polystyrene 25cm^2 culture flasks and 10 ml TSY medium. For the purpose of isolating large quantities of intra- and extracellular EBs of *P. amoebophila*, symbiont-harboring amoebae were grown at room temperature in sterile polystyrene 500cm^2 culture flasks (Nunc) and 150 ml TSY medium. In order to be able to restrict the iron supply, endosymbiont-free amoebae and asynchronously infected amoebae needed for Fe-depletion experiments were cultivated in either DGM-21A medium for *Acanthamoeba* sp. (see chapter 2.8) or in PYG medium.

Medium exchange was carried out depending on morphological criteria examined by light microscopy as well as need for cells, so that exchange finally took place once or twice a week when cultures were needed for experiments, and only twice a month in periods of rare usage

since amoebic cysts are capable of recovering from starvation. Morphological signs that resulted in medium exchange when cultures were extensively used included large amounts of detached or encysted amoebae as well as large quantities of extracellular bacteria in infected cultures. In order to maintain a well-grown culture, flasks that were densely populated with amoebic trophozoites were subjected to regular shaking off and subsequent medium exchange when not needed. A culture was considered well-grown and therefore ready to use when the flask surface was densely covered with attached amoebal cells (trophozoites) and the proportion of floating cells was low. The medium exchange was simply accomplished by pouring the old medium out into a glass bottle leaving a small volume of medium behind, and in turn pouring in a standardized volume of sterile TSY or PYG medium. Defined medium was transferred using disposable 10 ml plastic pipettes. Fresh medium was either provided in standard-sized glass culture tubes (TSY, PYG) or glass bottles (TSY, DGM-21A).
New or poorly grown cultures were inoculated with respective cells from well-grown cultures. For this purpose cultures were shaken vigorously and 1-2 ml of suspensions were transferred to target culture flasks by disposable single-use pipettes.

2.11 Harvest and quantification of amoebal cells

Culture flasks were shaken vigorously in order to displace amoebae from the surface and suspensions were poured out into 50 ml plastic tubes leaving just a small volume of liquid in the flask, and then centrifuged at 3900 rcf for 6 minutes. Supernatants were discarded, pellets resuspended in 1 ml 1x PAS and pooled. Another centrifugation step (3900 rcf, 6 minutes) was again followed by resuspension of cells in 1 ml 1x PAS. Depending on the number of amoebae needed for an experiment, the number of culture flasks to be harvested was estimated. One small well-grown culture yielded about 1.5×10^6 cells whereas one large well-grown culture allowed for a yield of about 1×10^7 amoebae.
Cell concentrations of harvested amoebae were determined using a Neubauer counting chamber (Paul Marienfeld GmbH). To do so, 10 µl of amoebal suspensions were – depending on the cell density – diluted with either 90 µl or 990 µl 1x PAS. 12 µl of these dilutions were subsequently pipetted into each of the two chambers per slide that were generated by placing a damp cover glass over the counting surface and cells were immediately subjected to counting using an inverse phase contrast microscope (10x objective, no immersion) (Zeiss). Cells that were located within 8 different large squares (16 x 8 small squares) were counted. The concentrations (cells/µl) were calculated as follows: The total number of counted cells multiplied by the dilution

factor (10 or 100) was divided by the counting area (8 mm^2) multiplied by the depth of the chamber (0.1 mm).

2.12 Purification of *P. amoebophila*

Six to twelve large culture flasks containing endosymbiont-harbouring amoebae were harvested as described before, so that eventually all cells were pooled in one 50 ml reaction tube. The volume was adjusted to 10 ml using 1x PAS. As a first step to break up amoebae, two successive freeze/thaw steps (-20°C/45°C) were performed. To further lyse the host cells, 5 ml sterile glass beads (Roth) were added to the cells, the suspension was vortexed for 3 minutes and amoebal cell debris was pelleted by centrifugation at 300 rcf for 10 minutes at 4°C. The supernatant was then transferred to a sterile ultracentrifuge tube, the five remaining tubes were balanced with $_{dd}H_2O$ to 0.0 g difference from the the supernatant-containing tube, tubes were placed in $ethanol_{70\%}$-sterilized tube holders which were mounted on the SW 41 Ti rotor. *P. amoebophila* was pelleted by ultracentrifugation at 17000 rpm for 40 minutes and 4°C. The supernatant was removed and the pellet was resuspended in 3 ml precooled SPG buffer followed by another ultracentrifugation step carried out as described above. The pellet was again resuspended in 3 ml precooled SPG buffer. In order to break up clusters of bacteria the suspension was passaged through a single-use 0.45 mm needle (B. Braun Melsungen AG) several times. Finally, the *P. amoebophila* suspension was filled up with SPG buffer to a total volume of 7 ml, mixed and split up into 1 ml aliquots. Before storage at -80°C, 10 µl and 1 µl samples per aliquot were taken to test for contamination and to quantify the purified endosymbionts, respectively. Also, 0.5 ml of one of the aliquots was taken in order to isolate DNA. Purifications were expected to contain mostly elementary bodies (EBs) of *P. amoebophila*, since the reticulate bodies (RBs) are considered unstable in an extracellular environment.

2.13 Testing for contamination of cultures and purifications

Three different approaches were regularly used to test for contaminants of pure amoebal cultures as well as cultures containing *P. amoebophila*-infected amoebae and purified endosymbionts, and to control for proper identity of symbionts. First, purified bacteria were transferred to medium in order to promote growth of free-living contaminants. Second, cultures and purifications of symbionts were screened by detection and identification of 16S rRNA genes, thereby making DNA extraction, PCR using 16S rDNA-specific primers, and finally identification of PCR-products by either RFLP or sequencing necessary. Third, detection of

organisms by fluorescent staining using DAPI or specific oligonucleotide probes (fluorescence *in situ* hybridization or FISH, see chapter 2.19) was performed.

2.13.1 Transfer of purified *P. amoebophila* to medium

Multiwell dishes containing PYG medium were inoculated with 10 µl of each aliquot that resulted from the purification procedure. After incubation for one week at room temperature wells were visually controlled for growth of organisms, which would indicate contaminanation since *P. amoebophila* is an obligate intracellular organism.

2.13.2 Isolation of total DNA

The extraction of DNA was carried out using the DNeasy Blood & Tissue Kit which relies on selective binding of DNA to a membrane while contaminants are removed by centrifugation. All reagents needed except for $EtOH_{abs.}$ were supplied by the manufacturer. $EtOH_{abs.}$ was added to buffers AW1 and AW2 as indicated on the bottles.
As a first step, 10 ml of a well-grown culture were harvested (centrifugation: 7300 rcf for 10 minutes) or 0.5 ml of purified EBs were centrifuged at full speed (20800 rcf) for 15 minutes. After washing the cells once, the pellet was resuspended in 180 µl lysis buffer (buffer ATL) before the addition of 20 µl proteinase K and incubation at 56°C for 2 hours using a thermomixer. Subsequently, samples were vortexed for 15 seconds, 200 µl buffer AL was added, the mixture was vortexed and incubated at 70°C for 10 minutes. After the incubation step 200 µl $EtOH_{abs.}$ were added and the samples were mixed again. This mixture was transferred to a supplied spin column, placed in a 2 ml collection tube and centrifuged at 6950 rcf for 1 minute. The flow-through was discarded, the spin column was placed in a new collection tube and 500 µl of the first washing buffer (buffer AW1) was added. The second washing step using 500 µl buffer AW2 was performed after repeated centrifugation at 6950 rcf for 1 minute and removal of the flow-through. This time washing was followed by centrifuagtion at full speed for 3 minutes in order to dry the membrane. Finally, the spin column was placed in a 1.5 ml reaction tube. DNA was eluted by adding 50-100 µl $_{dd}H_2O$ directly onto the center of the membrane and centrifugation at 6950 rcf for 1 minute.
The DNA dissolved in $_{dd}H_2O$ was ready for spectrophotometrical determination of the DNA concentration using the Nano Drop® device (see 2.10.3), as well as for the subsequent use as a PCR template.

2.13.3 Polymerase-chain-reaction (PCR)

To select specifically for chlamydial DNA, chlamydial 16S rRNA genes were targeted by either PanF/R or PcF/R primer pairs. Bacterial contaminants other than *Chlamydiae* were targeted by the universal bacterial primer pair 27F/1492R. In either case DNA isolated from endosymbiont-harbouring amoebae, endosymbiont-free cultures as well as from purified EBs was tested.
Depending on the concentration of isolated DNA, 1 or 2 µl of template DNA per reaction was utilized, thereby ensuring about 100 ng of template DNA per reaction. As a negative control, template DNA was substituted by $Aqua_{bidest.}$, positive controls were either *P. amoebophila* and *Parachlamydia* sp. DNA (kindly provided by Eva Heinz) when screening for chlamydial presence, or α-proteobacterial DNA (kindly provided by Barbara Sixt) when searching for general bacterial DNA. Further PCR reaction components and concentrations are listed in table 14. The PCR program was as follows: 35 cycles with 30 s of 94°C denaturation, 30 s primer annealing (temperature depends on primer pair used, see Table 9) and 90 s of 72°C elongation. Initial denaturation was done at 94°C for 3 minutes, final elongation at 72°C for 10 minutes.
PCR product quality and size was controlled by gelelectrophoresis prior to purification. Fragment sizes expected were approximately 1260 bp for amplification with PcF/R, 1445 bp for PanF/R and 1480 bp for 27F/1492R.

Table 14. Components and concentrations used for PCR

Components	Manufacturer	Final concentration	Volume/50 µl reaction (µl)
$MgCl_2$ (25 mM)	Fermentas Inc., Hanover, MD, USA	2 mM	4
10 x Taq buffer (with KCl)	Fermentas Inc., Hanover, MD, USA	1 x	5
dNTP mix (2 mM each)	Fermentas Inc., Hanover, MD, USA	0,2 mM of each	5
Taq DNA polymerase (5 u/µl)	Fermentas Inc., Hanover, MD, USA	1 u/50 µl	0.2
Forward primer (50 pmol/µl)	Thermo Fisher Scientific GmbH, Ulm, Germany	25 pmol/50 µl	0.5
Reverse primer (50 pmol/µl)	Thermo Fisher Scientific GmbH, Ulm, Germany	25 pmol/50 µl	0.5
$Aqua_{bidest.}$	Mayrhofer Pharmazeutika GmbH & Co KG, Leonding, Austria	____	32.8-33.8
DNA template/positive controls		~100 ng/50 µl	1-2

All steps except for the addition of positive controls were carried out in a UV sterilizing PCR hood to prevent contamination of PCR reactions. For the same reason, PCR reaction tubes, $Aqua_{bidest.}$, $MgCl_2$ solution, the Taq buffer and the reaction tube used to prepare the PCR mastermix were exposed to UV light before use.

2.13.4 Purification of PCR products and determination of DNA concentration

PCR products were purified in order to remove reaction mix components that could disrupt subsequent DNA measurement and sequencing. Purification was conducted by using the QIAquick PCR purification Kit (Qiagen) and precisely following the manufacturer's instructions. Briefly, the whole volume of the PCR sample was mixed with five volumes of buffer PBI, the mixture was applied to a spin column placed in a 2 ml collection tube and centrifuged for 1 minute at maximum speed (20800 rcf) in order to bind the DNA to the membrane. Flow-through was discarded, and washing took place by adding 750 µl $EtOH_{abs.}$-containing buffer PE and subsequent centrifugation for 1 minute at maximum speed. The centrifugation step was repeated after removal of flow-through. Elution of DNA was carried out by placing the spin column into a clean reaction tube, adding 30 µl $_{dd}H_2O$ to the center of the membrane and centrifugation for 1 minute at maximum speed.

Concentrations (ng/µl) and purity (A260/A280) of DNA were determined using the NanoDrop® device, which allows measurements of very small volumes (0.5-2 µl) and highly concentrated samples (up to 3700 ng/µl dsDNA). For each measurement 1.5 µl blank sample followed by 1.5 µl DNA sample was loaded onto the end of a fiber optic cable, a second fiber optic cable was then brought into contact with the liquid sample and the sample was spectrophotometrically analysed based on Beer's law. Data were provided by the NanoDrop software.

2.13.5 *Vsp*I digestion

As an alternative to sequencing, chlamydial 16S rRNA genes amplified by PCR were assigned to either *P. amoebophila* or *Parachlamydia* sp. via restriction fragment length polymorphism (RFLP) using the restriction enzyme *Vsp*I (Fermentas). *Vsp*I recognizes the palindromic sequence 5'-ATTAAT-3' which is present twice in the 16S rRNA gene of *Parachlamydia* sp. and just once in *P. amoebophila*.
The digestion reaction was performed as follows: 5 µl non-purified chlamydial PCR product generated by using either PanF/R or PcF/R primer pairs were mixed with 3.8 µl $_{dd}H_2O$, 1 µl 10x buffer O (Fermentas) and 0.2 µl (2 u) *Vsp*I enzyme. The mixture was incubated for 3 hours in a 37°C room. The reaction was stopped by adding 5 µl loading buffer.

2.13.6 Gel electrophoresis

To check for success of PCR and *Vsp*I digestion, 5 µl per 50 µl PCR reaction or 10 µl of *Vsp*I-digestion reaction was mixed with 5 µl loading buffer. PCR products and 5µl Gene Ruler™ 1kb DNA ladder (Fermentas) were loaded on 1% agarose gels (1 g agarose, 100 ml 1x TBE buffer)

and ran at 125 V for 1 hour. *Vsp*I-generated fragments were separated using 2.5% agarose gels (2,5 g agarose, 100 ml 1x TBE buffer) and 5 µl of GeneRuler™ 100 bp DNA ladder, since fragments smaller than 1000 bp were expected. These gels ran at 80 V for 90 minutes. To stain DNA bands gels were incubated in an ethidium bromide bath (100 µl ethidium bromide stock solution in 1 l $_{dd}H_2O$) for about 30 minutes, visualization of bands was done by UV transillumination.

2.13.7 Sequencing of PCR products

Sequencing was performed by our technician Christian Baranyi using the ABI 3130*xl* DNA sequencer and the BigDye Terminator Cycle Sequencing Kit v3.1 (Applied Biosystems) thereby allowing for highly automated fluorescent-based cycle sequencing reactions based on Sanger's chain-termination dideoxynucleotide method for sequencing and PCR. Briefly, labeled ddNTPs, each of the four bases linked to a different fluorescent dye, are recognized by a laser after electrophoretic separation of the differently terminated DNA fragments. 16 capillaries allow for 16 separations at a time, since one template requires only one sequencing reaction.
Small amounts of purified DNA template (5-20 ng PCR product/reaction) and the primer SigF2 to sequence chlamydial PCR products or 27F/1492R for bacterial and mitochondrial products (Thermo Fisher Scientific GmbH) were used to sequence at least about 800 nucleotides in one direction. Output files are chromatograms of DNA sequences in which colored peaks represent one of four bases. Sequences were manually proof-read using the FinchTV software (Geospiza). Ambiguous sequence positions were resolved where possible and start and end sequences were removed due to poor sequence quality. Ultimately, edited sequences were subjected to a BLAST search using the general nucleotide collection database and default settings to find the most similar sequence.

2.13.8 DAPI staining

Pure amoebae cultures as well as endosymbiont-harbouring amoebae cultures were shaken vigorously, 1-2 ml cell suspension were transferred to reaction tubes using disposable plastic pipettes and centrifuged at 3900 rcf for 6 minutes. After washing with 1x PAS and repeated centrifugation, the pellet was resuspended in 50-200 µl 1x PAS, the volume depending on the size of the pellet. 20 µl of the suspension were incubated on 10-well microscope slides (Paul Marienfeld GmbH) for 30 minutes to allow attachment of amoebae, residual fluid was removed, cells were fixed by incubation with 20 µl of 4% paraformaldehyde (PFA) for 10 minutes and subsequently washed once with $_{dd}H_2O$ and dried at room temperature. Fixed cells on slides were

either stored at -20°C or immediately subjected to DAPI staining. To do so, 15 µl of DAPI working solution was placed on the fixed cells, incubated for 4 minutes in the dark, washed once with $_{dd}H_2O$ and finally dried at room temperature. Subsequent inspection of the cells by epifluorescence microscopy (100x objective, oil immersion) was aimed at general detection of any intra- and extracellular biological contaminants, since DAPI is a fluorescent dye that binds to the DNA of all organisms.

2.14 Quantification of purified and extracted *P. amoebophila* cells

P. amoebophila suspensions were quantified by filtration of particles (> 0.22 µm diameter) onto a membrane. This approach ensured accurate counting of cells since they are evenly distributed over the membrane.

1 µl of purified *P. amoebophila* or aliquots (10-70 µl) of thawed lysates and supernatants (see chapter 2.16) were diluted with 5 ml 1x PBS that had been filter-sterilized using a 0.2 µm filter fixed to a disposable 50 ml syringe. Subsequently, suspensions were stored on ice until use. The glass funnel of the filter device was rinsed with $EtOH_{abs}$ and flame-sterilized. The filter device was assembled using a black 0.22 µm polycarbonate membrane filter (Millipore) and a 0.45 µm cellulose acetate membrane support (Sartorius) underneath the filter. To first rinse the funnel, 5 ml filter-sterilized 1x PBS were filtered by applying a vacuum pump (Millipore) running at 250 mmHg (millimeter of mercury). The same pressure was used throughout the experiment. The bacterial suspension was filtered next, followed by another rinsing step to wash away bacteria that were possibly attached to the glass walls of the funnel. Subsequently, the vacuum pump was switched off so that the membrane could be incubated with 200 µl of a 1:1000 DAPI solution for 5 minutes in the dark. The DAPI solution was removed by applying the vacuum pump and repeated rinsing with 5 ml 1x PBS. Therefore, each sample to be quantified needed about 20 ml filter-sterilized 1x PBS in total.

The membrane was transferred to a microscope slide (Roth), a drop of the anti-bleaching mounting medium Citifluor (Agar Scientific Ltd.) was applied to the center of the membrane and a cover glass (24 x 50 mm) was added. Embedded membranes were either stored for a few hours at 4°C in the dark or immediately subjected to epifluorescence microscopy.

DAPI signals either within the 10 x 10 grid (purified bacteria) or the entire visual field (lysates and supernatants) were counted using the 100x objective (oil immersion). Depending on the density of stained cells on the membrane, signals within 10-20 fields were counted per quantification. Only clearly coccoid DAPI signals were considered to be *P. amoebophila* cells. Concentration of cells was calculated as follows:

$$\text{cells/ml} = \frac{\text{number of counted cells}}{\text{number of fields}} \times M \times DF$$

$$M_1 \text{ (microscope factor 1)} = \frac{\text{membrane area exposed to filtration } (\varnothing = 15 \text{ mm})}{\text{grid area } (\varnothing = 12.5 \text{ mm}/100)} = \frac{\pi \times r^2}{a^2}$$

$$= \frac{\pi \times 7.5\ (\text{mm})^2}{0.125\ (\text{mm})^2} = \frac{176\ \text{mm}^2}{0.015625\ \text{mm}^2} = 11264$$

$$M_2 \text{ (microscope factor 2)} = \frac{\text{membrane area exposed to filtration } (\varnothing = 15 \text{ mm})}{\text{area of visual field } (\varnothing = 25 \text{ mm}/100)} = \frac{\pi \times r^2}{\pi \times r^2}$$

$$= \frac{\pi \times 7.5\ (\text{mm})^2}{\pi \times 0.25\ (\text{mm})^2} = \frac{176\ \text{mm}^2}{0.049087\ \text{mm}^2} = 3585.4$$

DF = dilution factor for 1 ml (e.g. 100 if 10 µl suspension are quantified)

Microscope factor 1 (M_1) was used when counting DAPI signals within the ocular grid; whereas microscope factor 2 (M_2) was used when expanding the counting area to the entire visual field because of low density of DAPI signals.

2.15 Infection of *Acanthamoeba sp*. with *P. amoebophila* to visualize the cycle

A. castellanii Neff or *Acanthamoeba* sp. UWC1 cells were harvested and quantified, and 10^5 cells were seeded in 2 ml TSY in 6-well plates (Nunc). One well per time point of interest and technical replicate was inoculated. After one to two hours of amoebal attachment to the well surface at room temperature. *P. amoebophila* EBs were thawed at 37°C in a water bath, put on ice, and added at a theoretical multiplicity of infection (MOI) of 10, namely 10^6 EBs. When necessary, EBs were diluted in SPG buffer prior to usage. The plate was carefully shaken by hand in order to equally distribute the inoculum. To stimulate the uptake of EBs, plates were centrifuged at 130 rcf for 15 minutes at 20°C. Immediately after centrifugation the media was exchanged to remove bacteria that had not been taken up by amoebae. Subsequently, time point 0 hours post infection (hpi) was harvested by resuspension, the suspension was transferred to a 2 ml reaction tube, centrifuged (3900 rcf, 10 minutes, 20°C), washed once with 1x Page's amoebic saline (PAS) and resuspended in 50-100 µl 1x PAS. 20 µl aliquots of amoebic suspensions were incubated on 10-well microscope slides (Paul Marienfeld GmbH) for 30 minutes, cells were fixed with 20 µl 4% paraformaldehyde (PFA) for 10 min at room temperature (RT), washed once with $_{dd}$H2O and slides were stored at -20°C. Later time points were harvested 6, 12, 24, 48, 72, 96, 120, 144, 168, 192 hpi and treated as described above for the 0 hpi time point. The uninfected control was harvested at the last time point post infection and also processed as

described above. Each infection experiment was carried out in technical duplicates. Biological duplicates were performed for time points 0-96 hpi with both amoebal strains, 120 hpi was performed once with *A. castellanii* Neff and twice with *Acanthamoeba* sp. UWC1 as a host, and later time points were just conducted once with each organism. Fixed samples were subjected to analysis by FISH.

2.16 Infectivity assay

2.16.1 Primary infection

A. castellanii Neff was infected with purified *P. amoebophila* EBs as described in chapter 2.15. Also, an uninfected control was carried along. However, the number of amoebae to be infected as well as the number of infecting bacteria was doubled in order to be able to split the cells into two identical parts during harvest of cells at different time points post infection (0, 24, 48, 72, 96, 120 and 168/216 hpi). The two parts per time point (1 ml each) were treated identically throughout the following procedure to ensure equal numbers of bacteria for the two different but connected final experiments, namely the quantification of total intra- and extracellular bacteria throughout the initial infection cycle and the quantification of the infectious proportion based on the total bacterial numbers that had been determined before (Fig. 3).

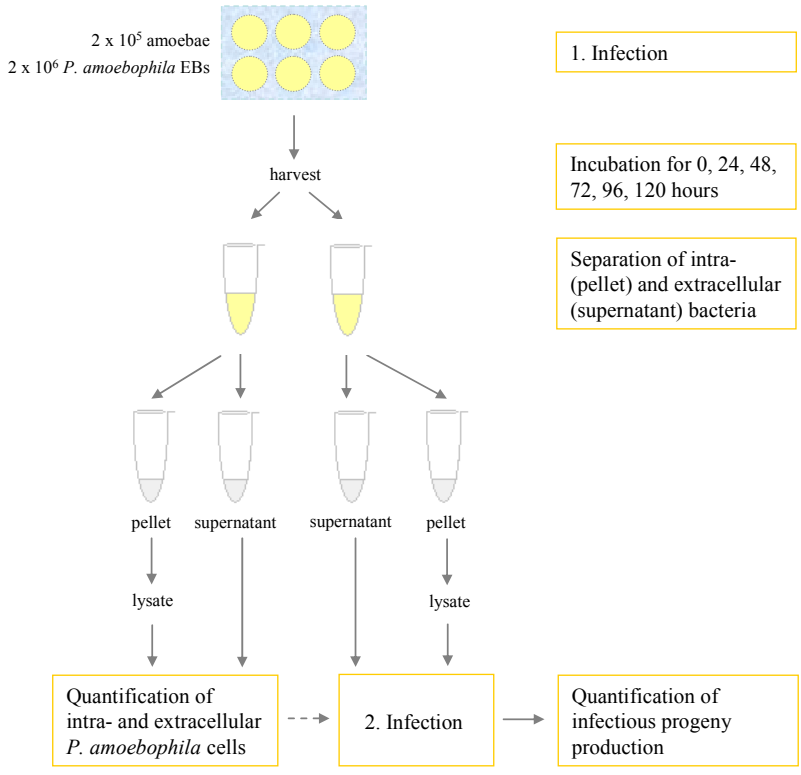

Figure 3. Schematic illustration of the approach to quantify intra- and extracellular infectious forms of *P. amoebophila* over 5 days of a synchronized infection.

The entire infectivity experiment was conducted in one biological duplicate and one technical duplicate of the first biological replicate for time points 0-120 hpi, so that three sets of data for each time point post infection and fraction (inta-, extracellular) were available for evaluation.

2.16.2 Collection of intra- and extracellular bacteria

After harvest and splitting of cells at the different time points post infection, bacteria that were located within host cells were separated from extracellular bacteria due to different behaviour during low-speed centrifugation. The centrifugal force was chosen based on the established protocol for purification of *P. amoebophila* (chapter 2.12) – specifically the removal of amoebal debris after break up of host cells. Consequently, the required separation was carried out by centrifugation at 300 rcf for 10 minutes at 4°C, thereby expecting only (infected) amoebae to be pelleted and the extracellular bacteria to be in the supernatant.

The amoebal pellet and the pellet that was generated by centrifugation of the supernatant to collect extracellular bacteria (20800 rcf, 30 minutes, 4°C) were resuspended in 100 µl of precooled SPG buffer in order to stabilize all forms of chlamydiae and stored at -20°C and -80°C, respectively. The protocol proceeded when all time points and the uninfected control had been collected and processed.

Amoebal pellets at -20°C were thawed at RT and frozen and thawed a second time, about 50 µl sterile glass beads were added, suspensions were vortexed for 3 minutes and host cells debris was pelleted by centrifugation at 300 rcf for 10 minutes at 4°C. To further break up host cells, supernatants were subjected to several passages through a single-use 0.45 mm needle (B. Braun Melsungen AG) and broken amoebae were again pelleted by centrifugation at 300 rcf for 10 minutes at 4°C. The supernatant representing the purified amoebal lysate containing intracellular forms of *P. amoebophila* at respective time points post infection was transferred to a new reaction tube and at stored at -80°C.

Stored lysates (about 70 µl) and stored collected supernatants (100 µl), each being present twice per time point, were subjected to quantification of bacteria by filtration (chapter 2.14) and a second round of infection in order to determine infectivity (next chapter). Samples that had not been used for quantification, namely late time points and the uninfected control, were controlled for proper identity of bacteria by FISH using the genus-specific probe E25-454.

2.16.3 Secondary infection

A. castellanii Neff were harvested, quantified and 5 x 10^3 cells were seeded in 150 µl PYG medium per well of a Lab-Tek™ 16-well chamber slide system (Nunc). Also, asynchronously

infected amoebae were harvested and seeded in one well, serving as a positive control for immunofluorescence. One well per primary-infection-time point was inoculated. During one to two hours of amoebal attachment to the well surface, quantified *P. amoebophila* cells that had been collected from intra- and extracellular fractions were thawed at 37°C in a water bath and subsequently pelleted by centrifugation at 20800 rcf for 30 minutes and 4°C. All supernatant but a small volume of about 10 µl was aspirated, in which the pellet was resuspended. These suspensions were added to the attached amoebae and the plate was carefully shaken by hand in order to equally distribute the inoculum. Therefore, a definite number of amoebae was exposed to different numbers of chlamydiae resulting in different amoebae-to-chlamydiae ratios. Uninfected amoebae served as a negative control for immunofluorescence. To stimulate the uptake of infectious forms (EBs), plates were centrifuged at 130 rcf for 15 minutes at 20°C, as described before. Immediately after centrifugation, media were exchanged to remove bacteria that had not been taken up by amoebae. After incubation for 12 hours, the infection cycle was stopped by methanol fixation. Subsequent immunofluorescence (chapter 2.20) allowed for counting of numbers of amoebae as well as numbers of specific intracellular *P. amoebophila* signals per visual field as accomplished by epifluorescence microscopy (100x objective, oil immersion). Between 10 and 20 fields were subjected to counting per replicate, fraction (intra-, extracellular) and time point post infection. One intracellular bacterial signal was assumed to represent a single infectious particle since binary fission of *P. amoebophila* in *Acanthamoeba* sp. was found to be detectable at 24 hpi but not at 12 hpi (see results).

2.17 Preparation of iron-deprived growth conditions for *P. amoebophila*

The introduction of environmental stress by severe reduction of iron availability for chlamydial endosymbionts was aimed at inducing *P. amoebophila* to transform into morphologically aberrant forms that could be a first hint for persistance of *Chlamydia*-like bacteria. Iron deprivation experiments involved identification of appropriate deprivation conditions including culture medium tests and host cell viability experiments when adding the iron (III) chelator deferoxamine mesylate (DAM). DAM was always added when iron depletion experiments were performed, since it is reported to be cell-permeable and therefore manipulates the host's intracellular iron levels (Jacobs, 1977).

2.17.1 Development of a host viability assay using propidium iodide (PI)

The assessment of host cell viability, which is enabled by differentiation between dead and living amoebae, was used as a tool to examine the optimal DAM concentration to generate possible

iron deprivation effects on *P. amoebophila*. Viability tests were conducted using the fluorescent nucleic acid stain propidium iodide (PI), since it is excluded by viable cells and conversely penetrates cells whose membrane integrity is disrupted, and therefore considered dead. Fluorescence was monitored by exitation at 485 nm and emission at 580 nm.

2.17.1.1 Approach 1: Fixation-based propidium iodide (PI) staining on coverslips

Glass coverslips (12 mm, Roth) stored in $EtOH_{abs.}$ were flame-sterilized and placed in wells of a 24-well dish. Medium was added to the wells, uninfected *A. castellanii* Neff cells were harvested and quantified as described before and 1 x 10^5 amoebae were seeded. After attachement of cells, the medium was aspirated and cells were rinsed with 1 ml 1 x PBS. In order to fix cells either 1 ml methanol or 1 ml Mg-Ethanol solution plus 100 µl RNase A solution (see chapter 2.9 and "Staining apoptotic cells with propidium iodide" online protocol from www.scientistsolutions.com) were added to the cells. The methanol was removed after 10 minutes of incubation at RT, the Mg-Ethanol/RNase A solution was aspirated after one hour of incubation at 37°C. In either case fixation was followed by addition of 1 ml 1x PBS in order to equilibrate the samples, replacement by 300 µl of a 1.5 µM PI solution in 1x PBS (1:1000 dilution of stock solution) and incubation in the dark for either 2 minutes at RT (methanol fixation) or 1 hour at 37°C (Mg-Ethanol/RNase A fixation). After incubation, cells were rinsed with 1x PBS three times, the buffer was completely removed from the wells, coverslips were displaced from the wells and inversely placed on a 1.5 µl drop of Mowiol mounting medium (chapter 2.8) which had been applied to a microscope slide (Roth). PI-stained samples were ready for evaluation by epifluorescence microscopy after hardening of Mowiol for 30 minutes at RT (40x objective, oil immersion).

2.17.1.2 Approach 2: Propidium iodide (PI) staining on coverslips without fixation

Uninfected *A. castellanii* Neff cells were harvested and transferred to coverslip-containing 24-well dishes as described for approach 1 in chapter 2.17.1.1. After attachement of cells, the medium was aspirated, cells were rinsed with 1 ml 1 x PBS and 300 µl of a 1.5 µM PI solution in 1x PBS (1:1000 dilution of stock solution) were added per well. The cells were exposed to PI in the dark at RT for 30 and 50 minutes respectively. Finally, the coverslips were displaced from the wells and inversely placed on microscope slides (Roth). Cells were mounted with PBS buffer and immediately subjected to inspection by epifluorescence microscopy (40x objective, oil immersion). Alternatively, coverslips were sealed with nailpolish, mounted with a drop of Citifluor (Agar Scientific Ltd.) or Vectashield® mounting medium with DAPI (Vector

Laboratories Ltd.), or mounted with additional 1x PBS (2 µl), 3 µl precooled SPG buffer, or 3 µl precooled SPG buffer containing twice the amount of sucrose (150 g/l). Cells mounted in SPG buffer were also microscopically inspected after storage of mounted cells at 4°C for 1 hour.

2.17.1.3 Approach 3: Propidium iodide (PI) staining in Lab-Tek™ Chambered Coverglass

Uninfected *A. castellanii* Neff cells were harvested, quantified and 1 x 10^4 cells were seeded in 8-well Lab-Tek™ Chambered Coverglass (Nunc) containing 300 µl medium per well. After attachment of amoebae cells were rinsed once with 1x PBS and 150 µl of a 1.5 µM PI solution in 1x PBS (1:1000 dilution of stock solution) were added per well. The cells were exposed to PI in the dark at RT for 50 minutes and subsequently inspected by inverse fluorescence microscopy using a confocal laser scanning microscope (CLSM, Zeiss). Due to a coverglass thickness of just 0.13-0.16 mm in combination with a proper microscopic objective (40x, water immersion), direct microscope viewing of cells in the chambered coverglass system was possible.

2.17.2 Search for a proper medium

The proper medium for iron deprivation experiments should support growth of both uninfected and *P. amoebophila*-infected amoebae. Also, a host cell response to iron restriction by DAM, namely reduced viability, should be producible.

2.17.2.1 Cultivation in DGM-21A defined medium

Cultivation in defined medium was aimed at eventually controlling the iron content by reducing or omitting the iron compound ($FeSO_4*7H_2O$, 32 µM) in order to generate a detectable effect on the endosymbionts. Prior to iron deprivation experiments however, amoebae had to be maintained in defined medium.

The four different solutions that make up the defined medium were mixed as described in chapter 2.9, adjusted to RT and transferred to small culture flasks (8 ml per flask). Endosymbiont-free *Acanthamoeba* sp. UWC1 and *A. castellanii* Neff as well as respective *P. amoebophila*-infected amoebae in PYG or TSY were harvested as described before and about 1 x 10^5 cells were used to inoculate the defined medium-containing small flasks. After one week of incubation at 20°C amoebae in defined medium were shaken and aliquots of about 1 ml were transferred to new culture flasks containing defined medium aimed at increasing the number of available amoebae in defined medium. Subsequently cultures were repeatedly subjected to routine treatments such as medium exchange (feeding) and harvest for different screening

approaches (DNA isolation and PCR, DAPI staining). Also, amoebal growth and health status were regularly inspected by inverse phase contrast microscopy (10x objective, no immersion).

2.17.2.2 Testing of and cultivation in PYG-based medium

Since components of PYG are more defined compared to TSY, iron deprivation by addition of DAM was tested in regular PYG and PYG without $Fe(NH_4)_2(SO_4)_2*6\ H_2O$ (modified PYG) and assessed by visual inspection and PI-measured host cell viability.

Endosymbiont-free *Acanthamoeba* sp. UWC1 and *A. castellanii* Neff as well as respective *P. amoebophila*-infected amoebae in PYG were harvested and quantified. 700 µl of regular PYG or modified PYG were added to 4-well Lab-Tek™ Chambered Coverglass (two wells per medium and organism) and 5 x 10^4 amoebae per well were seeded. After attachment of amoebae, cells in regular PYG and modified PYG were exposed to either 0 µM or 1000 µM DAM, which was assumed to be a rather high dose according to the literature. DAM addition was followed by sealing of the chamber system using parafilm and incubation for 4 days at 20°C. The effect on host cell viability for non-exposed and DAM-exposed organisms was evaluated by PI staining as described in chapter 2.17.1.3. However, due to the larger volume capacity of 4-well Lab-Tek™ Chambered Coverglass (Nunc) cells were incubated in 300 µl instead of 150 µl PI solution. Viability was visually assessed by inverse phase contrast microscopy (10x objective, no immersion) and quantified by counting of total number of amoebae and PI-stained amoebae per 10x10 ocular grid using an inverse fluorescence microscope (CLSM, 40x objective, water immersion). Numbers of amoebae in ten randomly chosen fields per condition were documented. This test was performed twice although quantified only once.

Additionally, endosymbiont-free *A. castellanii* Neff and respective *P. amoebophila*-infected amoebae were transferred to small culture flasks containing modified PYG. These cultures were incubated at 20°C for 3 months during which they were routinely subjected to medium exchange, shaking and microscopic inspection.

2.17.3 Determination of the optimal concentration of deferoxamine mesylate (DAM)

Since DAM was primarily used to deprive endosymbionts of iron, the highest DAM concentration that did not impair viability of uninfected hosts but at the same time adversely affects viability of infected amoebae was a matter of investigation.

Therefore, endosymbiont-free *A. castellanii* Neff and respective *P. amoebophila*-infected amoebae that had been grown in PYG medium were harvested and quantified. 1 x 10^4 cells per well were added to 8-well Lab-Tek™ Chambered Coverglass (Nunc), each well containing 300

µl modified PYG. After attachment of amoebae, cells were exposed to 0, 25, 50, 100, 180, 250, 500 and 1000 µM DAM by adding and carefully distributing respective volumes of a freshly prepared DAM solution (10 mg/ml ddH_2O). These concentrations were tested and identified in several experiments that were based on each other, so that eventually only a core set of DAM concentrations – 0, 100, 180, 250, 500 µM DAM – was tested more exensively for each organism.

Also, viability of synchronously infected amoebae at 0, 25, 50, 100, 180, 250 µM DAM was tested, the core set being only 0 µM and 250 µM DAM. Infection was carried out immediately after DAM addition and was basically conducted as described in chapter 2.15. In difference to the procedure described above the medium was not exchanged after centrifugation and MOI 20 (in accordance with the effect-visualization experiment described in the next chapter) was used.

Chambers were sealed with parafilm and incubated for 5 days at 20°C. Finally, host cell viability after 5 days of iron deprivation by various concentrations of DAM was evaluated by PI staining as described in chapter 2.17.1.3 and subsequent quantification of the total number of amoebae and the number of PI-stained amoebae per 10x10 ocular grid using an inverse fluorescence microscope (CLSM, 40x objective, water immersion). Numbers of amoebae in ten randomly chosen fields per condition and organism were documented.

Overall, viability effects of different DAM concentrations on uninfected amoebae were tested most often since respective information about amoebae to be infected was most useful for further experiments. Precisely, the mentioned core set of DAM concentrations was tested in two biological replicates or more. Additionally, each experiment was performed in technical replicates thereby considering 1000-2000 cells in total for 0, 100, 180 and 250 µM DAM, and more than 300 cells for 500 µM DAM. Non-core set DAM concentrations (25, 50, 1000 µM DAM) were just performed once but in technical duplicates.

Viability experiments on asynchronously infected amoebae were conducted on more than 700 cells in total for 0, 100, 180 and 250 µM DAM, and more than 300 cells for 500 and 1000 µM DAM. Each DAM concentration was tested in technical duplicates. Since viability experiments on synchronously infected amoebae were aimed at monitoring viability during the ultimate effect-generating experiments, viability data for the entire range of DAM concentrations are rather poor except for the two key concentrations 0 and 250 µM DAM which were tested in biological duplicates on more than 400 cells in total. DAM concentration in between were just tested once counting more than 100 cells in total.

2.17.4 Iron deprivation to generate an effect on morphology of *P. amoebophila*

Since possible morphological effects were visualized in three different ways, three slightly different procedures of cell handling were exerted. However, each procedure involved harvesting of PYG cultures of endosymbiont-free *A. castellanii* Neff, quantification of amoebae and infection of endosymbiont-free *A. castellanii* Neff. The infection was performed as described before (chapter 2.17.3). Iron deprivation effects on endosymbionts were tried to be generated during synchronized infection in the first place, but were also searched for in asynchronously *P. amoebophila*-infected amoebae.

For initial visualization by DAPI alone 1 x 10^4 uninfected amoebae were seeded in 8-well Lab-Tek™ Chambered Coverglass (Nunc), each well containing 300 µl modified PYG. After attachment of amoebae cells were exposed to 0, 25, 50, 100, 180 and 250 µM DAM by just adding and carefully distributing respective volumes of a freshly prepared DAM solution (10 mg/ml $_{dd}H_2O$). Immediately after DAM addition infection was conducted, chambers were sealed and incubated for 5 days at 20°C. For detection cells were harvested by resuspension and transferred to reaction tubes followed by washing, PFA-fixation and DAPI staining as described in chapter 2.13.8. The effect of 25 µM and 50 µM DAM was just examined in a single experiment, whereas 0, 100, 180 and 250 µM DAM were investigated in two independent experiments.

For visualization by immunofluorescence (IF) 5 x 10^4 uninfected as well as *P. amoebophila*-infected amoebae were seeded on sterile 12 mm glass coverslips (Roth) in 24-well dishes (Nunc), each well containing 1 ml modified PYG. After attachment of amoebae cells were exposed to 0, 100 and 250 µM DAM. Immediately after DAM addition infection of *A. castellanii* Neff was conducted, dishes were sealed and incubated for 5 days at 20°C. For detection of endosymbionts, IF was performed directly on the coverslips in the 24-well dishes, and involved either methanol or paraformaldehyde fixation prior to exposure to antibodies. IF experiments were conducted twice, although the second time only focusing on iron deprivation at the key concentration of 250 µM DAM and the non-exposed control, but including asynchronously infected amoebae. The first IF experiment was performed in two technical replicates on synchronously infected amoebae. Controls for the procedure of IF involved uninfected and asynchronously infected amoebae not exposed to DAM.

For visualization by FISH 5 x 10^4 uninfected as well as *P. amoebophila*-infected amoebae were seeded in 24-well dishes (Nunc), each well containing 1 ml modified PYG. After attachment of amoebae cells were exposed to either 0 or 250 µM DAM. Immediately after DAM addition infection of *A. castellanii* Neff was conducted, dishes were sealed and incubated for 5 days at 20°C. For detection, cells were harvested by resuspension, transferred to reaction tubes,

centrifuged at 3900 rcf for 6 minutes, washed once with 1x PAS and eventually resuspended in 20 µl 1x PAS. The entire volume of 20 µl per condition was transferred to 10-well microscope slides (Paul Marienfeld GmbH). Subsequent incubation at RT for 30 minutes allowed for attachment of amoebae. Residual fluid was removed, 20 µl 4% PFA (fixative) was added per well, removed again after 10 minutes and cells were rinsed once with 20 µl $_{dd}H_2O$. Prior to storage at -20°C, fixed samples were dried at RT. The FISH visualization was performed once, but was conducted simultaneously to the second IF experiment meaning use of the same cell pool and DAM solution. An uninfected control not exposed to DAM was carried along.

2.18 Fluorescence *in situ* hybridization (FISH) and DAPI staining to monitor infection and iron deprivation

Table 15. Composition of buffers used for FISH (20% formamide)*

Hybridization buffer (HB)	5 M NaCl	180 µl	**Washing buffer** (WB)	5 M NaCl	2150 µl
	1 M Tris/HCl (pH 8)	20 µl		1 M Tris/HCl (pH 8)	1 ml
	$_{dd}H_2O$	600 µl		0.5 M EDTA	500 µl
	Formamide	200 µl		$_{dd}H_2O$	ad 50 ml
	10% (w/v) SDS	1 µl		10% (w/v) SDS	50 µl
	Total volume	1000 µl		Total volume	50 ml

* Buffers were prepared freshly immediatly before hybridization. HB was stored at room temperature, WB in a 48°C water bath until use. All solutions except for formamide (4°C) were stored at room temperature.

PFA-fixed samples on 10-well microscope slides were briefly thawed at RT and 9 µl hybridization buffer (HB) were applied onto each sample. Subsequently, 1 µl per oligonucleotide probe working solution (50 ng/µl in $_{dd}H_2O$) was mixed with the applied HB and immediately after the slide was horizontally placed in a 50 ml plastic tube (hybridization chamber) that contained a folded paper towel soaked with the remaining HB. Tubes were closed and incubated in a 46°C hybridization oven in order to provide stringency for specific hybridization of oligonucleotide probes to complementary rRNA. After 90 minutes of hybridization slides were quickly transferred into washing buffer (WB)-containing 50 ml tubes that had been warmed up to 48°C in a waterbath in order to maintain stringency during removal of excess probes. Slides were incubated in the WB at 48°C for 10 minutes, briefly rinsed in ice-cold $_{dd}H_2O$ and immediately dried by blowing off the liquid through an air flow. Dry slides were either stored at -20°C or subjected to DAPI staining as described in chapter in 2.13.8 in order to visualize all cells of a sample.

The following probes were used to visualize the infection cycle of *P. amoebophila* in *Acanthamoeba* sp. (chapter 2.15): The combination of probes EUK516 and Acanth412a, both targeting the amoebal host cells and labeled with FLUOS (green), was aimed at obtaining a strong background signal against the scattered and small-sized intracellular bacterial signals that were obtained with either the *Chlamydiales*-specific Cy3-labeled probe Chl523 (red) or *P. amoebophila*-specific Cy3-labeled probe E25-454 (red). Only the metabolically active chlamydial forms (RBs) are theoretically detected by FISH due to their higher ribosome content and their more permeable cell wall relative to EBs.

The visualization of iron deprivation effects on *P. amoebophila* was accomplished by two different probes, namely Acanth412a linked to FLUOS (green) to label the host cells and the *P. amoebophila*-specific Cy3-labeled probe E25-454 (red) to prove identity of affected forms.

The control of endosymbiont identity in various samples, as for example in extracted endosymbionts in the course of the infectivity assay, was performed using the EUBmix probes linked to FLUOS (green) in combination with the *P. amoebophila*-specific Cy3-labeled probe E25-454 (red). Thereby, most of *Bacteria* versus *P. amoebophila* endosymbionts were detected.

In general, probe working solutions were protected from light and kept on ice during the hybridization procedure. Also, probe-treated slides were only exposed to light when necessary. The formamide concentration of 20% (v/v) for all probes used in this work had been established before this study.

Hybridized slides were examined using either an epifluorescence microscope (100x objective, oil immersion) or a confocal laser scanning microscope (CLSM, 60x objective, oil immersion) equipped with two helium-neon-lasers (543 nm and 633 nm) and an argon laser (458-514 nm) thereby being able to visually document FLUOS/FITC- and Cy3-stained samples but not DAPI staining. Image analysis was performed with Axio Vision 4 and LSM Image Browser 3.2 respectively.

2.19 Monitoring of infection and iron deprivation by immunofluorescence and DAPI staining

Table 16. Buffers and solutions used specifically for immunofluorescence

Blocking buffer	Bovine serum albumin (BSA) 1x PBS	20 g 1 l	This buffer was stored in 50 ml aliquots at -20°C before and at 4°C after first use.
Lysozyme solution	5 mg/ml Lysozyme stock solution 10 mM Tris-HCl, pH 6.5	1:1000 dilution	The stock solution was stored at -20°C, the working solution was prepared freshly.
Tween 20 solution	Tween 20 1x PBS	0.05% (v/v)	

2.19.1 Antibody inactivation

Polyclonal *P. amoebophila*-antibodies that had been inactivated against *A. castellanii* Neff to prevent non-specific binding to host cell components were provided by Karin Aistleitner. Briefly, a small culture of endosymbiont-free amoebae was harvested and cells were resuspended in 500 µl blocking buffer and subjected to two successive freeze/thaw steps in order to mechanically lyse the cells. 500 µl of antibody solution was added, the mixture was incubated for 24 hours at 4°C, mixed, and again incubated at 4°C for 30 minutes. Finally, antibodies reactive against the host cell lysate were removed by centrifugation at 6800 rcf for 2 minutes. The supernatant containing inactivated anti-*P. amoebophila* antibody was stored at -20°C.

2.19.2 Methanol fixation

Methanol fixation precipitates proteins quickly but provides only low structural preservation. It worked for both primary antibodies used in this work.
Cells were rinsed once with 150 µl (16-well Lab-Tek™ Chamber Slides) or 1 ml (24-well dishes) 1x PBS, the same volumes of methanol were added and cells were incubated with methanol for 10 minutes at RT. Methanol was finally replaced by 1x PBS. Fixed cells in 1x PBS were either stored at 4°C for a few hours or subjected to immunofluorescence.

2.19.3 Paraformaldehyde (PFA) fixation

The cross-linking reagent PFA preserves cell structure better but requires the addition of a permeabilization step to allow access of antibodies to antigens. The PFA fixation protocol was established by co-workers and only worked for the anti-*P. amoebophila* antibody.
Cells were rinsed once with 1 ml 1x PBS, 500 µl of thawed 4% PFA was added and cells were incubated for 1 hour at RT. PFA treatment was followed by again rinsing with 500 µl 1x PBS and incubation in 500 µl of Tween 20 solution for 25 minutes at RT. Cells were ready for immunofluorescence after final permeabilization of amoebae by incubation with 500 µl of lysozyme solution for 1 hour at RT.

2.19.4 Indirect immunofluorescence procedure

IF was performed in the chambers of the 16-well Lab-Tek™ Chamber Slides and the coverslip-containing 24-well dishes respectively. 1x PBS was replaced by 150 µl/1 ml thawed blocking buffer and cells were incubated for 20 minutes at RT on a rocking platform in order to block unspecific binding sites. In the meanwhile the primary antibodies were diluted 1:1000 in cooled

blocking buffer. The blocking buffer was aspirated, 100 µl/300 µl of antibody solution was then added to each chamber/well and samples were incubated with primary antibodies for 60 minutes at RT on a rocking platform. Fluorochrome-labeled secondary antibodies were prepared by a 1:1000 dilution in cooled blocking buffer and kept on ice protected from light. To remove unbound primary antibodies samples were washed with 100 µl/300 µl 1x PBS three times. 100 µl/300 µl diluted secondary antibodies were added to each chamber/well after removal of 1x PBS, dishes were placed in a box to provide protection from light and sample were again incubated for 60 minutes at RT on a rocking platform. Finally, samples were twice washed with 100 µl/300 µl 1x PBS, 100 µl/300 µl 1:10000 DAPI solution in 1x PBS was added and incubated for 4 minutes in the dark followed by another two PBS washes.

The last volume of 1x PBS was left in the wells in the case of experiments that involved coverslips, which were subsequently transferred to microscope slides and inversely placed on 1.5 µl of Mowiol for mounting. Samples were ready for viewing by fluorescence microscopy after hardening of Mowiol for 30 minutes at RT. Microscopy and image analysis was performed as described for experiments visualized by FISH (chapter 2.18).

Immunofluorescence in chamber slides was differently processed after the final washes, since chambers had to be removed before mounting. Therefore, the last volume of 1x PBS was removed leaving a thin film of buffer so that samples did not desiccate. Chambers were gently displaced from the slide followed by removal of the entire gasket and all residual irregularities. Residual buffer was removed and samples were immediately covered with several drops of citifluor and coverglass thereby being ready for evaluation by epifluorescence microscopy.

The following primary and secondary antibodies were used in this work: For visualization of iron deprivation effects on *P. amoebophila* polyclonal anti-*P. amoebophila* antibodies raised in chicken or rabbit were detected by either Cy3-conjugated (donkey anti-chicken IgG) or FITC-conjugated (goat anti-rabbit IgG) secondary antibodies. Additionally, anti-Hsp60 antibody in combination with Cy3-conjugated secondary antibody (goat anti guinea pig IgG) was used in the first immunofluorescence experiment. Experiments aimed at quantification of *P. amoebophila* infectivity just involved the anti-*P. amoebophila* antibodies generated in chicken combined with Cy3-conjugated secondary antibody (donkey anti-chicken IgG).

2.20 Statistical analysis

Analysis of the quantitative data collected in this work was conducted following standard statistical methods (Motulsky, 1995). Calculations, statistical tests and graph constructions were performed using Microsoft Excel 2002 and GraphPad Prism version 5.01.

2.20.1 Quantification of extracted *P. amoebophila*

The number of bacteria per ml and field was calculated according to the equation presented in chapter 2.14. Dilution factors varied depending on the sample volume that had been subjected to quantification. Based upon the assumption that the data were sampled from a population that follows a Gaussian distribution, cell concentration values from each experiment were combined and averaged for each condition (time point post infection, intra- or extracellular), standard deviation (SD) and standard error of the mean (SE) were determined. For comparison of either intra- or extracellular mean number of cells per ml of 6 different time points (0-120 hpi) the one-way analysis of variance (ANOVA) was performed. Individual time point-pairs within a fraction were post-tested for statistical significance of observed differences using the Tukey-Kramer test.

2.20.2 Evaluation of *P. amoebophila* infectivity

For each field the number of infectious particles per amoebal cell was calculated and then normalized to the number of cells per amoebal cell that had been introduced when performing the second round of infection. Calculation of these theoretical MOIs was possible due to quantification of total chlamydial cells throughout the cycle and the defined number of amoebae that were subjected to infection. Therefore, the proportion of infectious bacteria per individual field was determined. The combination of all three data sets resulted in a total number of fields of 31-44 per time point and fraction (intra-, extracellular). Based upon the assumption that the data were sampled from a population that follows a Gaussian distribution, outliers were detected using the Grubb's test ($P < 0.05$) and mean proportions of infectious bacteria as well as standard deviations (SD) and standard errors of means (SE) were calculated. To test for the presence of statistically significant differences of either intra- or extracellular mean infectivity values of 6 different time points (0-120 hpi) the one-way analysis of variance (ANOVA) was performed. Individual time point pairs within a fraction were post-tested for statistical significance of observed differences using the Tukey-Kramer test.

2.20.3 Evaluation of host cell viability during iron deprivation

The numbers of total PI-stained amoebae per condition and organism were expressed as proportions of dead and alive cells respectively. Proportions were calculated both for each field individually and also summarized for every treatment and organism. Individual proportions were used to detect outliers in a set of data that included all available values for a treatment (Grubb's test, $P < 0.05$), and summarized proportions were used to define the optimal DAM concentration.

The uncertainty of summarized values was determined by calculating the 95% confidence intervals (95% CI) for proportions (Clopper-Pearson method). A two-sided Fisher's exact test was used to compare the outcome of different DAM treatments to the control (0 μM DAM), thereby asking for statistical significance of observed differences of means. Differences between treatments were further analysed by calculating relative risks (ratio of two proportions) and corresponding 95% CIs.

3 Results

3.1 *Parachlamydia* sp. versus *P. amoebophila*

One of the first cycles completed involved the infection of *A. castellanii* Neff with elementary bodies (EBs) that had been partially purified a few months earlier, but had never been controlled for correct identity or contamination. That infection was aimed at monitoring major phenotypic events of the cycle through visualization of metabolically active bacteria by fluorescence *in situ* hybridization (FISH) combined with the not consistently succeeding general DNA stain DAPI over a period of time of 5 days (120 hours post infection, hpi).

Since the *Chlamydiales*-targeting probe Chls-0523 was used for hybridization, the development of bacteria shown in figure 4 could not be explicitly assigned to *P. amoebophila*, the organism of interest. In fact, the visualized inclusion-forming behaviour of these bacteria was considered as being abnormal, and therefore strongly indicated an unintended infection with chlamydiae different from *P. amoebophila*. In contrast to regularly distributed, individual bacterial signals observed in amoebae asynchronously infected with *P. amoebophila*, cauliflower-like structures appeared 48 hpi (Fig. 4C), that presumably represent amoebae densly packed with replicating clusters of bacteria within inclusion membranes. It was assumed, that the infection of amoebae was performed using EBs of ambiguous identity rather than acquisition of a contamination during the experimental procedure, since the control cells remained uninfected throughout the cycle (Fig. 4G).

Due to the synchronized infection and the observed dominance of unexpected intracellular FISH signals that either indicate a higher replicative power or a higher initial dose of infectious chlamydial organisms relative to *P. amoebophila*, developmental features of this organism within *A. castellanii* Neff can be carefully inferred from this erroneous infection experiment. Knowledge about the developmental cycle of this organism, which was subsequently identified as *Parachlamydia* sp., might be interesting to contrast with the cycle of *P. amoebophila*.

At 0 hpi only a low proportion of total bacterial cells was detected by FISH, which was in contrast to the high proportion of Cy3-labeled cells at 24 hpi. The FISH signals at 24 hpi did not have the coccoid appearence typical for individual chlamydial cells, but were rather square-shaped and slightly enlarged when compared to 0 hpi. Amoebae contained, and were dominated, by multiple clusters of Cy3-stained bacteria located close to each other at 48 hpi as well as at 72 hpi. At 96 hpi and 120 hpi characteristic cauliflower structures were clearly diminished. Instead, amoebal cells were densly packed with small-sized bacterial cells so that no amoebal structures except for the nuclei were recognized 4 and 5 days post infection.

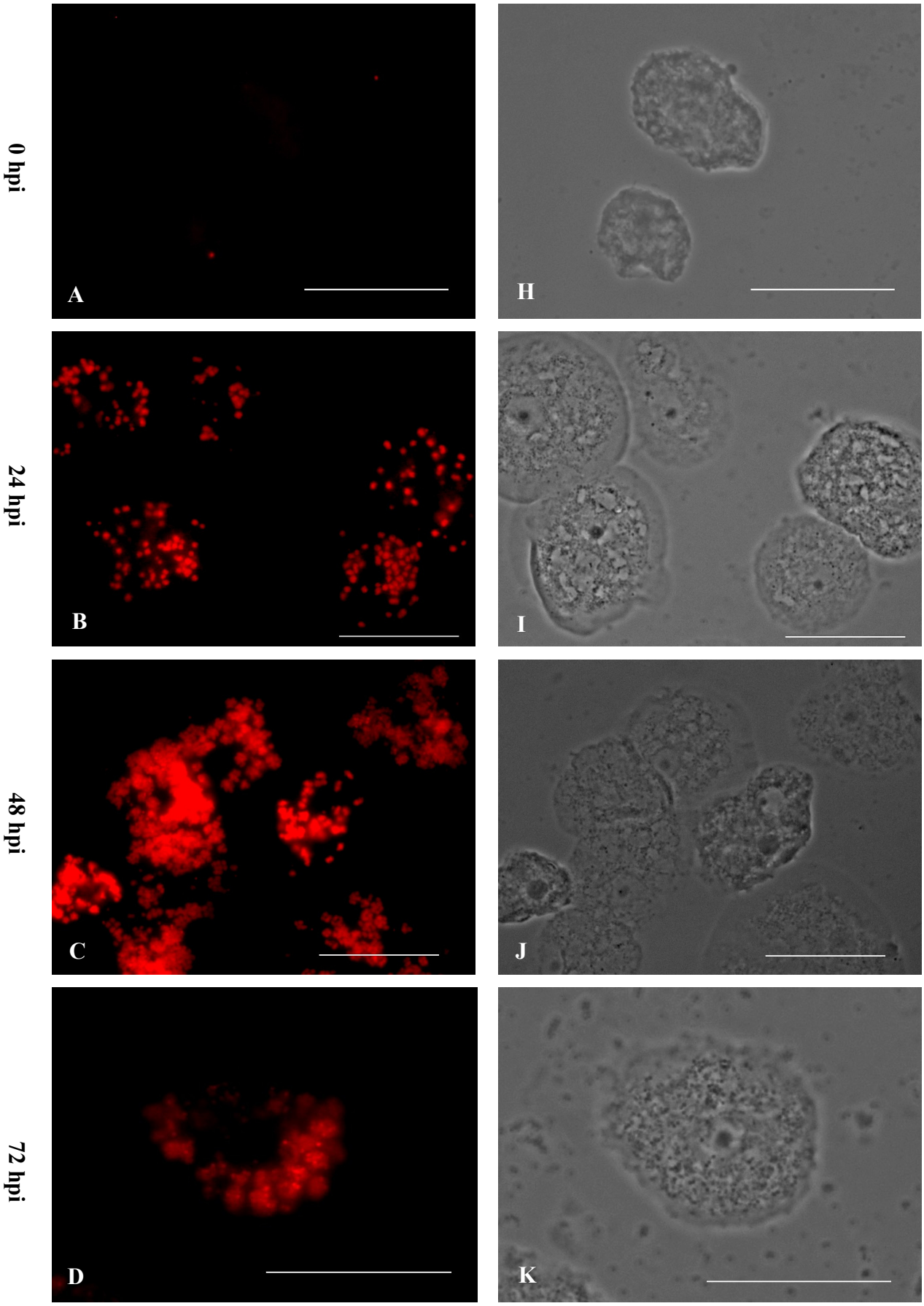
0 hpi
24 hpi
48 hpi
72 hpi
A
B
C
D
H
I
J
K

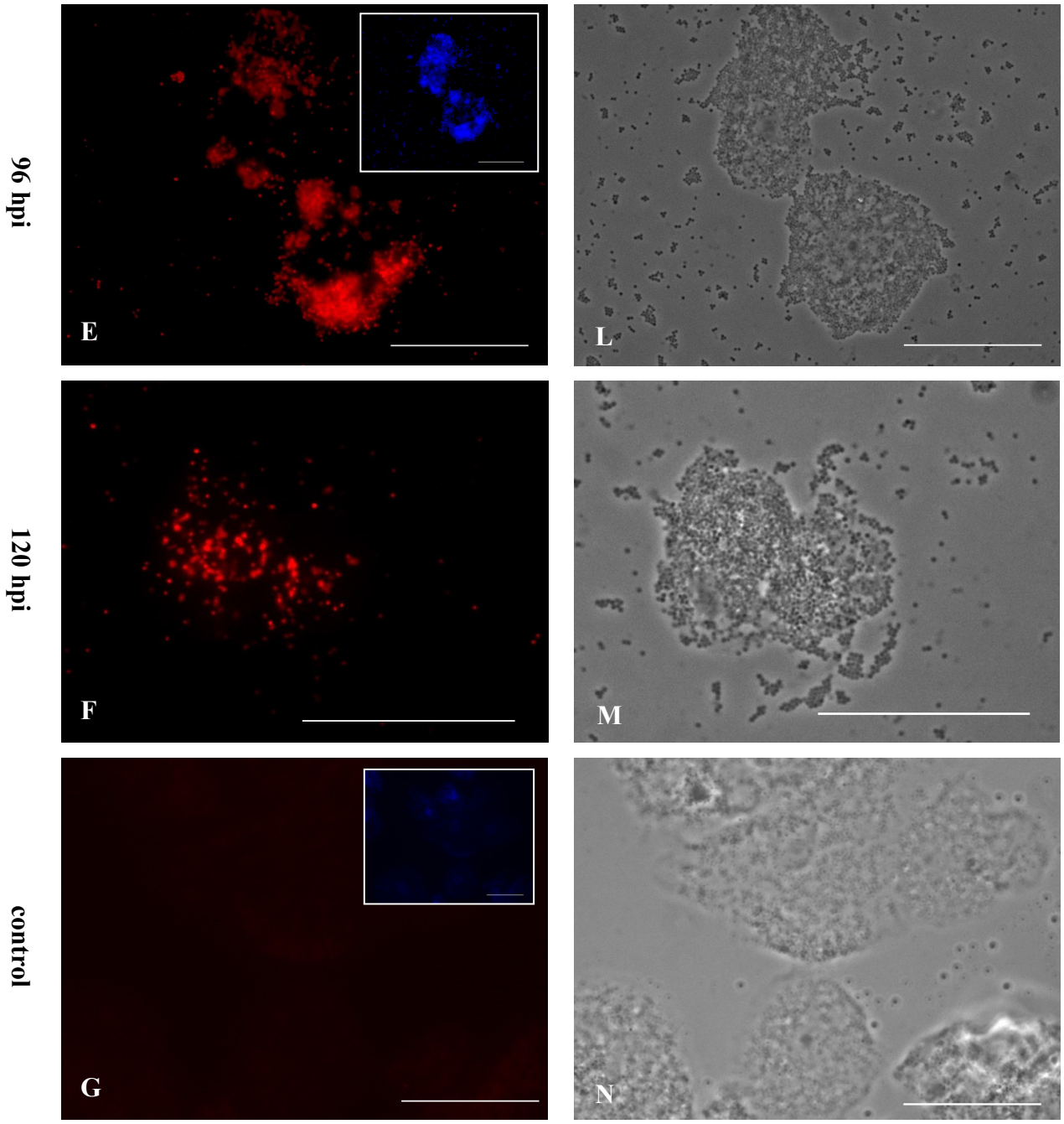

Figure 4. Different time points post infection after infection (MOI 10) of *A. castellanii* Neff with EBs of mixed identity visualized by FISH and DAPI staining. The FISH images (A to G) show hybridization with Cy3-labeled Chls-0523 probe, which targets 16S rRNA of *Chlamydiales*. (H to N) Corresponding phase-contrast images demonstrate boundaries of amoebal cells. Insets in (I) and (G) show DAPI-stained total bacteria at 96 hpi (I) and mitochondria of uninfected controls (G). Bar, 10 µm.

This chlamydial dominance was even more obvious when comparing phase contrast images of 96 and 120 hpi to the uninfected control, where host cell boundaries were well-preserved (Fig. 4L, M, and N). FISH signals relative to total bacterial cells were clearly reduced at the last two time points post infection (Fig. 4E, L, F, and M). The amount of extracellular, only DAPI-stained bacteria increased from 72 hpi on, and was evident at 96 hpi (Fig. 3L). At 120 hpi Cy3-labeled bacteria made up about half of the total number of extracellular cells.

3.2 Screening of purified elementary bodies (EBs) and endosymbiont-free amoebae

The identity of purified EBs that were used to synchronously infect amoebae was controlled by restriction fragment length polymorphism (RFLP) analysis using *Vsp*I as well as sequencing of chlamydial 16S rRNA genes. Application of these two screening methods to EBs that had been used for the infection described above (chapter 3.1.1) revealed the presence of two phylogenetically different chlamydial 16S rRNA genes, namely from *Parachlamydia* sp. and *P. amoebophila* (Fig. 5). Therefore, amoebae were potentially infected with a mixture of these two *Chlamydia*-like bacteria, although only DNA was demonstrated to be existent in the EB purification.

Sensitivity of detection of parachlamydial DNA by RFLP analysis was tested by performing standard 16S rRNA gene-targeted PCR with template DNA that had been mixed in defined ratios followed by the restriction enzyme digestion and standard gel electrophoresis. This test revealed that 20 ng, but not 10 ng, of either para- or protochlamydial DNA can be reliably detected in a mixture with the respective other DNA that sums up to 100 ng starting DNA. Since isolated DNA always includes both DNA from amoebal host cells and from endosymbionts, 20 ng DNA must be further resolved in order to be able to determine a detection limit. According to the genome size of *P. amoebophila* (2.4 Mb) and the mass of one nucleotide pair (1 x 10^{-9} pg), one *P. amoebophila* cell contains 2.4 x 10^{-3} pg DNA. The mass of DNA of one amoebal cell was determined to be 2 to 5 pg (Coulson and Tyndall, 1978), and is therefore assumed to be 3 pg for the calculation presented here. Assuming that one amoeba contains 50-100 endosymbionts in an

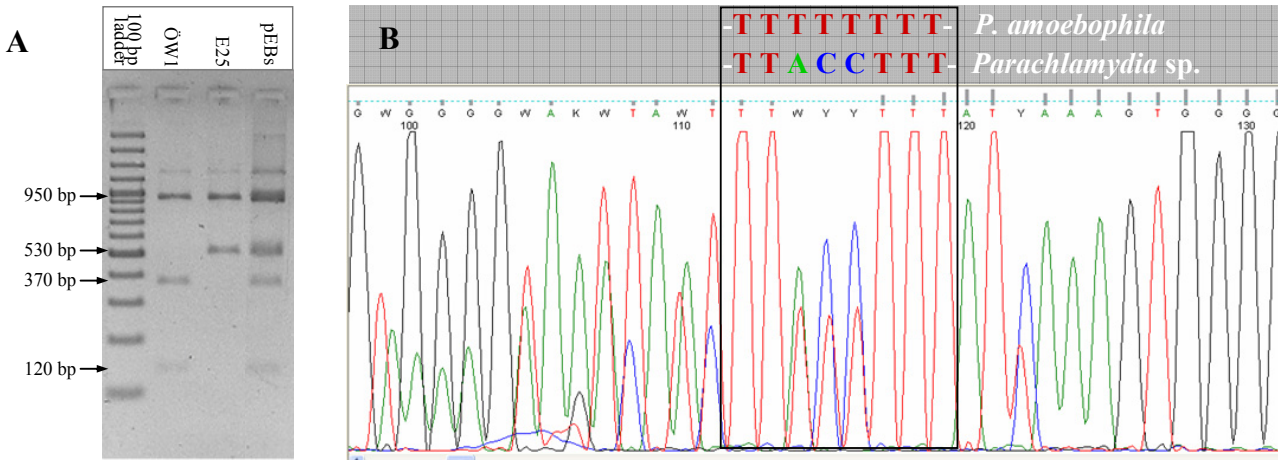

Figure 5. Mixed endosymbionts as detected by RFLP analysis (A) and sequencing of chlamydial 16S rRNA genes (B). (A) The *Vsp*I restriction enzyme digestion produces two distinctive sets of fragments for 16S rRNA genes that have been PCR-amplified from either pure *Parachlamydia* sp. DNA (ÖW1) or *P. amoebophila* DNA (E25) as visualized by gel electrophoresis. Therefore, DNA from purified EBs of a mixed culture shows a mixed/combined fragment pattern after PCR and *Vsp*I digestion. (B) A detail of the 16S rRNA gene sequence of purified EBs shows the presence of two different sequences that could be assigned to *P. amoebophila* and *Parachlamydia* sp. The black rectangle highlights a stretch characteristic for *Parachlamydia*-contamination. Bp, base pairs. ÖW1, *Parachlamydia* sp. strain ÖW1. E25, *P. amoebophila* strain UWE25. pEBs, purified elementary bodies.

asynchronously infected culture, bacterial DNA would make up 3.9 to 7.5% of total DNA. Since a 1:5 dilution of mixed DNA is still detectable, RFLP analysis can detect 0.8 to 1.5% of (contaminating) bacterial DNA in a DNA mixture, which corresponds to 0.8-1.5 ng bacterial DNA or 3.2 x 10^5 to 6.2 x 10^5 bacterial cells. In other words, about 1 ng or more DNA of both *Parachlamydia* sp. and *P. amoebophila* must have been present to be detectable on the RFLP gel showed in figure 5A.

Subsequent experiments were routinely controlled for contaminats as described in chapter 2.13. Briefly, amoebae to be infected were checked for DAPI signals other than those weak signals derived from mitochondria, purified EBs had to show just a single chlamydial 16S rRNA gene sequence after sequencing, a single RFLP-fragment pattern characteristic for *P. amoebophila* and no PCR product when targeting the 16S rRNA gene via the universal primer pair 1492R/27F. Also, testing for contamination using FISH required a 100% overlap of *P. amoebophila*-specific (E25-454 probe) and universal bacterial signals (EUBmix probes) for endosymbiont-containing cultures, and no bacterial signals for endosymbiont-free cultures, in order to be qualified for experiments. Morphological signs for a parachlamydial infection of amoebae are high numbers of extracellular coccoid bacteria combined with severely reduced amoebal growth and increased detachment from the culture flask surface.

3.3 The developmental cycle of *P. amoebophila* as monitored by fluorescence *in situ* hybridization (FISH)

Synchronized infections were performed using two related amoebal strains as hosts, that both belong to the genus *Acanthamoeba*. The infection procedure and the visualization method were identically conducted for both *A. castellanii* Neff and *Acanthamoeba* sp. UWC1 in order to allow for comparison of the intracellular development of *P. amoebophila* and determination of distinctive phenotypic events over a period of time. Since interpretations of observations will take place mainly in the discussion chapter, this chapter is focused on descriptive characterization of the developmental cycle of *P. amoebophila*.

The selection of visualized time points shown in this work was initially based on literature (see Table 3), but is also a result of this work. The end of the experiment was initially set for 96 hours post infection, but this period of 4 days turned out to be too short to specify the end of the cycle. Therefore, the infection experiment was extended to regular monitoring within a period of 14 days. Since time points after 5 days post infection (120 hpi) do not provide any detectable differences from the 120 hpi time point, the cycle in FISH images is restricted to time points 0, 6, 12, 24, 48, 72, 96 and 120 hpi. The relatively close early time points (0, 6, 12, 24 hpi) should

specify the time of differentiation of EBs to RBs. In combining FISH with DAPI staining, changes from one chlamydial form to another was expected to be detectable. Discrimination of mitochondrial and bacterial DAPI signals was generally accomplishable by visual inspection as well as by the CCD camera (AxioCam HRc, Zeiss) used for taking photomicrographs, since amoebal mitochondria appear as bluish, evenly and densly scattered dots whereas *P. amoebophila* gives bright signals that stand out against the mitochondrial background. The metabolically less active EBs presumably account for star-like, extremely compact DAPI signals, that could be explained by the condensed DNA present in EBs.

As depicted in figures 6 and 7, major changes of *P. amoebophila* in growth and appearance as detected by fluorescently labelled oligonucleotides follow a similar timeline in both *Acanthamoeba* strains. Therefore, the following description of observable changes over time is true for synchronously infected *A. castellanii* Neff (Fig. 6) as well as for *Acanthamoeba* sp. UWC1 (Fig. 7).

The 0 hpi time point, which was processed right after infection by centrifugation, revealed that the theoretical multiplicity of infection (MOI) 10 could not truly be achieved, meaning a lower mean number of intracellular bacteria per amoeba than 10 as assessed by the number of intracellular bacterial DAPI signals. Also, not every amoebal cell was found to be infected at 0 hpi, but instead only estimated 50-70% of amoebae. Assuming that 50-70% of amoebae were infected with 5 bacteria, the mean effective MOI 2.5-3.5 can be reported for the infection experiments described in this chapter. At 0 hpi all bacteria could be detected with DAPI, but generally not with FISH probes (Fig. 6A, 7A). Rarely, however, bacteria targeted by Cy3-linked probes could be detected both intra- and extracellularly at this first time point. Whether the seemingly intracellular chlamydial FISH signals were truly derived from bacteria within host cells or were rather extracellular signals adhering to the exterior of the amoebae was not determined. Intracellular signals were unevenly distributed within host cells. The low number of extracellular signals (approximately 1 per host cell) suggests that most of infectious chlamydial forms (EBs) had been taken up by amoebae, thereby excluding a lack of physical contact between host cells and bacteria or a low infectious capacity as a possible reason for the low effective MOI.

At 6 hpi and 12 hpi the number of intracellular bacterial signals was comparable with the number of signals at 0 hpi. However, different from the start of infection was the appearance of weak FISH signals overlapping with intracellular DAPI signals 6 hpi (Fig. 6B, 7B). FISH signals 12 hpi seemed slightly increased in size and intensity compared to 6 hours earlier (Fig. 6C, 7C). Admittedly, not every intracellular bacterium showed up with both DAPI and FISH probes at

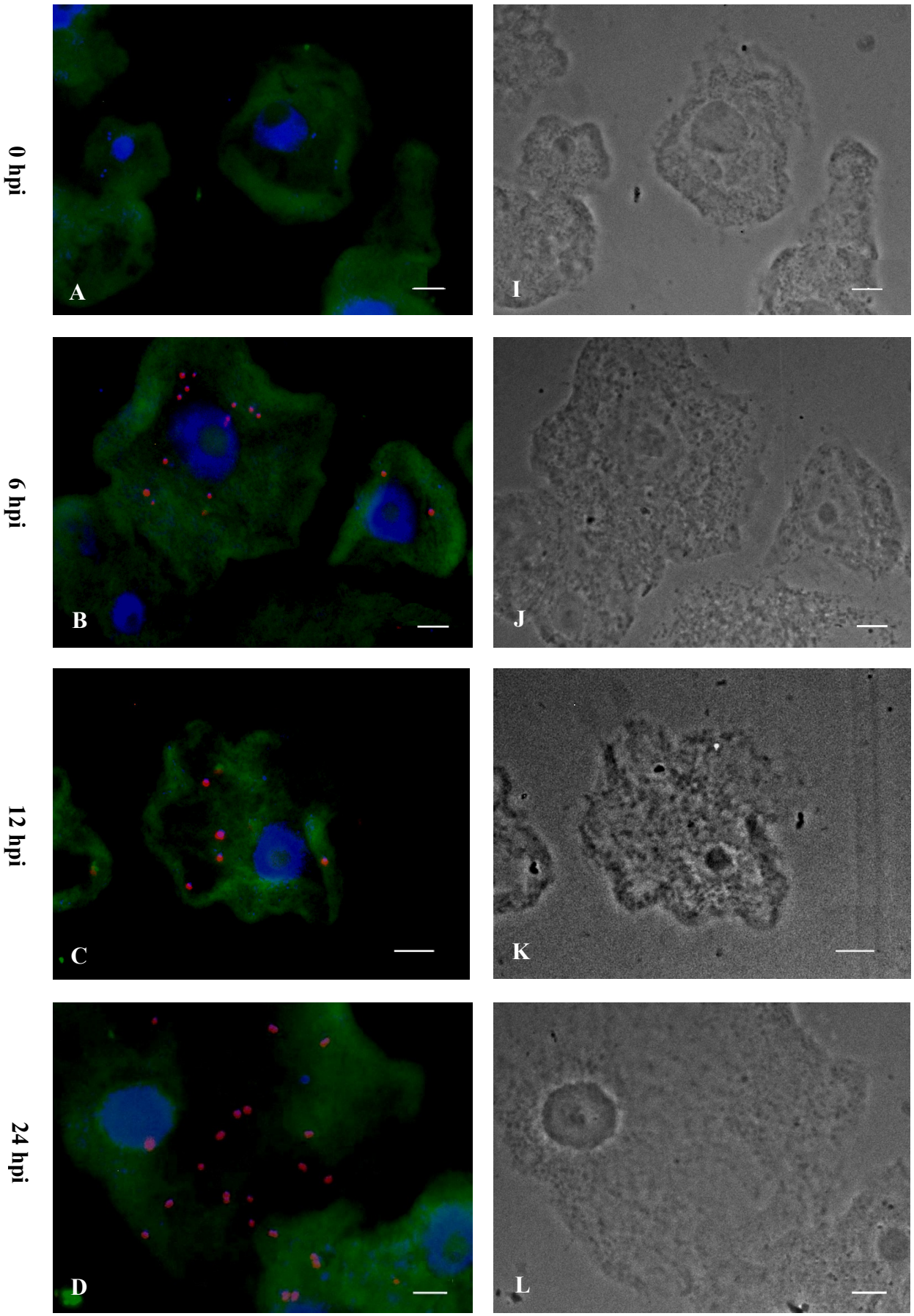
0 hpi
6 hpi
12 hpi
24 hpi
A
B
C
D
I
J
K
L

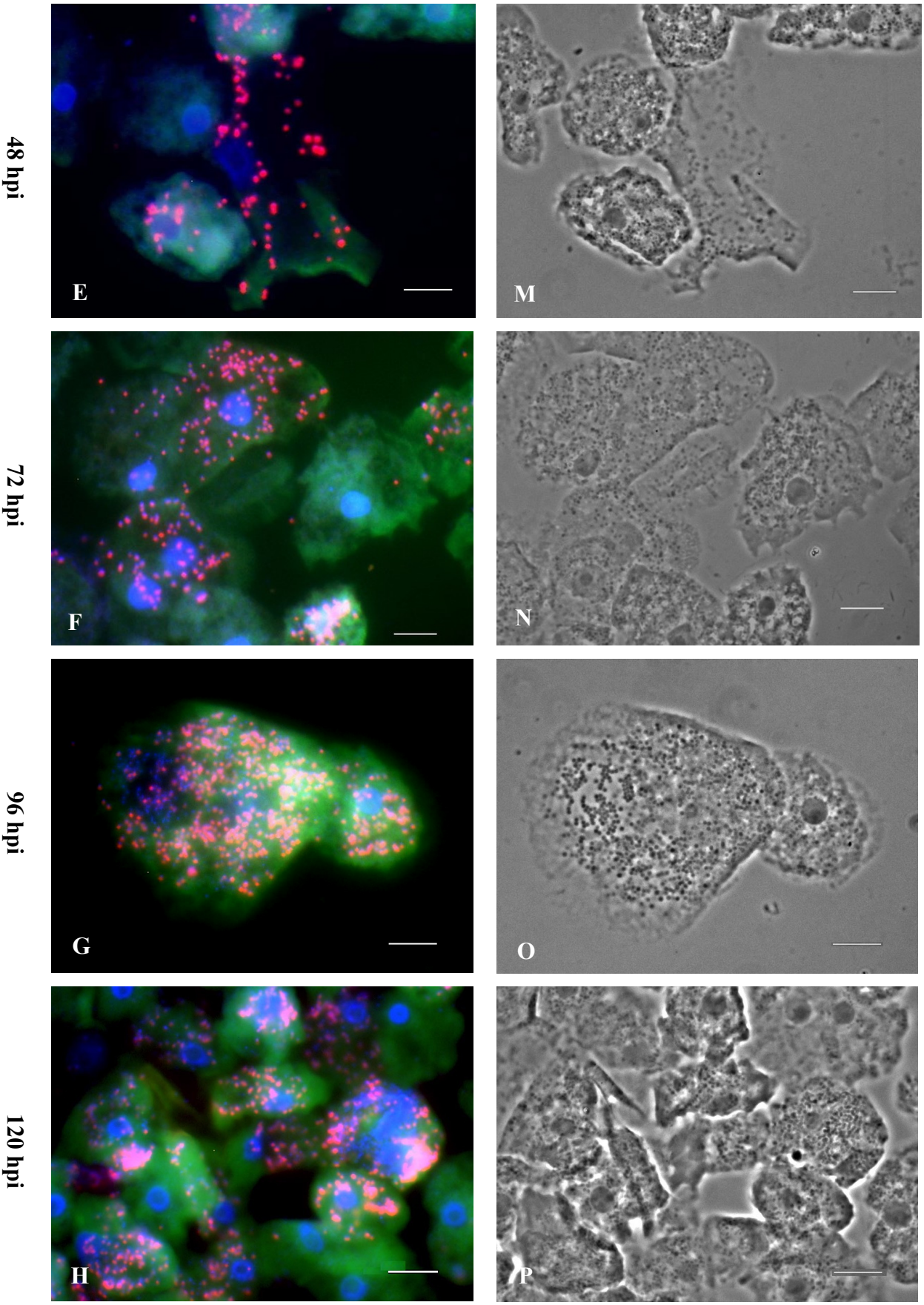
48 hpi
72 hpi
96 hpi
120 hpi
E
M
F
N
G
O
H
P

Figure 6. Synchronized infection of *A. castellanii* Neff with *P. amoebophila* (MOI 10) visualized by FISH and DAPI staining. (A-H) Different hours post infection (hpi) are shown. FISH was performed by targeting the host cells with probes Acanth412a and EUK516 linked to FLUOS (green), and the chlamydial endosymbionts with Chls-0523 linked to Cy3 (red). Amoebal nuclei and endosymbionts appear in blue due to DAPI staining. Bacterial cells that were stained with both Cy3-linked probe Chls-0523 and DAPI are pink. (I-P) Corresponding phase contrast images. The uninfected control which was processed together with the latest time point post infection did not show any chlamydial FISH signals or DAPI signals other than DAPI-stained amoebal mitochondria. Bar, 10 µm.

these two early time points. Instead, the appearance of both signals in contrast to only DAPI-stained bacteria could be observed frequently, but not until 24 hpi, or was inconsistent between experiments and individual cells (Fig. 6B and C, 7B).

At 24 hpi every single bacterium could be consistently detected with DAPI and the Cy3-linked chlamydial probe indicating universal metabolic activity. Also, the shape of the FISH signal changed from roundish to irregular and square-shaped signals (Fig. 6D, 7D). A closer look at the corresponding DAPI signals revealed the presence of pairs of cells at this time point which clearly indicates binary fission of endosymbiont (Fig. 8A).

At 48 hpi and 72 hpi chlamydial FISH signals appeared strikingly bright and relatively large. Again, every bacterial DAPI signal was represented by a FISH signal, and the number of signals was already elevated at 48 hpi (Fig. 6E, 7E) but even more increased at 72 hpi (Fig. 6F, 7F).

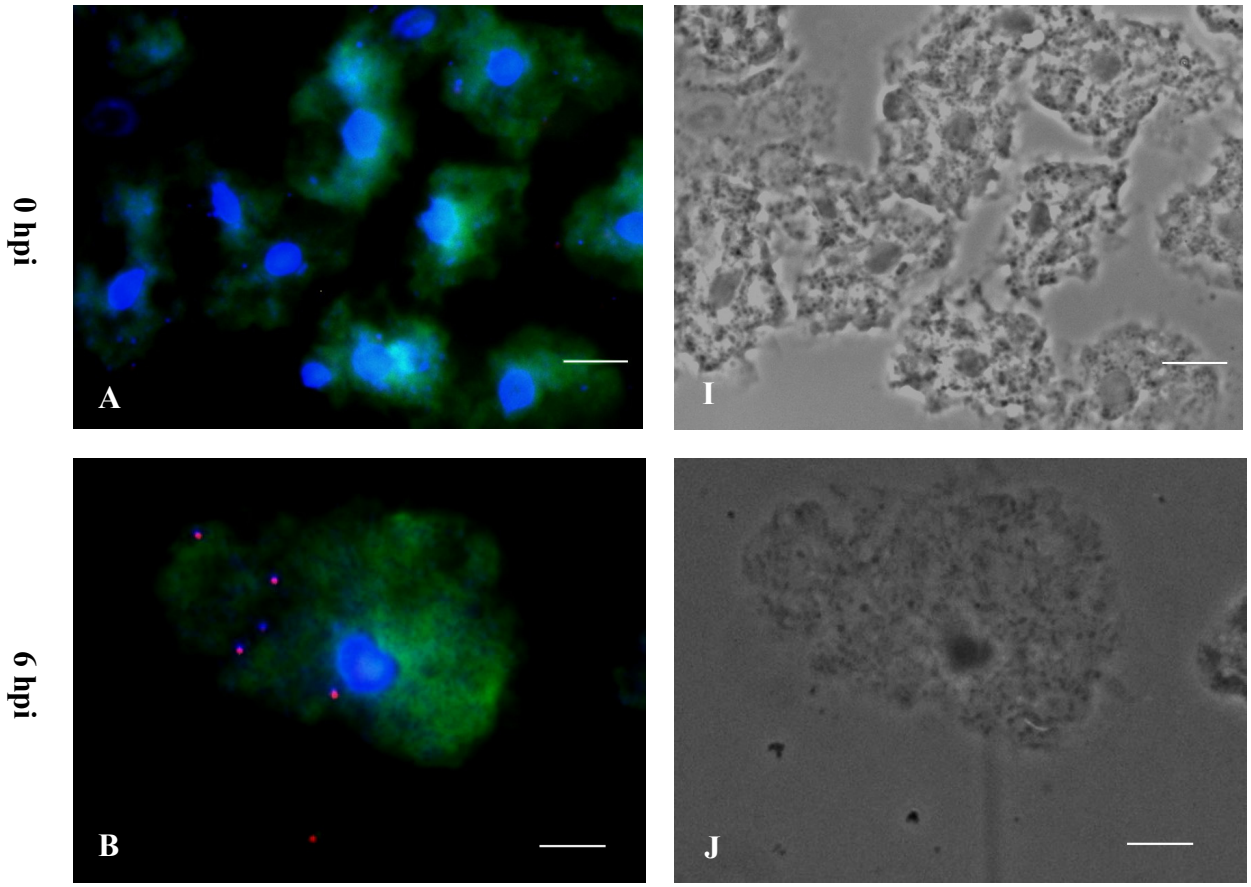

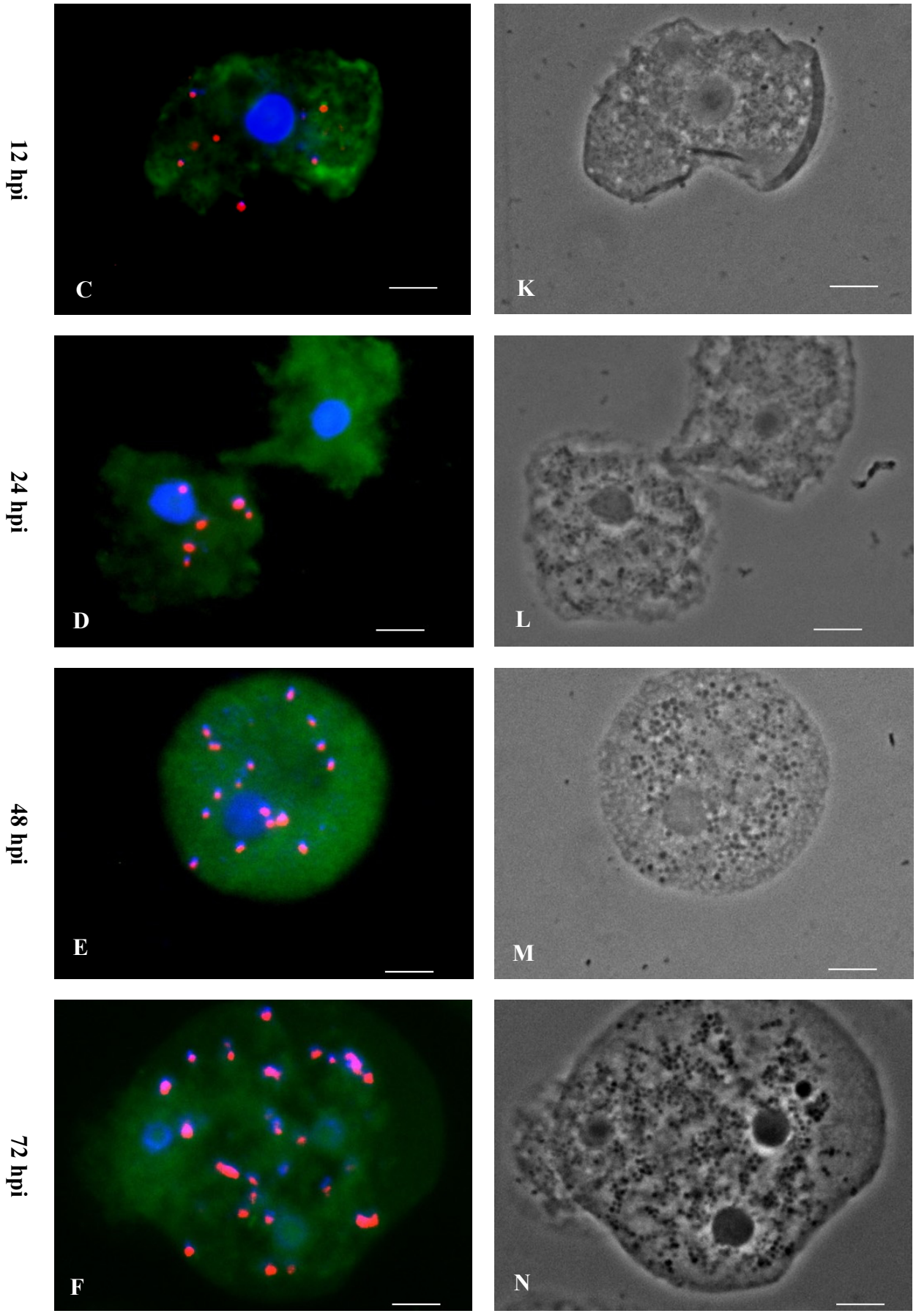
12 hpi
24 hpi
48 hpi
72 hpi
C
K
D
L
E
M
F
N

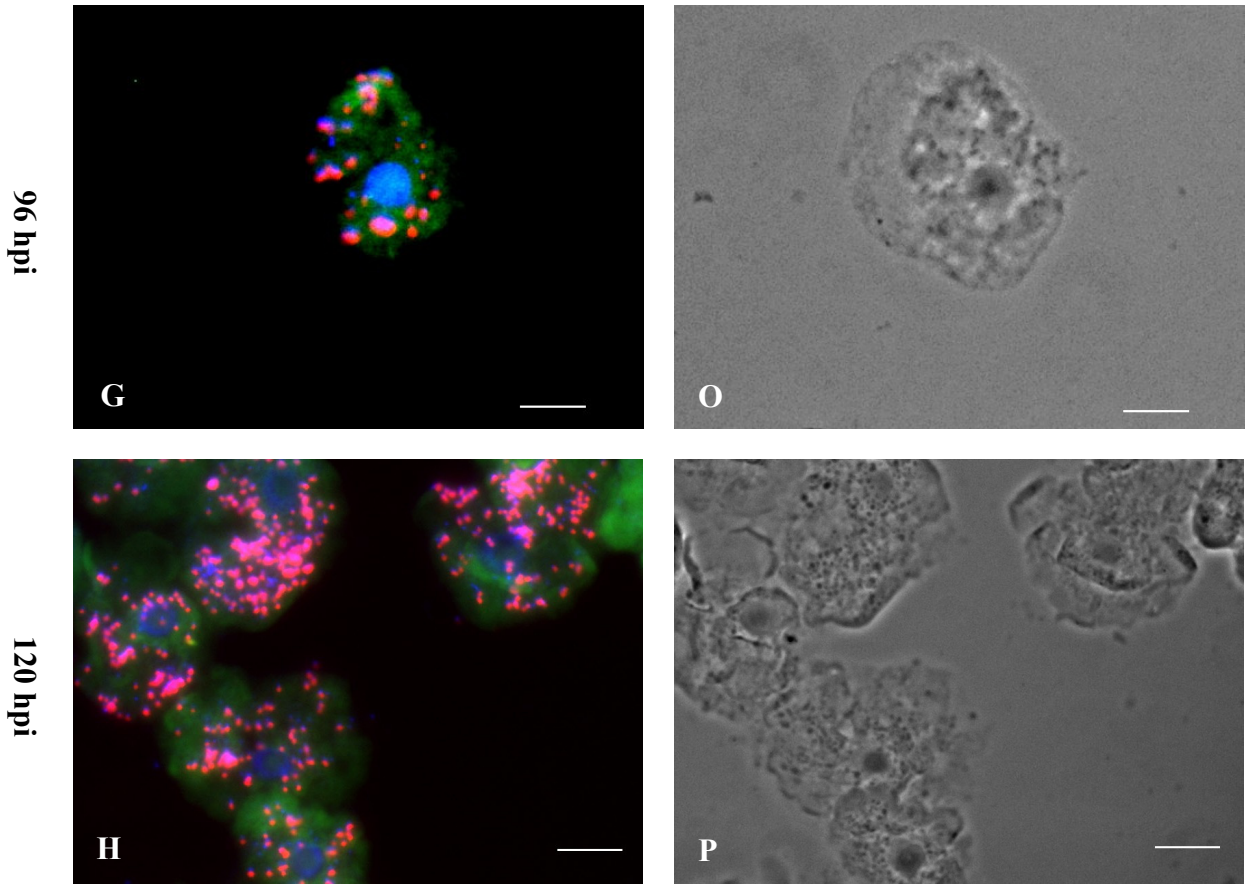

Figure 7. Synchronized infection of *Acanthamoeba* sp. UWC1 with *P. amoebophila* (MOI 10) visualized by FISH and DAPI staining. (A-H) Different hours post infection (hpi) are shown. FISH was performed by targeting the host cells with probes Acanth412a and EUK516 linked to FLUOS (green), and the chlamydial endosymbionts with Chls-0523 linked to Cy3 (red). Amoebal nuclei and endosymbionts appear in blue due to DAPI staining. Bacterial cells that were stained with both Cy3-linked probe Chls-0523 and DAPI are pink. (I-P) Corresponding phase contrast images. The uninfected control which was processed together with the latest time point post infection did not show any chlamydial FISH signals or DAPI signals other than DAPI-stained amoebal mitochondria. Bar, 10 µm.

Ongoing cell division at 72 hpi is evident when looking at the DAPI image in figure 8B, where small clusters of presumably 2-4 cells are evenly distributed over one amoebal cell.

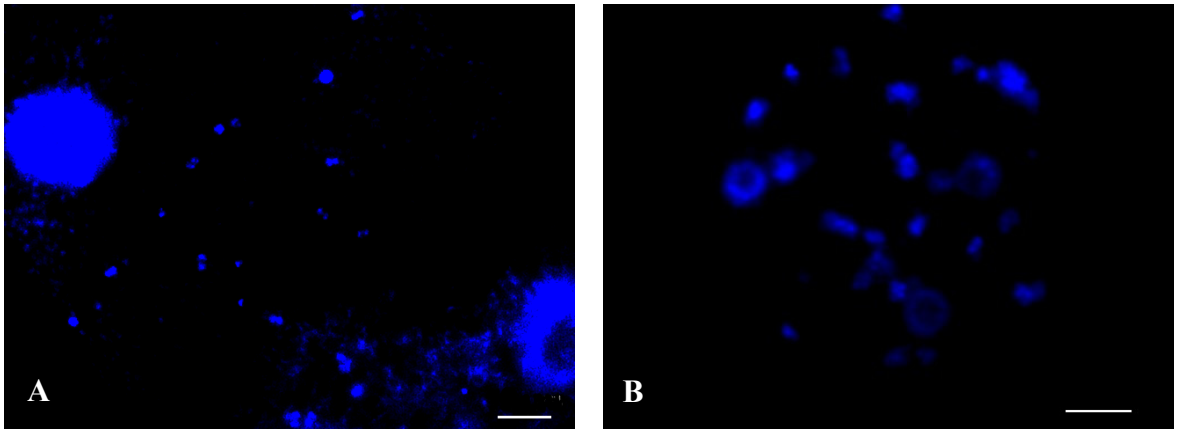

Figure 8. Enlarged DAPI images of time points 24 (A) and 72 hours post infection (hpi) (B) showing two or more adjacent chlamydial signals. Note that in addition to bacterial DAPI signals nuclei of amoebae are DAPI-stained as well. Two nuclei are visible in (A), three smaller nuclei are present in (B).

Corresponding merged FISH images and phase contrast micrographs are shown in figures 6D, L and 7D,L. Bar, 10 µm.

At 96 hpi a small proportion of total intracellular bacterial cells could not be detected with FISH probes anymore, but only with DAPI. These DAPI signals were small, compact and coccoid compared to previous time points. FISH signals 4 days post infection tended to be less bright and voluminous, although larger signals indicative for replicating forms were still present. In general, a high number of individual bacterial signals were uniformly dispersed within amoebae thereby taking up a major part of the host cells. Also, an increased number of extracellular DAPI signals that occasionally also showed up with FISH probes could be detected at this time point.

The 120 hpi time point was generally very similar to the 96 hpi time point. Specifically, the presence of three different intracellular chlamydial appearances, as detected by FISH and DAPI staining, could be observed at both time points: DAPI only; weak and individual FISH signals; and bright and enlarged FISH signals. Also, extracellular signals were increased. Additionally, more amoebae seemed to be infected compared to the 0 hpi time point, thereby indicating a spread of infection. Later time points share the simultaneous presence of a mixture of different chlamydial appearances, probably reflecting different chlamydial states. About 10 days after infection with MOI 10 all amoebal cells were infected.

The results on major phenotypic changes throughout the development of *P. amoebophila* presented here could be obtained when using either the family-specific probe Chls-0523 or the organism-specific probe E25-454, thereby confirming the correct identity (Fig. 9). The reason for

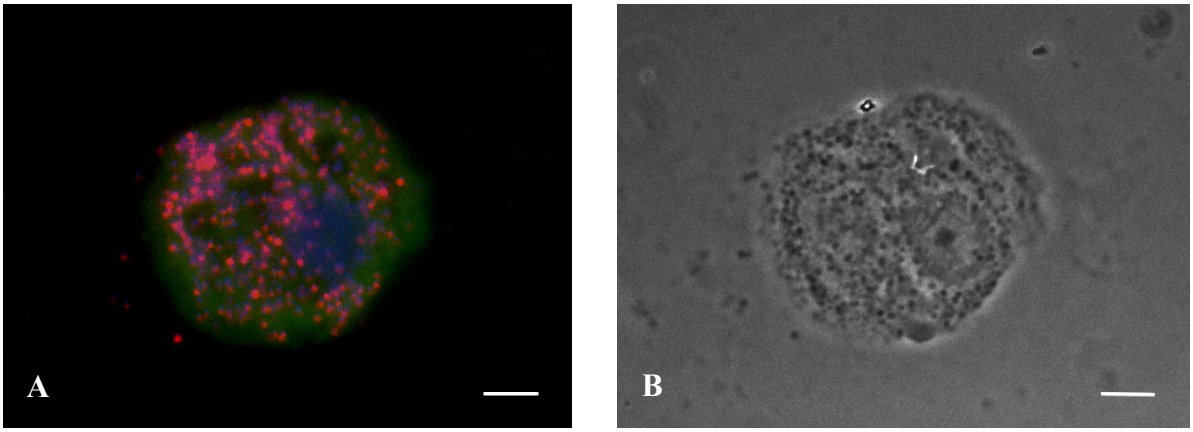

Figure 9. Identity of endosymbionts in synchronously infected *A. castellanii* Neff (MOI 10) as confirmed by FISH using the genus-specific Cy3-linked probe E25-454 (red). The probe specific for *P. amoebophila* was used in parallel FISH experiments combined with DAPI staining (all cells, blue) and FLUOS-linked Acanth412a and EUK516 (amoebae, green). (A) 96 hpi time point. (B) Corresponding phase contrast image. Bar, 10 µm.

presenting the cycle in FISH images showing the Cy3-linked Chls-0523 probe is the generally lower signal intensity and therefore poor quality of photomicrographs when using the E25-454 probe.

3.4 The developmental cycle of *P. amoebophila* as monitored by quantification of infectious progeny throughout the cycle

The developmental cycle of *P. amoebophila* in amoebae should be monitored by determining the infectious proportion of total bacteria that were collected from either amoebal lysates thereby representing intracellular bacteria or the host cell-free fraction (extracellular bacteria) at different time points after a synchronized infection. Since infectious forms are considered to be EBs, assessment of infectivity of the progeny throughout an infection cycle should allow for observation of crucial events during chlamydial development such as RB/EB transition and release of EBs.

3.4.1 Quantification of total bacteria over time

In order to be able to determine the proportion of infectious bacteria, numbers of total available bacteria per time point post infection and fraction (intra-, extracellular) were defined. Also, bacterial concentrations over time, which should reflect the course of total bacterial numbers and consequently the extent of growth within host cells, were determined and are shown in figure 10. Theoretically, cell numbers should include both EBs and RBs. However, this assumption is to be questioned, since there was no increase of intra-amoebal cell numbers within the first three days (72 hours) of a synchronized infection as inferred from the graph in figure 10. This obvious stagnation is reflected by the indication of statistically insignificant differences of mean intracellular bacterial concentrations between 0 and 72 hpi, which resulted from a statistical analysis that tested statistical significance of differences between all pairs of means expressed through P values (Tukey's Multiple Comparison Test). Tukey's test was chosen since the pre-test 1-way ANOVA (one-way analysis of variance) yielded P values less than 0.05 for each data set (intra-, extracellular bacteria) meaning that at least one mean within each data set significantly differs from the rest (Fig. 10).

A statistically significant increase in intracellular cells/ml was observable between time points 0, 24, 48, 72 hpi and 120 hpi, namely an increase from 2.3 x 10^5 cells/ml (mean of 0-72 hpi) to 4.9 x 10^5 cells/ml within 2 days after a 3 day-period of undetectable growth. In other words, on day 5 of a synchronized infection there were about twice as many intracellular bacteria present as on day 3.

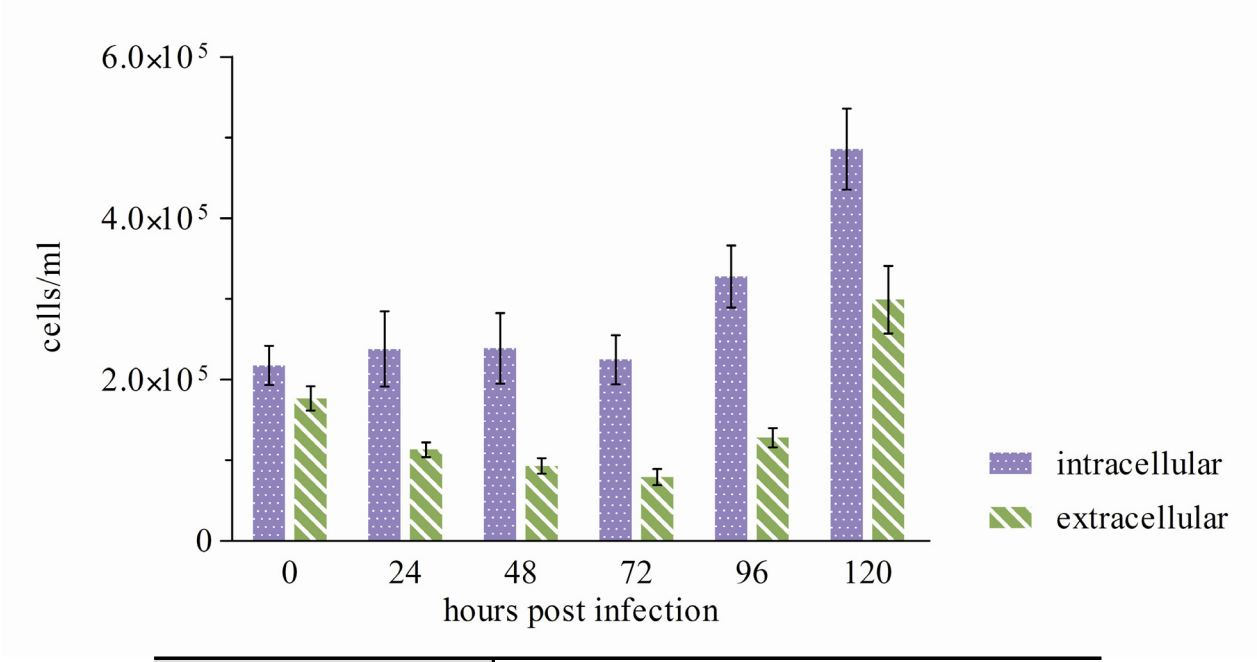

1way ANOVA	intracellular	P < 0.0001				
	extracellular	P < 0.0001				
Statistical significance (Tukey's Multiple Comparison Test, P < 0.05)	0	24	48	72	96	120 hpi
0		no	no	no	no	yes
24	no		no	no	no	yes
48	yes	no		no	no	yes
72	yes	no	no		no	yes
96	no	no	no	no		no
120 hpi	yes	yes	yes	yes	yes	

Figure 10. Number of intracellular (purple) and extracellular (green) *P. amoebophila* cells over 120 hours of a synchronized infection of *A. castellanii* Neff as quantified by filtration and subsequent DAPI staining of collected bacteria. The graph shows mean concentrations of bacterial cells (cells/ml) ± standard error of the mean (SE) at time points 0, 24, 48, 72, 96 and 120 hpi. The uninfected control did not show any detectable intra- or extracellular bacteria. Results from tests for statistical significance of differences among the means (1-way ANOVA, Tukey's Multiple Comparison Test) are summarized in the table below the graph. Differences were considered statistically significant when P values were smaller than 0.05.

In contrast to the intracellular progression of bacterial concentrations where basically only one change could be detected, numbers of extracellular bacteria showed an additional trend earlier in development. More precisely, there was a decrease from 1.8 x 10^5 to 7.9 x 10^4 extracellular bacteria per ml between 0 and 72 hpi, which could be supported by statistical analysis for significance of mean differences (Fig. 10). Therefore, there was a twofold reduction of

extracellular bacteria within the first 3 days of the infection cycle. Again, a statistically significant increase can be reported for days 3 to 5 (Fig. 10). During this period of 2 days, extracellular bacterial concentration rose from 7.9 x 10^4 to 3.0 x 10^5 which corresponds to a 3.8-fold increase of cells/ml. Overall, the 72 hpi time point seems to be a turning point in the developmental cycle of *P. amoebophila*, since both groups of data – the intracellular as well as the extracellular – follow a significantly different trend from this time point.

Since two later time points, namely 168 hpi and 216 hpi, were quantified only once each in two different experiments and thereby rely on a small sample size, these data were not integrated into the graph and the table presented in figure 10. However, the data could contribute to a better understanding of the infection cycle and are therefore summarized in table 17. Compared to the earlier time points outlined in figure 10, there was a statistically significant twofold increase of intracellular bacterial concentration between 120 hpi and 168 hpi (7 days post infection), and another 1.35-fold increase between 168 hpi and 216 hpi (9 days post infection). Therefore, a 5.4-fold increase of intracellular bacteria within 6 days (72-216 hpi) could be observed. This is again in contrast to the trend of extracellular bacteria, whose concentration did not change significantly compared to 120 hpi, but would have possibly decreased if the experiment had been extended.

Table 17. Summarized analysis of *P. amoebophila* cell concentration at two late time points*

		Mean cells/ml	SE	Sample size	Tukey's test
intracellular	168 hpi	**1.02 x 10^6**	1.1 x 10^5	13	P < 0.05 for each pair of time point means
	216 hpi	**1.38 x 10^6**	7.1 x 10^4	10	
extracellular	168 hpi	**3.25 x 10^5**	2.8 x 10^4	13	P < 0.05 for each pair except for 120 vs. 168, 120 vs. 216, 168 vs. 216 hpi
	216 hpi	**2.35 x 10^5**	9.3 x 10^3	12	

* SE, standard error of mean;

As mentioned at the beginning of this chapter total cell numbers for each time point and fraction (intra-, extracellular) were calculated to determine infectious proportions (see next chapter), since relatively low bacterial numbers obtained from the primary infection required the infection of a constant number of 5 x 10^3 amoebae with total available bacterial cells. Therefore, numbers of introduced bacterial cells per amoeba – corresponding to theoretical MOIs – varied among the different conditions. As shown in table 18, theoretical MOIs were generally higher for bacteria that had been collected as the intracellular fraction (MOI 1.5-16.0), and consequently lower for the extracellular fractions (MOI 0.8-9.2). Interestingly, the percentage of bacteria that could be retained after primary infection and subsequent quantification procedure was consistently low, as determined from total bacteria at 0 hpi (intracellular + extracellular bacteria) per initially

introduced bacteria (1 x 10^6 purified EBs). More precisely, mean 3.8% of 10^6 bacteria could be recovered and mean 42.6% of total recovered bacteria were found to be intracellular.

Notably, neither intracellular nor extracellular fractions of uninfected controls contained detectable bacteria. As controlled by FISH, extracted bacteria could be confirmed to be *P. amoebophila*.

Table 18. Total cell numbers available for secondary infection and resulting theoretical MOIs when infecting 5 x 10^3 amoebae

		Experiment 1		Experiment 2		Experiment 3	
	Hpi	Number of bacteria	MOI	Number of bacteria	MOI	Number of bacteria	MOI
intracellular	0	1.9 x 10^4	3.8	1.1 x 10^4	2.3	1.1 x 10^4	2.3
	24	2.5 x 10^4	5.0	9.7 x 10^3	1.9	2.4 x 10^4	4.9
	48	2.2 x 10^4	4.4	7.5 x 10^3	1.5	3.1 x 10^4	6.1
	72	3.0 x 10^4	6.0	9.6 x 10^3	1.9	2.5 x 10^4	5.0
	96	4.4 x 10^4	8.8	1.4 x 10^4	2.9	2.5 x 10^4	5.0
	120	8.0 x 10^4	16.0	2.4 x 10^4	4.8	7.9 x 10^4	15.8
	168			7.1 x 10^4	4.3		
	216					1.1 x 10^5	21.5
extracellular	0	8.6 x 10^3	1.7	1.8 x 10^4	3.5	4.6 x 10^4	9.2
	24	6.5 x 10^3	1.3	7,3 x 10^4	1.6	3.5 x 10^4	7.0
	48	5.2 x 10^3	1.0	5.6 x 10^3	1.1	3.1 x 10^4	6.1
	72	3.9 x 10^3	0.8	4.4 x 10^3	0.9	2.9 x 10^4	5.7
	96	1.2 x 10^4	2.4	1.1 x 10^4	2.1	4.2 x 10^4	8.4
	120	1.6 x 10^4	3.2	4.4 x 10^4	8.7	4.0 x 10^4	8.1
	168			3.3 x 10^4	6.5		
	216					5.9 x 10^4	11.8

* Numbers in grey indicate incomplete data for the respective time points. Thus, these numbers were excluded from general statements.

3.4.2 Quantification of infectious progeny over time

The chlamydial progeny that were produced during the primary infection were used to infect a defined number of 5 x 10^3 amoebae in order to determine the proportion of infectious progeny.

For this purpose, intracellular chlamydial signals detected by immunofluorescence were quantified 12 hpi, since at that time point no cell division takes place according to FISH analysis. Consequently, each intracellular chlamydial signal should represent a single infectious descendant. Statistical analysis corresponds to analysis that was performed for the number of chlamydial cells at different time points (previous chapter), since the organization of data (two fractions and several time points within each fraction) had not changed.

The graph in figure 11 shows that both the intracellular as well as the extracellular progeny contained a starting level of about 10% infectious chlamydial particles, or differently phrased the bulk of bacteria in either fraction consisted of uninfectious chlamydial cells. According to Tukey's test for statistically significant differences between pairs of means, this low infectivity did not significantly change for the intracellular progeny until 72 hpi, although intracellular sample means slightly rise from 9% to 29% infectivity within these 3 days. However, there was a sudden increase in infectious intracellular progeny observable between 72 and 96 hpi, namely from 29% to 66%. This rapid increase is even more evident if mean intracellular infectious proportions of 0, 24, 48 and 72 hpi are combined and averaged to 15% infectivity, assuming that there is no significant increase in infectious progeny within the first 3 days. Consequently, an increase of 51% within 24 hours, or more generally expressed a 3.4-fold increase in infectious intracellular progeny between infection and 4 days post infection (96 hpi) can be reported. At time point 96 hpi the intracellular chlamydial population consisted of 66% infectious and 34% non-infectious bacteria, which is obviously the peak of infectivity, since 24 hours later the infectious proportion significantly dropped to a level of 35% infectious progeny. Noteably, this number represents a sudden reversion of the peak-ratio from 66/34 to 35/65. Also, the intracellular infectivity at 120 hpi is not significantly different from infectivity at 72 hpi, thereby highlighting the reversion to a relatively low infectious proportion. Interestingly, the late but insufficiently tested time point 216 hpi or 9 days post infection confirmed this trend of decreasing infectious progeny (Table 18).

The curve for the infectivity of extracellular progeny was similar to the curve addressing the intracellular progeny, but shows a 1 day-delay of increase in infectious progeny (Fig. 11). More precisely, there was no significant change in infectivity of extracellular bacteria between 0 and 96 hpi according to the results of the statistical analysis (Fig. 11). Nevertheless, a slight decrease of sample means from 9% to 1-2% infectious progeny between 0 and 72 hpi as well as a slight increase from 2% at 72 hpi back to 10% at 96 hpi could be detected. However, infectivity within the first four days of infection seems to be low, since 90-99% of total extracellular bacteria are

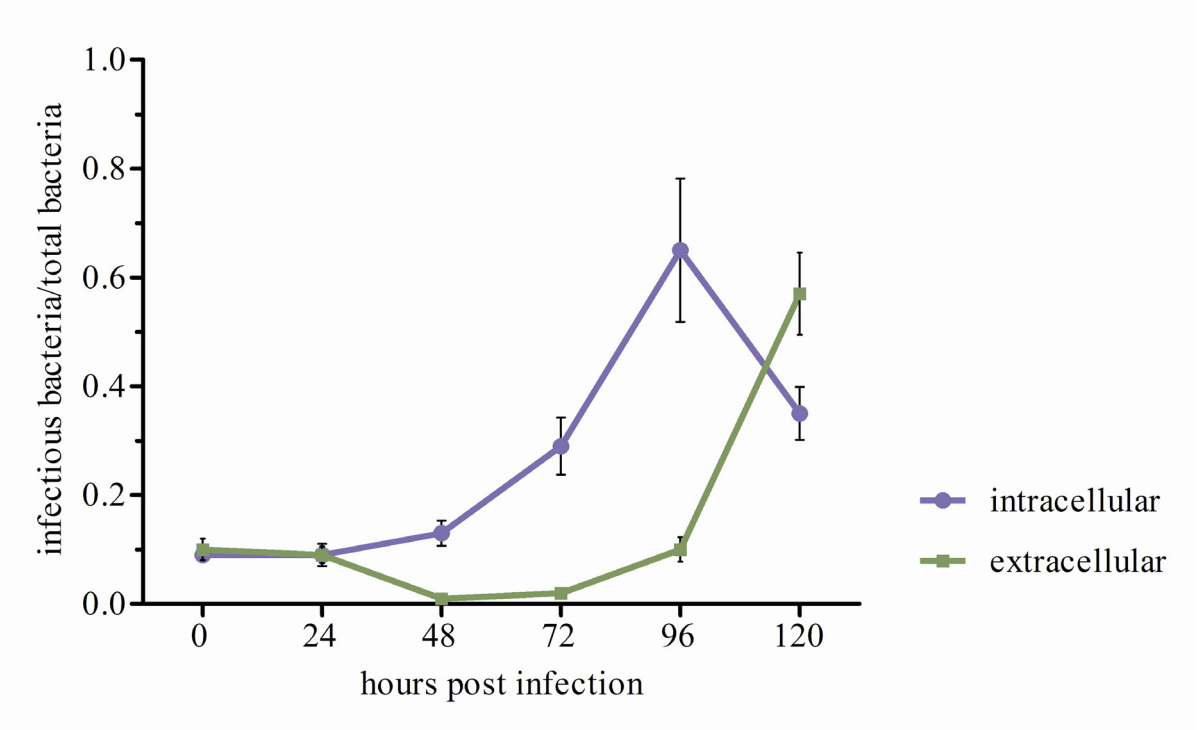

1way ANOVA	intracellular	P < 0.0001				
	extracellular	P < 0.0001				
Statistical significance (Tukey's Multiple Comparison Test, P < 0.05)	0	24	48	72	96	120 hpi
0		no	no	no	yes	yes
24	no		no	no	yes	no
48	no	no		no	yes	no
72	no	no	no		yes	No
96	no	no	no	no		yes
120 hpi	yes	yes	yes	yes	yes	

Figure 11. Proportion of infectious intracellular (purple) and extracellular (green) *P. amoebophila* at time points 0, 24, 48, 72, 96 and 120 hpi as determined by quantification of intracellular bacterial immunofluorescence signals 12 hpi. The graph shows mean proportions of infectious bacteria (infectious bacteria over total bacteria) ± standard error of mean (SE). The uninfected control did not show any detectable bacterial signal. Results from tests for statistical significance of differences among the means (1-way ANOVA, Tukey's Multiple Comparison Test) are summarized in the table below the graph. Differences were considered statistically significant when P values were smaller than 0.05.

non-infectious. Between 96 and 120 hpi a sharp increase from 10 to 57% infectious progeny could be detected, which corresponds to a 5.7-fold increase within 24 hours. In other words, more than half of all extracellular bacteria at this time point were infectious, whereas in the

meanwhile the percentage of infectious intracellular progeny had already dropped. As depicted in table 19, decrease of extracellular infectivity similar to the intracellular trend could be observed, so that both curves reached a similar low level of infectivity (8%) at 216 hpi.

Table 19. Summarized analysis of infectious progeny of two late time points[1]

		Infectious bacteria/total bacteria	SE	Sample size	Tukey's test
intracellular	168 hpi[2]	no data			P < 0.05 only for 96 vs. 216 hpi
	216 hpi	**0.07**	0.01	11	
extracellular	168 hpi	**0.43**	0.04	11	P < 0.05 for 0 vs. 168, 24 vs. 168, 48 vs. 168, 72 vs. 168, 96 vs. 168, 120 vs. 216, 168 vs. 216 hpi
	216 hpi	**0.08**	0.01	14	

[1] SE, standard error of mean;
[2] No data available due to technical problems.

In order to rule out that infectivity curves reflect the different MOIs used for secondary infection in each experiment and condition, all MOIs used (table 18) were plotted against normalized infectious proportions of each condition (fraction, time point) and experiment, thereby plotting 18 different MOIs per fraction (intra-, extracellular) against 18 corresponding normalized

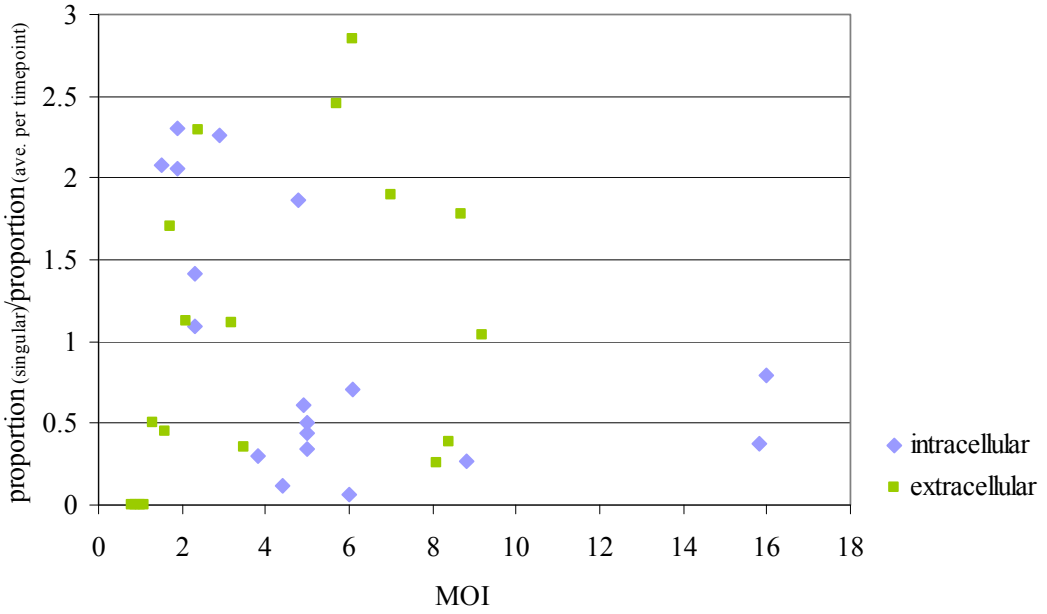

Figure 12. Relation of the MOI to infectious proportions at different time points post infection. All MOIs used in secondary infection were plotted against corresponding infectious proportions that were normalized to combined average infectious proportions in order to account for an unbiased analysis of the effect of MOI on observed changes of infectious proportions.

proportions (Fig. 12). The number of 18 resulted from the number of experiments (3) multiplied by the number of time points (6). Normalization was performed by dividing the average

infectious proportion for each condition and experiment by the combined average infectious proportion for each time point in order to account for the time-based trends in levels of infectious bacteria. This normalization procedure facilitates an unbiased analysis of the effect of MOI on infectious proportion by accounting for the effect of time in the data set.
Since data points in figure 12 do not follow any trend, but instead are clearly randomly distributed, increase in infectivity with increasing MOI can be rejected for the range of MOIs used in this work (MOIs 0.8-16). For example, the two highest MOIs 15.8 and 16 resulted in low infectivity values, whereas MOIs less than 2 were able to yield very high values of infectivity.

3.5 The host cell viability assay

Since iron deprivation would have an effect on viability of the host *Acanthamoeba* sp., a reproducible test for viability was required that could reliably reflect ratios of dead and viable amoebae. The results regarding the different approaches to assess viability of amoebae via propidium iodide (PI) staining are summarized in table 20. Notably, differentiation between dead and viable cells could not be accomplished when amoebae were either pre-treated (fixation) or post-treated by mounting with common anti-fadent media (Citifluor, Vectashield/DAPI, Mowiol), since either all cells or an unnaturally high proportion of cells were PI-stained and therefore considered dead. In general, only approaches that just involved buffer allowed for high viability of host cells. However, the simplest approach – mounting of PI-stained amoebae attached to coverslips with 1x PBS and immediate microscopic inspection – facilitated differentiation (Fig. 13), but viability values varied considerably between experiments. This was presumably due to relatively quick but spatially uneven desiccation of cells, which could be followed by a change of amoebal morphology during evaluation of the assays. More precisely, while the bulk of cells exhibited structures typical for viable amoebae such as pleiomorphic appearance and needle-like projections (pseudopodia) immediatly after mounting, amoebae started to round up, pseudopodia disappeared and the cytoplasm lost its structures soon after mounting.
Nevertheless, mounting in 1x PBS provided an insight into the PI staining behaviour: A 50 minutes-incubation with PI was found to result in a more distinctive staining of cells than the 30 minutes-incubation, namely a clear differentiation between the bright-red nuclei and the scattered PI staining of the cytoplasm (Fig. 13C). It could be also observed that some dying cells show dynamic blebs of PI-stained material located at the cell boundaries (Fig. 13E). Interestingly, PI-stained cells could be correleated to granular cell morphology and absence of

vacuoles in the majority of cases and notably not only for death due to desiccation, as observed by phase contrast microscopy (Fig. 13).

Although mounting with the viscous SPG buffer as well as with the modified SPG buffer (2x sucrose) facilitated high viability of amoebae at the beginning of evaluation, there was again an increase in dying cells detectable after about one hour of inspection – a time period that was likely to be exceeded when quantifying viability under different conditions.

Table 20. Performance of different PI staining approaches to differentiate between dead and viable amoebae

	Method	Staining device	Viability of untreated amoebae	Comment
Pre-treatment before PI staining	Methanol-fixation	Coverslips	100% cells are PI-stained	
	Mg-EtOH incubation	Coverslips	100% cells are PI-stained	
No pre-treatment before PI staining	Mounting with 1x PBS	Coverslips	Proportion of PI-stained cells: 72/634 = 0.11 (11%) 95% CI [0.09;0.14]	Viability was highly variable due to desiccation of cells
	Mounting with Vectashield/DAPI	Coverslips	50-70% cells are PI-stained	PI staining correlated with DAPI staining
	Mounting with Citifluor	Coverslips	50-70% cells are PI-stained	
	Mounting with Mowiol	Coverslips	100% cells are PI-stained	
	Sealing with nailpolish	Coverslips	100% cells are PI-stained	
	Mounting with precooled SPG buffer	Coverslips	Proportion of PI-stained cells: 6/254 = 0.02 (2%) 95% CI [0.01;0.05]	Desiccation of cells about one hour after mounting
	Mounting with precooled modified SPG buffer	Coverslips	Almost no cells are PI-stained	Decreased number of viable cells about one hour after mounting
	Direct inspection in chambers	Chambered coverglass	Proportion of PI-stained cells: 12/394 = 0.03 (3%) 95% CI [0.02;0.05]	Viability did not change within several hours

The drawback of desiccation could ultimately be resolved by relocating the staining procedure as well as the evaluation by microscopy to a single device – chambered coverglass (Nunc) – thereby allowing for high viability over several hours, since cells were residing in closed buffer-containg chambers throughout the entire procedure. Desiccation-independent features of PI-stained amoebae that were observed for amoebae mounted with 1x PBS, could be confirmed for the chamber-method (Fig. 14).

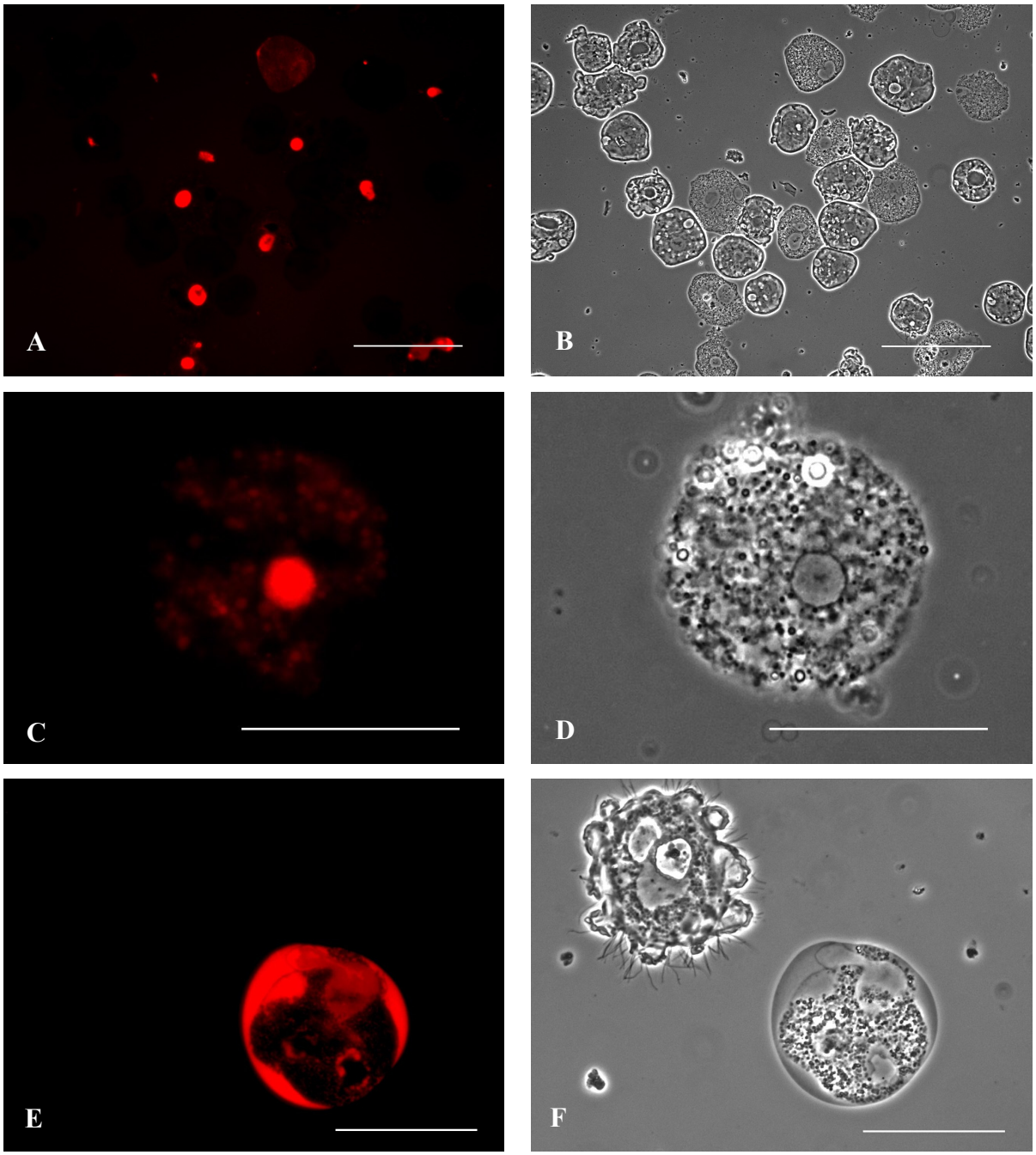

Figure 13. Differentiation between dead and viable *A. castellanii* Neff via PI staining. Dying cells are stained red due to membrane permeability and hence binding of PI to nucleic acids (A, C, E), but are also clearly recognizable by phase contrast microscopy (B, D, F). (A, B) Relatively low viability due to desiccation of cells. (C, D) Amoebal cell death not caused by desiccation. (E, F) Direct comparison of a viable and a dying cell. All images show PI-stained amoebae mounted with 1x PBS. Bars, 10 µm.

Interestingly, PI-stained heavily infected amoebal cultures showed PI-stained moving coccoid forms of bacterial size within vacuoles and in the surrounding buffer. These amoebae were not considered to be dead, since they looked viable as inferred from morphology. Instead, PI-stained forms could represent dead and phagocytosed endosymbionts which had been released from lysed host cells and as a consequence had died. Floating amoebal cysts were thought to be partially removed during a washing step before PI staining, so that the extent of encystment was

not included in the assessment of the effect of DAM in subsequent experiments. Remaining encysted amoebae showed either no PI staining or a very bright and homogeneous PI signal.

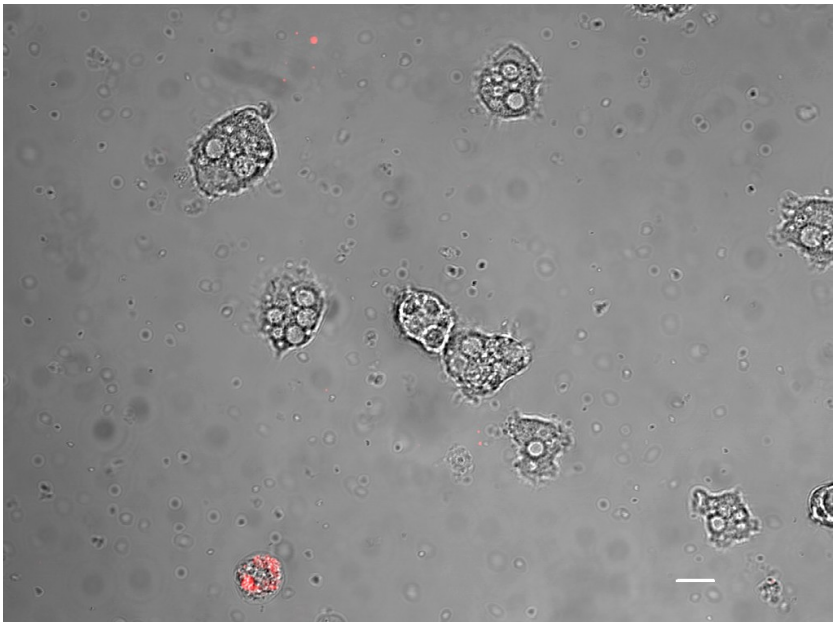

Figure 14. The viability assay performed in chambered coverglass. The image shows an overlay of the DIC (differential interference contrast) and the corresponding PI image. Note the amoebal vacuoles characteristic for viability. Bar, 10 µm.

3.6 Growth in DGM-21A defined medium

Endosymbiont-free and infected amoebae were maintained in DGM-21A medium in order to eventually perform iron deprivation studies in a definable environment. Both *A. castellanii* Neff and *Acanthamoeba* sp. UWC1, as well as the respective *P. amoebophila*-infected amoebae initially attached to the culture flask surface when transferred from TSY or PYG medium to defined medium and stayed attached for about one week. Within this week infected amoebae exhibited limited growth as reflected by lower cell density when compared to endosymbiont-free counterparts. When infected amoebae were harvested within 2 to 7 days after initial inoculation and transferred to a new culture flask containing defined medium, they failed to re-attach or detached after a few hours in both the original culture that had been subjected to shaking and the freshly inoculated culture. In contrast, uninfected amoebae seemed to be unaffected since they behaved similar to amoebae in TSY or PYG. Once infected amoebae were detached, no recovery through threefold exchange of defined medium within one week could be observed. Also, newly prepared DGM-21A medium could not prevent detachment of infected amoebae. However, 1 ml TSY medium added to 8 ml defined medium allowed for re-attachment of infected amoebae after the harvesting procedure.

3.7 Effects of iron chelation in modified PYG medium

Since infected amoebae could not be maintained in DGM-21A defined medium, modified PYG medium (without $Fe(NH_4)_2(SO_4)_2*6\ H_2O$) was tested for effects on amoebal viability upon iron chelation through deferoxamine mesylate (DAM). At that point it was assumed that normal growth of untreated amoebae would not be impaired in modified PYG, since 2g/l yeast extract should account for the lack of the withdrawn iron compound, at least within a limited period of time. Afterwards, normal growth of amoebae in modified PYG as concluded from morphology and comparison with amoebae cultivated in regular PYG could be maintained for several weeks.
As depicted in figure 15, exposure to a high concentration of the iron-chelating compound DAM for 4 days only exerted an effect in terms of decreased viability, when iron chelation was performed in modified PYG. This effect was particularly clear for infected amoebae since the non-exposed controls showed a very low percentage of dead cells as well as the exposed amoebae in regular PYG, whereas the DAM-exposed amoebae in modified PYG showed an elevated level of dead cells (17%, 95% CI 14.1% to 20.5%).
However, the effect of iron chelation on uninfected amoebae could not be explicitly assessed, since the percentage of dead cells for the non-exposed control in modified PYG was too high (10%) and the 95% CI too wide (6.9% to 16.2%) to state a significant difference between the control and the corresponding DAM-exposed cells. At least an effect on uninfected amoebae in regular PYG could be excluded due to the high viability of these cells when exposed to DAM. Notably, the following studies of viability under iron-deprived conditions (next chapter) resulted in much lower non-exposed control values for proportions of dead uninfected cells in modified PYG.

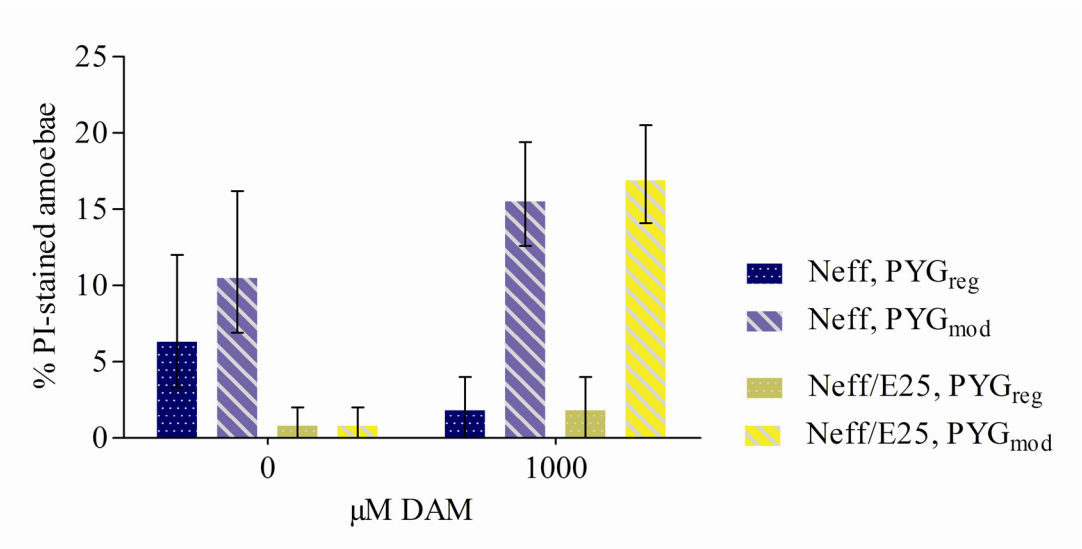

Figure 15. The effect of iron chelation in regular PYG (PYG_{reg}) and modified PYG (PYG_{mod}) on uninfected

(Neff) and asynchronously infected amoebae (Neff/E25) 4 days after exposure to DAM. Bars show % PI-stained amoebae and 95% CIs for proportions. Note that similar results could be obtained for *A. castellanii Neff* and *Acanthamoeba* sp. UWC1.

Generally, amoebal morphology and cell density on day 4 of DAM exposure reflected the results described above, namely a clear increase of non-viable cells upon exposure to 1000 µM DAM for amoebae in modified, but not in regular, PYG. Cells challenged with reduced iron availability, due to the lack of additional iron in the medium as well as the chelating of free iron, showed restricted growth and a higher number of detached cells, whereas the controls and the DAM-exposed cells in regular PYG exhibited similar cell density. Also, a morphological change to elongated and narrow amoebal bodies could be observed for amoebae exposed to 1000 µM DAM in modified PYG.

3.8 Effects of different deferoxamine mesylate (DAM) concentrations on host cell viability

The determination of host cell viability under different iron-chelating conditions was required to set an upper DAM concentration limit for subsequent studies about phenotypic effects on the endosymbiont. As shown in figure 16, the percentage of viable endosymbiont-free and synchronously infected amoebae after 5 days of DAM exposure slightly fluctuated but did not drop dramatically between 0 and 250 µM DAM. In fact, there was an overall change of viability of 3% within the mentioned range of DAM concentration, so that not less than 95% of cells were

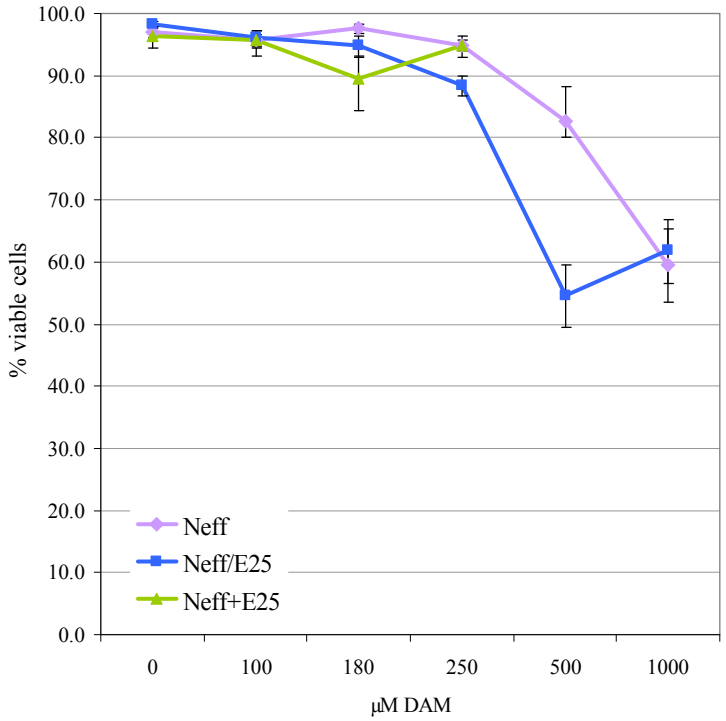

Organism	µM DAM	Proportion of viable cells		95% CI
Neff	0	(2005/2066)	0.970	0.962 to 0.977
	25	(1037/1059)	0.979	0.969 to 0.986
	50	(762/778)	0.979	0.967 to 0.988
	100	(1260/1317)	0.957	0.944 to 0.966
	180	(1454/1489)	0.976	0.968 to 0.983
	250	(2347/2473)	0.949	0.940 to 0.957
	500	(254/307)	0.827	0.802 to 0.883
	1000	(155/260)	0.596	0.536 to 0.654
Neff/E25	0	(3406/3466)	0.983	0.978 to 0.987
	25	(1139/1156)	0.985	0.976 to 0.991
	50	(590/617)	0.956	0.937 to 0.970
	100	(776/807)	0.962	0.946 to 0.973
	180	(668/704)	0.949	0.930 to 0.963
	250	(1275/1441)	0.885	0.867 to 0.900
	500	(201/368)	0.546	0.495 to 0.569
	1000	(206/333)	0.619	0.565 to 0.669
Neff + E25	0	(436/452)	0.965	0.943 to 0.978
	25	(139/147)	0.945	0.895 to 0.974
	50	(136/158)	0.861	0.798 to 0.907
	100	(377/394)	0.957	0.932 to 0.973
	180	(172/192)	0.896	0.845 to 0.932
	250	(657/692)	0.949	0.930 to 0.963

Figure 16. Viability of uninfected (Neff), asynchronously infected (Neff/E25) and synchronously infected (Neff + E25) amoebae after 5 days of iron deprivation by DAM exposure in modified PYG medium. The gaph shows percentage of viable cells and corresponding 95% CI for proportions. The table below lists all values (in proportions) that were used to generate the graph and additionally shows values for 25 and 50 µM DAM. Note that proportions were calculated by dividing the number of viable cells by the number of total cells (brackets). Besides, there were no experiments performed for synchronously infected amoebae exposed to 500 and 1000 µM DAM.

found to be viable. However, the viability value for 250 µM DAM, which is identical for both uninfected and synchronously infected amoebae, represented the lower end of this spectrum (95%), which corresponds to the upper limit of the percentage of dead cells (5%) when viability was for the first time assess by the chamber-method (table 20).

The percentage of viable uninfected host cells clearly decreased when exposed to 500 µM DAM, and further dropped when the iron chelator concentration was raised to 1000 µM. While 60% of uninfected cells were viable when exposed to 1000 µM DAM for 5 days, about 85% viable cells could be observed after 4 days under similar conditions (previous chapter) – an increase in percentage of dead cells that was expected due to prolonged DAM exposure time.

Asynchronously infected amoebae reacted differently with increasing DAM concentrations. While cells exposed to 0-180 µM exhibited viability values similar to uninfected and

synchronously infected amoebae (95-98% viable cells), a discrepancy of 6.5% was observable for exposure to 250 µM DAM, since the percentage of viable infected cells dropped below 90%. Importantly, control values (0 µM DAM) and values for 250 µM DAM were derived from relatively large samples (Fig. 16).

A higher sensitivity of asynchronously infected amoebae towards 500 µM DAM could be observed when compared to the corresponding value for uninfected amoebae, thereby causing a steeper decrease of viable cells. This viability value of about 55% could never be undercut but instead represented the lowest detectable level. However, 95% confidence interval (CI) values for exposure of asynchronously infected amoebae to 500 µM and 1000 µM DAM as well as for exposure of uninfected amoebae to 1000 µM DAM overlap, so that (1) these viability values can be considered similar and (2) asynchronously infected amoebae seem to reach this low level earlier in terms of increased iron chelation.

Statistical analysis of viability data as summarized in proportions on the one hand asked for statistical significance of observed differences in viability between the non-exposed control (0 µM DAM) and DAM-exposed samples as expressed by the P value. On the other hand, scientific relevance of statistically significant differences was assessed by determining relative risks of cells to die when exposed to DAM (Table 21). For example, uninfected amoebae exposed to 250 µM DAM were 1.73 times more likely to die than the non-exposed cells. However, the difference between the two proportions was statistically significant. When asynchronously

Table 21. Statistical analysis of DAM exposure

	µM DAM	P values of control (0µM DAM) vs. DAM exposure (Fisher's exact test)	P < 0.05	Relative risk*	95% CI of relative risk
Neff	100	0.0349	yes	1.47	1.03 to 2.09
	180	0.2488	no	0.80	0.53 to 1.20
	250	0.0003	yes	1.73	1.28 to 2.33
	500	< 0.0001	yes	5.85	4.13 to 8.28
	1000	< 0.0001	yes	13.68	10.26 to 18.25
Neff/E25	100	0.0006	yes	2.22	1.45 to 3.40
	180	< 0.0001	yes	2.95	1.97 to 4.43
	250	< 0.0001	yes	6.65	4.99 to 8.88
	500	< 0.0001	yes	26.21	19.92 to 34.50
	1000	< 0.0001	yes	22.03	16.56 to 29.32
Neff + E25	100	0.5966	no	1.22	0.62 to 2.38
	180	0.0011	yes	2.94	1.56 to 5.55
	250	0.244	no	1.43	0.80 to 2.55

* Note that for the calculation of relative risks proportions of dead cell were used.

infected amoebae were exposed to 250 µM DAM, they were 6.65 times more likely to die than the non-exposed control. The P value for this pair is rather low, thereby concluding that sample proportions are highly significally different. Interestingly, the relative risks for exposure to 1000 µM DAM considerably differ for uninfected (13.7) and infected amoebae (22.0), although viability values are located closely to each other at about 60% viability (Fig 16).

No differences in morphology were observable for DAM concentrations below 1000 µM, but slightly less dense amoebae could be observed with increasing DAM concentration. However, iron-deprived amoebae exhibited a dark-red fluorescence other than the fluorescence derived from PI staining, which faded shortly after exposure to light. The intensity of fluorescence was observed to be dose-dependent.

3.9 Effect of iron deprivation on *P. amoebophila*

A phenotypic effect of iron deprivation as conducted by iron chelation in modified PYG medium could be observed using three different methods for visualization, namely DAPI staining, immunofluorescence and FISH. As first detected by DAPI staining (Fig. 17), iron-deprived synchronously infected amoebae showed clearly enlarged bodies, which was in contrast to non-DAM-exposed but also infected controls. More precisely, while controls only exhibited regular-sized bacterial signals typical for 120 hpi, iron-deprived samples generally contained four different types of amoebae. In addition to the three types that could also be observed in non-exposed controls, namely uninfected, highly infected and newly infected amoebae, host cells harbouring large-sized roundish or irregularly shaped DAPI signals could be visualized. These aberrant bodies were non-uniformly in size and numbers per cell, since slightly enlarged as well

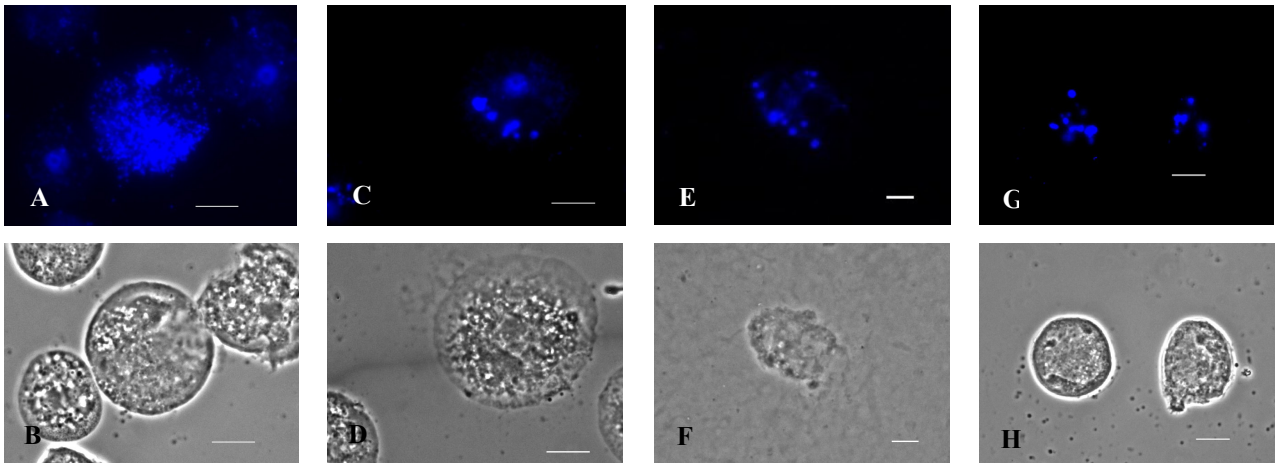

Figure 17. Iron-deprived synchronously infected amoebae as detected by DAPI staining 5 days after infection (120 hpi) and DAM exposure. Iron chelation was performed in modified PYG medium. Iron-deprived amoebae contained either normal-sized endosymbionts (A and B) or aberrantly large forms as shown for 25 µM DAM (C and D), 180 µM DAM (E and F) and 250 µM DAM (G and H). Bars, 10 µm.

as dramatically enlarged forms were present in numbers of one to ten per cell (Fig. 17). Amoebal cells showing aberrant bodies often were additionally infected with regular-sized bacteria, but overall these amoebae seemed to be less strongly infected than amoebae that were packed with only small-sized endosymbionts (Fig. 17A). Enlarged DAPI signals appeared mostly as homogenously stained, unstructured bodies.

Enlarged forms already appeared at the lowest examined DAM concentration (25 µM, Fig. 17C), although the frequency of amoebae with aberrant signals was estimated to be slightly lower than at 100, 180 and 250 µM DAM. However, no detectable differences in appearance between different DAM concentrations as well as no difference in frequency between samples exposed to 100, 180 and 250 µM DAM could be discovered. 1-3 amoebae per 10 infected amoebae are estimated to show enlarged forms. Also, infected amoebae exposed to 500 µM DAM did not show an obvious increase in number of cells containing enlarged forms.

The results obtained by DAPI staining could be confirmed by immunofluorescence (Fig. 18). However, the first immunofluorescence experiment could not properly confirm the identity of enlarged bodies, since the *P. amoebophila*-specific antibody exhibited a high background signal, so that endosymbionts could not be consistently detected or insufficiently intense signals against the background were observed. This observation was true for regular endosymbionts as well as for aberrant forms. Also DAPI staining could not be obtained consistently. For example, the amoebal cell nucleus could be detected in figure 18B but not in figure 18A. Similarly, bacteria were detected by DAPI only occasionally.

However, signals derived from anti-Hsp60 antibody confirmed the presence of aberrantly large bodies of presumably bacterial origin under iron deprivation. These signals were homogenous as described for DAPI signals, but noticeably rather regular-shaped, equally-sized and often located close to each other. Also, generally less aberrant signals per amoebal cell could be observed.

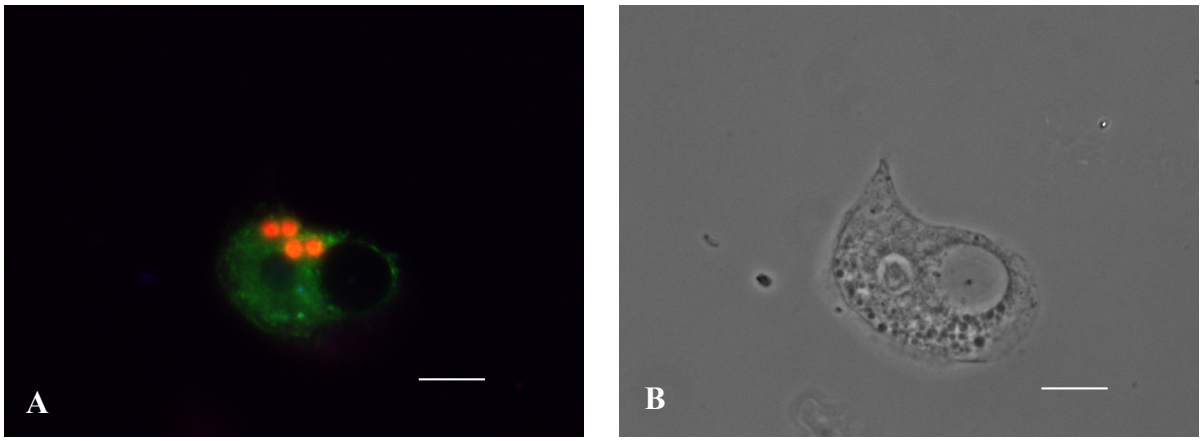

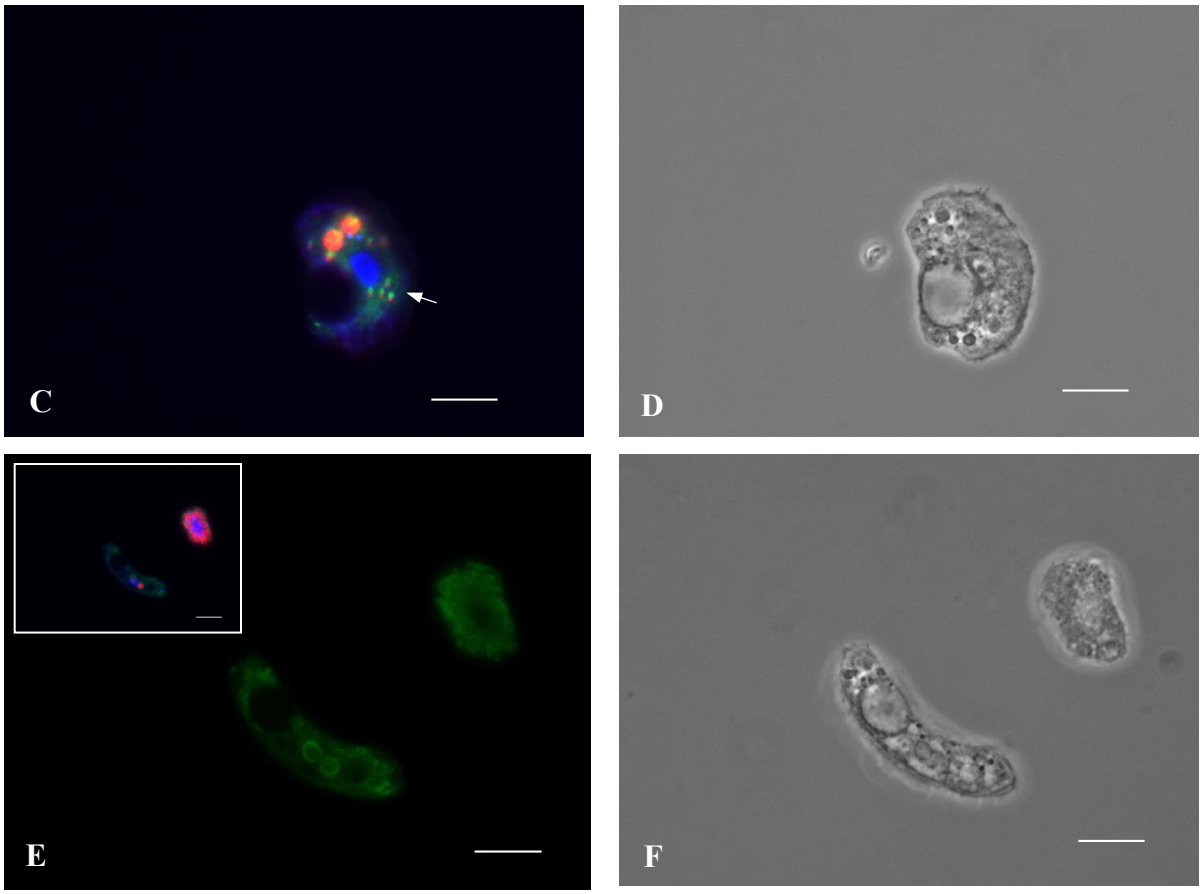

Figure 18. Iron-deprived synchronously infected amoebae as detected by immunofluorescence 5 days after infection (120 hpi) and DAM exposure. Endosymbionts were targeted with anti-Hsp60 antibody detected by Cy3-conjugated secondary antibody (red) and anti-*P. amoebophila* antibody visualized by FITC-conjugated secondary antibody (green). Additionally, cells were DAPI-stained. (A) Large bacterial bodies when exposed to 100 µM DAM. (C) Large bacterial bodies and regular-sized endosymbionts at 250 µM DAM (arrow). (E) Large ring-shaped anti-*P. amoebophila* signals (green) within the lower cell at 250 µM DAM. The inset shows the corresponding three-channel overlay revealing the upper amoebal cell to be infected with regular-sized endosymbionts. Corresponding phase contrast images are shown in B, D and F. Note that cells were methanol-fixed before antibody incubation. Bars, 10 µm.

Recognizable signals derived from anti-*P. amoebophila* antibody formed large rings corresponding to the shape of anti-Hsp60 signals (Fig. 18E), as can be usually observed for regular protochlamydial forms.

Two examples for the difference in size were determined through the measurement tool offered by the LSM image analysis software (Zeiss). While a single regular-sized endosymbiont of figure 19A exhibited an approximate area of 0.92 µm^2 (r = 0.54 µm), two differently sized but clearly enlarged forms showed areas of 7.53 µm^2 (r = 1.55 µm) and 13.94 µm^2 (r = 2.10 µm) respectively. Aberrant forms were therefore found to be 8 to 15 times larger than regular forms. Corresponding bacterial cells in figure 19A are shown by arrows.

The aberrant forms could be assigned to *P. amoebophila* when identity was confirmed by detection through *P. amoebophila*-specific antibody (Fig. 19A) and the *P. amoebophila*-specific FISH probe (Fig. 19C). Notably, the images of figure 19 show iron-deprived asynchronously

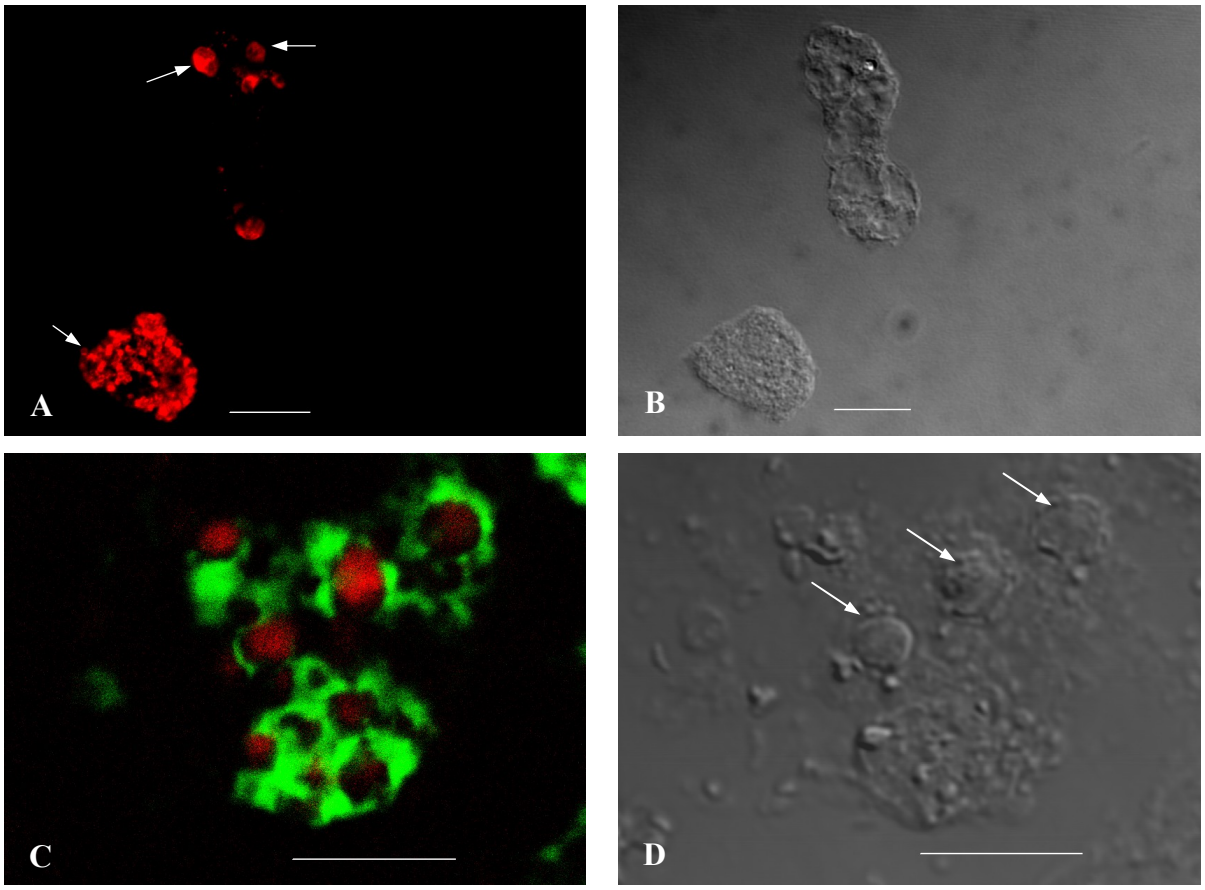

Figure 19. Specific detection of enlarged *P. amoebophila* cells 5 days after exposure to 250 µM DAM. (A) Anti-*P. amoebophila* antibody visualized by Cy3-conjugated secondary antibody (red) was used for immunofluorescence after PFA-fixation. The image shows an amoebal cell infected with a high number of regular-sized endosymbionts and above another cell exhibiting enlarged bacterial bodies. Cells whose sizes were measured are labeled by arrows. (C) Cy3-linked E25-454 oligonucleotide probe specific for *P. amoebophila* (red) in combination with *Acanthamoeba*-specific Acanth412a probe linked to FLUOS (green) was used for detection by FISH. Corresponding DIC images are shown in (B) and (D). Three enlarged forms denoted by arrows can be observed in (D). Note that asynchronously infected amoebae were used in this iron deprivation experiment. Bars, 10 µm.

infected amoebae. However, no difference in morphology or frequency of aberrant forms could be observed compared to synchronously infected amoebae. Remarkably, FISH signals could not always be obtained for enlarged forms, as concluded when comparing DAPI and *P. amoebophila*-specific FISH signals. Existent FISH signals were weaker than regular signals and appeared again homogenous and unstructured. Most of the endosymbiont-specific regular and aberrant immunofluorescence signals in figure 19A were ring-shaped, as could be observed before for this antibody. However, this distinctive signal-shape could not be photographed.

It should also be mentioned that individual aberrantly-sized bodies were rarely present in infected amoebae that had been cultivated under normal conditions. Deprivation of iron however resulted in a clearly increased occurrence of enlarged forms.

4 Discussion

The increased appearance of endosymbionts exhibiting an aberrant morphology under iron-deprived conditions but not under highly nutritious conditions suggests that the two different modes of chlamydial existence – the productive and the aberrant mode – depend on the growth conditions which are determined by the host cell's environment. Therefore, the discussion of the results that were obtained in this work is divided into two main parts, namely the discussion of the developmental cycle under conditions that are supposed to be optimal for host cell growth on the one hand, and the speculative switch to a persistent state presumably caused by nutrient deprivation on the other hand.

4.1 The phenotypic developmental cycle of *P. amoebophila* under favourable conditions

4.1.1 The cycle as observed by fluorescence *in situ* hybridization (FISH)

The application of fluorescence *in situ* hybridization (FISH) to track the chlamydial developmental cycle was already suggested earlier (Poppert *et al.*, 2002), but has so far only been used to provide proof of suitability of this approach but not to follow the development of newly discovered chlamydial organisms although identification of previously unknown chlamydial organisms is ongoing (Corsaro *et al*., 2007; Israelsson, 2007; Karlsen *et al*., 2008; Thomas *et al*., 2006). In the study mentioned above, FISH was used to specifically track the developmental cycle of the pathogen *C. pneumoniae*, a well-characterized relative of *P. amoebophila*. However, what was proposed to be a shortcoming for clinical application – the detection of *C. pneumoniae* from 12 hours post infection (hpi) but not earlier as well as the absence of detectable FISH signals for purified elementary bodies (EBs) – was considered to be advantageous for this work. More precisely, the detection of 16S rRNA through fluorescently-labeled oligonucleotide probes allows only for visualization of viable and metabolically active cells thereby facilitating detection of earliest chlamydial metabolic activity. Consequently, the transition from metabolically inert EBs to metabolizing reticulate bodies (RBs) as well as the transition back to EBs should be temporally definable when comparing FISH signals to total intracellular bacteria. In other words, targeting *P. amoebophila* with FISH probes combined with the general nucleic acid stain DAPI during a synchronized infection as conducted in this work should allow for differentiation between EBs and RBs and therefore characterization of major phenotypic events of the developmental cycle of *P. amoebophila* within their amoebal hosts, provided that this *Chlamydia*-like organism and *C. pneumoniae* share the distinctive EB and RB qualities.

Notably, it has been shown in our laboratory that samples of highly purified *P. amoebophila* EBs occasionally show FISH signals (Barbara Sixt, diploma thesis), which is in contrast to the observation for purified *C. pneumoniae* EBs, as mentioned above (Poppert *et al*., 2002). However, the detection of FISH signals probably indicates variation in rRNA levels due to the presence of metabolically active transitory forms (intermediate bodies) that had been co-purified due to similar density rather than metabolic activity of EBs, since most of the cells did not show any detectable FISH signal. It can therefore be assumed for this qualitative work, that mature EBs of *P. amoebophila* are mostly not detectable by FISH, but instead only RBs and intermediate bodies (IBs).

In fact, differential detection of *P. amoebophila* forms during synchronous infection of both *Acanthamoeba castellanii* Neff (*A. castellanii* Neff) and *Acanthamoeba* sp. UWC1 by FISH could be observed in this work. While bacterial FISH signals were very rare immediately after infection (0 hpi), they began to appear as early as 6 hpi, thereby indicating an increasing number of ribosomes and/or accessibility of bacteria presumably due to a beginning transition from EBs to RBs 6 hpi. However, the inconsistent appearance of bacterial FISH signals 6 to 12 hpi suggests a slight asynchronism in early development of P. *amoebophila*. Since the 6 hpi time point was the earliest time point examined apart from 0 hpi, an even earlier time point such as 3 hpi would have been interesting in order to further narrow down the first metabolic activity as assessed by the appearance of bacterial FISH signals.

In accordance with the finding described above, the rare detection of extracellular bacterial FISH signals at 0 hpi suggests the presence of IBs or RBs in purified *P. amoebophila* samples that were used for infection. This is even more likely as purification in this work was not achieved by density gradient centrifugation as applied for purification of *P. amoebophila* EBs in the experiment mentioned above, but by a quicker method that just involves two successive ultracentrifugation steps in sucrose-phosphate-glutamate (SPG) buffer. Based on the assumption on extracellular FISH signals, the rarely observed FISH signals within amoebae 0 hpi could have been (1) in fact extracellular but attached to the amoebal cell, they could (2) represent IBs/RBs that were uptaken by phagocytosis and would subsequently be subjected to digestion, or (3) either IBs and/or RBs are infectious and therefore could be found intracellularly. The latter case can be carefully excluded, since the absence of infectious RBs is indicated in the experiment that examines infectious progeny production (see next chapter). For ultimate proof of non-infectious RBs however, purified *P. amoebophila* RBs should be used in infection experiments.

The steady number of intracellular bacteria between 0 and 12 hpi suggest that no bacterial cell division takes place within the first 12 hours of infection. However, bacterial FISH signals

appeared stronger and slightly larger 12 hpi when compared to 6 hpi. Again, this implies an even higher ribosome content that could reflect a still ongoing metabolic change towards the full metabolic capacity of RBs.

The results obtained in this study further suggest the first appearance of mature RBs to occur between 12 and 24 hpi, since pairs of closely associated but clearly separated DAPI signals 24 hpi indicate cell division of endosymbionts – a feature that has been only observed for RBs (AbdelRahman and Belland, 2005). The observation of pairs of bacterial cells whose number approximately corresponds to the number of single bacterial cells at the time points before 24 hpi, underlines the recent replication event. Furthermore, the presence of exclusively double-stained intracellular endosymbionts (FISH signal and DAPI staining) at this time point indicates that all endosymbionts undergo transformation from EBs to RBs.

Analysis of time points 48 hpi and 72 hpi revealed the occurrence of similar developmental events. First, the observation of increased numbers of intracellular signals when comparing 24 hpi to 48 hpi and again 48 hpi to 72 hpi suggests ongoing bacterial replication from 24 hpi. Moreover, the first round of replication could have been completed around 48 hpi, since the more abundant intracellular bacterial signals are scattered throughout the amoebal cells thereby suggesting physical separation of the pairs that were observed 24 hours earlier. Second, this increased number of FISH signals appeared very bright and relatively large at both time points, which could be due to the transient accumulation of slightly more than 1-2 replicating bacteria as revealed by DAPI staining at least for the 72 hpi time point, and/or an additional increase of ribosomes in RBs perhaps indicating the peak level of transcription and translation being at 2 to 3 days post infection. Third, the absence of DAPI-only signals at both time points indicates that the transition back to mature EBs does not occur until 72 hpi.

DAPI-only signals were observed as early as 96 hpi thereby indicating the presence of mature EBs at this time point. In other words, transformation from RBs to EBs probably started between 72 and 96 hpi but not earlier, since bacterial replication at 72 hpi was assumed to occur for all intracellular endosymbionts as inferred from the size and the intensity of FISH signals. Consistent with this assumption, FISH signals generally but not exclusively appeared less voluminous than before, which implies ongoing transition from RBs to metabolically less active forms, but at the same time proceeding replication. A high bacterial density within amoebae confirms that replication proceeds after 72 hpi. Thus, the developmental cycle seems to become asynchronous between 72 and 96 hpi. Also, increased extracellular DAPI signals as well as occasional FISH signals were detected for the first time 96 hpi, which suggests beginning release of mostly mature EBs and rarely IBs/RBs from the host cells. The end of the developmental

cycle of *P. amoebophila* in *Acanthamoeba* sp. can therefore be determined to occur between 72 and 96 hpi, provided that it is defined by the first release of intracellular bacteria.
However, the mode of release of *P. amoebophila* can not be assessed by this method, although host cell integrity seemed not to be impaired as inferred from phase contrast microscopy, especially when compared to the infection cycle that was unintentionally performed with *Parachlamydia* sp., thereby excluding host cell lysis as a main route of *P. amoebophila* release.
Five days after infection (120 hpi) and later, similar events have been observed, namely the existence of mature EBs as inferred from DAPI-only signals and the presence of transitory forms (IBs) and replicating forms (RBs). Since more amoebae seemed to be infected 120 hpi than between 0 and 96 hpi – an observation that was feasible due to the incomplete initial infection of amoebae – new infection by released EBs can be suggested. Therefore, transitory forms at this time point might be both RB-to-EB as well as EB-to-RB intermediates. In summary, constant release of EBs is assumed to take place from sometime between 72 and 96 hpi, resulting in continuous reinfection of amoebae after 96 hpi. All processes and chlamydial forms described in this chapter are believed to occur in parallel from sometime between 96 and 120 hpi, whereby a synchronously infected culture converts into an asynchronous culture during that time.
A thought that arose when observing the obviously replicating endosymbionts 24 hpi was as follows: On the one hand, pairs of adjacent chlamydial cells are formed after cell division. On the other hand, each individual cell is surrounded by an inclusion membrane and these single-cell inclusions are dispersed throughout the amoebal cytoplasm, as previously shown (Collingro *et al*., 2005a; Fritsche *et al*., 2000) and supported by the FISH/DAPI images presented in this work. Therefore, replication occurs within the inclusion membrane, but has to involve a subsequent separation of not only daughter cells but additionally the inclusion membrane. This additional step is not necessary for relatives of *P. amoebophila*, since they form large multi-cell inclusions where replicating bacteria presumably accumulate and inclusion membranes grow. Consequently, there must be a difference between *P. amoebophila* and the other *Chlamydiaceae* facilitating that two cells and the inclusion membrane are pulled apart.

4.1.2 Speculations about asynchronous infections

Based on routine microscopic observation of asynchronously infected cultures, speculations about the dynamics between *P. amoebophila* and their *Acanthamoeba* sp. hosts can be made when cultivated in complex media such as PYG and TSY. As mentioned before, continuous release of infectious particles (EBs) leads to continuous reinfection of amoebae, which replicate themselves thereby supplying new host cells. As long as nutrients are supplied, a release-

infection equilibrium should account for a stable host-endosymbiont relationship, provided that endosymbionts usually do not or marginally impair the host cells integrity as it is indicated by a low amount of amoebal cell debris and a steady amount of extracellular bacterial particles in synchronously infected cultures. A slower growth of *Acanthamoeba* sp. UWC1 infected with *P. amoebophila* in contrast to uninfected amoebae has been suggested (Collingro *et al*., 2004), thereby implying reduced fitness of infected amoebae. However, amoebae that had been infected shortly before the start of the growth rate experiment were used for that study, so that the growth rate of established asynchronous cultures was probably not assessed. According to observations in the course of this work, asynchronously infected amoebae of two different *Acanthamoeba* strains are as fit as uninfected amoebae after a phase of adaptation to their endosymbionts. More precisely, both uninfected and infected amoebae grow in complex medium, partly detach or encyst when attachment surface is limited or the medium has not been changed within about 1-2 weeks and are able to recover from starvation due to long periods of not changing the medium. Notably, no obvious differences regarding the cultivation of uninfected and asynchronously infected amoebae were noticed, although quantitative data were not collected. Moreover, viability data derived from propidium iodide (PI) staining of amoebae consistently showed slightly lower amoebal death for asynchronously infected than for uninfected amoebae under normal conditions. Taken together, observations indicate that the *P. amoebophila*-*Acanthamoeba* sp. interaction is stable and generally non-lytic for the amoebal hosts. The main exit mechanism for *P. amoebophila* could therefore be extrusion, as has been suggested to occur in addition to host cell lysis for *Parachlamydia* sp. (Greub and Raoult, 2002) and *C. trachomatis* (Hybiske and Stephens, 2007). However, since *P. amoebophila* can be found in single-cell inclusions, individual bacterial cells would be extruded from host cells. Demonstration of the presence of single-cell containing extracellular vesicles might be more difficult than detection vesicles filled with a higher number of chlamydial particles as it has been shown for the chlamydial relatives.

4.1.3 Validation of the course of infection by infectious progeny production over time

The developmental cycle of *P. amoebophila* in *Acanthamoeba* sp. was monitored by a second, quantitative approach that was aimed at supporting the FISH data by determining proportions of infectious intracellular and extracellular particles over a period of 10 days. Assuming that only mature EBs are able to infect host cells, significant changes in infectious proportions together with comparison between the intra- and extracellular course of infectivity were supposed to shed light on EB-related dynamics such as EB/RB transition and EB release. A comparable method has already been used before, namely for *C. caviae* in *Drosophila* cells (Derré *et al*., 2007) and

C. pneumoniae in epithelial-like cells (Mäurer *et al*., 2007), although the procedure as well as the evaluation performed in those studies slightly differed from the work presented here. More precisely, the quantification of intra- and extracellular bacterial cells at different time points post infection prior to determination of the infectious proportions in these collections of total bacterial cells was added as an intermediate step in this work, thereby theoretically facilitating a comparison of infectious proportions to total cell concentrations. Each intracellular bacterial signal 12 hpi was considered to represent one introduced infectious particle (EB), since cell division of *P. amoebophila* in *Acanthamoeba* sp. had been observed by FISH to be detectable not until 24 hpi.

Both parts of this experiment will be interpreted separately as well as combined, since they are experimentally connected and only the combination of bacterial concentrations with infectious proportions provides a comprehensive picture of dynamics during an initially synchronized and – according to the FISH data – later asynchronized infection with *P. amoebophila*. The integration of infectious proportions into bacterial concentrations is subsequently referred to as concentration of infectious bacteria.

The most striking discovery concerning bacterial concentrations over time is the apparent stagnation of intracellular bacterial cell numbers between 0 and 72 hpi, thereby implying the absence of bacterial growth during this period of time at first view. However, this finding would clearly contradict the previous results obtained by FISH analysis, which indicates start of growth of endosymbionts between 12 and 24 hpi. Considering the nature of different morphological forms, the detection only of rigid and structurally stable forms seems likely. In other words, RBs could have been lysed during the quantification procedure due to osmotic fragility. While most of the steps were conducted in sucrose-phosphate-glutamate (SPG) buffer – a buffer that is widely used in work with endosymbionts (Bovarnick *et al*., 1950) – the last step, namely the filtration onto membranes, was carried out in regular PBS buffer. Transfer of total collected bacteria from SPG buffer to PBS buffer could have caused osmotic lysis of RBs due to decreased osmolarity (from ~0.5 osmol/l to ~0.3 osmol/l), but not of EBs and possibly IBs, so that RBs were not included in the quantification. Therefore, a quantification method that would possibly detect both EBs and RBs, could have been real-time PCR, as previously performed for *Parachlamydia* sp. (Greub *et al*., 2003b).

Since suspensions used for quantification and re-infection were equally split prior to these two final experiments so that bacteria were not exposed to PBS buffer but only SPG buffer before determination of infectious progeny production, the presence of RBs can be assumed for bacterial suspensions that were used to infect amoebae. Therefore, the graph showing infectious

proportions over time (Fig. 11) rightly depicts the number of infectious bacteria over the number of bacteria that survived the quantification procedure (EBs, IBs), but notably when RBs were potentially present. Consequently, the number of introduced bacteria might have been higher than the theoretical multiplicities of infection (MOIs) determined through filtration and DAPI staining, depending on the extent of RB presence. Since infectious proportions depend on both number of infectious particles and number of introduced bacteria, smaller proportions would be expected when RBs are present, but proportions would not change in the absence of RBs. The curve for infectious extracellular proportions should reflect actual dynamics because RBs are not expected to be released or to survive an extracellular environment. The curve for infectious intracellular proportions indeed allows for monitoring major developmental changes, but probably lacks accuracy in varying degrees due to the presence of different amounts of RBs over time.

However, a major trend can be already inferred from the quantification of intracellular bacterial numbers, because presumably only EBs and IBs were detected: An exponential increase of intracellular cells (EBs/IBs) from 72 hpi until 7 days post infection (168 hpi) indicating the first transformation from RBs to EBs taking place between 72 and 120 hpi. This trend is confirmed by the data for infectious proportions showing that 65% of all intracellular bacteria are infectious 96 hpi, whereas 72 hpi a low proportion insignificantly different from values earlier in development was demonstrated to be infectious. Therefore, as already shown by FISH, mature EBs probably arise between 72 and 96 hpi. The presence of non-infectious bacteria shows that not only mature EBs but probably also IBs were detected and exist intracellularly 96 hpi. Moreover, the intracellular increase of EB/IB concentration suggests continuous replication and a still existent capacity of amoebae to harbour growing endosymbionts, which could be either due to growth of amoebae or capacity limit of amoebae had not been reached until 168 hpi. The increase of EBs/IBs flattens between 168 and 216 hpi, thereby indicating saturation of host cells with endosymbionts. Interestingly, this assumed period of 9 days to fill up host cells corresponds to the impression that has been received during the infections for FISH analysis, namely the complete infection of all amoebae at about 10 days post infection when infecting with a theoretical MOI 10. The relatively flat slope of the intracellular-curve (doubling within 72 and 120 hpi) can be explained by the asynchronous transformation of RBs to EBs, which was also indicated by the FISH data.

Remarkably, the value for 96 hpi is the highest proportion value that has been measured, thereby indicating lower amounts of mature EBs compared to total cell numbers at later time points which reflects the growth of endosymbionts at later time points as well as asychronism from 96

hpi leading to shifts in proportions but an overall stable concentration of infectious particles. More precisely, proportions of infectious bacteria decrease after 96 hpi while numbers of total bacteria rise, thereby establishing a constant concentration of mature intracellular EBs that are present among RBs and IBs. The data therefore suggest a steady state of intracellular EB concentration under favourable conditions. Thus, it is expected that time points later than 216 hpi would yield similar concentrations of infectious particles.

However, steady concentrations of intracellular EBs/IBs between 0 and 72 hpi are rather puzzling, since transformation to RBs should lead to a decrease of intracellular EBs/IBs, provided that only EBs/IBs were detected as proposed before. A possible explanation could be an incomplete separation of extra- and intracellular bacteria during low speed centrifugation. Combination of the information about the total quantification with the data for the infectious proportion shows that between 0 and 72 hpi only a constantly small proportion of intracellular bacteria are actually infectious. When converted to cell concentrations, it turns out that infectivity fluctuates corresponding to the cell concentration during this period of time (similar ratios), thereby indicating biased values for both bacterial cell concentrations and infectivity. Since the concentrations of infectious particles are constantly low and in fact represent the lowest values of all assessed time points, including the insignificantly different value for 72 hpi, it can be suggested that no major change in dynamics of mature EBs occurs within the first 3 days of infection. This finding is again in accordance with FISH data, since no increase in mature EBs has been detected. Moreover, intracellular infectious concentrations are low and do not significantly change in spite of assumedly high intracellular RB contents 24-72 hpi in fractions destined for re-infection, thereby indirectly indicating that *P. amoebophila* RBs are not infectious under given conditions. Also, intracellular infectious proportions would be expected to be lower 24 hpi than 0 hpi and lower 48 and 72 hpi than 24 hpi according to FISH observations (start of EB/RB transition before 24 hpi and absence of mature EBs 48 and 72 hpi), if RB numbers were included in cell concentrations.

The intracellular 0 hpi time point represents a special case because FISH data indicate that there is no or little metabolic activity shortly after infection thereby suggesting either no or beginning transition to RBs at that time point. Consequently, the question arises, whether endosymbionts are infectious shortly after infection. However, due to the putative uncertainty of bacterial concentrations this question can not be clearly answered. Assuming that the initial concentration represents truly all intracellular bacteria 0 hpi, which would be feasible since an increase can be observed later in development and RBs are not expected, only 10 % of bacteria were infectious and conversely 90% of bacteria were non-infectious according to the infectivity data. The

majority of bacteria would have already started transformation which could have led to a loss of infectivity.

According to the curve for the concentration of extracellular bacteria over time, not all EBs that were initially introduced actually infected the amoebae, as indicated by the presence of detectable cells 0 hpi. Assuming however, that not only EBs but also IBs survived the quantification procedure, the bars could also show IBs that were not able to infect due to the possible lack of the infectious quality. The subsequent gradual decrease in extracellular cell concentration confirms that (1) there is no release of bacteria within the first 3 days of infection and that (2) extracellular EBs/IBs are unstable and probably degrade during this period of time. The absence of release indirectly confirms the intracellular presence of RBs during that period of time. Although unstable, they are still detectable 72 hpi. However, infectious proportions show that detected bacteria are slightly infectious after infection, but loose this ability 48 hpi.

A significant rise in infectious extracellular bacteria was observed for 120 hpi, namely a 13-fold increase when compared to the concentration of infectious bacteria 96 hpi and a 100-fold increase compared to 72 hpi. Although statistical analysis revealed that infectious proportions 72 hpi and 96 hpi are not significantly different, an 8-fold rise in concentration of extracellular infectious bacteria as observed between 72 and 96 hpi seems biologically important. This indicates the first release of mature EBs taking place between 72 and 96 hpi, but the bulk of first generation infectious forms being released between 96 and 120 hpi, thereby possibly contributing to the noticeable increase in number of newly infected amoebae that has been observed with FISH. Moreover, the steep rise in infectious extracellular bacteria probably reflects the preceding rise in infectious intracellular bacteria, which was observed 96 hpi.

7 days post infection (168 hpi) the concentration of extracellular infectious bacteria is slightly decreased, but nevertheless elevated compared to initial numbers. This indicates a steady number of extracellular mature EBs from approximately 120 hpi, thereby possibly facilitating constant re-infection. The relatively high overall concentrations of extracellular but non-infectious bacteria might be a result of initially non-infectious bacteria that were detected throughout the 9-day infection experiment. Additionally, released EBs that did not infect and therefore degraded as well as possibly released IBs could have contributed to the non-infectious proportion.

Taken together, the quantitative data derived from the infectious progeny experiment (1) confirm the developmental cycle as observed by FISH and (2) imply a balance between infecting and released bacteria under favourable conditions that supports the impression of a stable host-endosymbiont relationship between *P. amoebophila* and *Acanthamoeba* sp. (Fig. 19). However, early events in development such as EB/RB transition and replication of RBs could not be

detected directly by this approach, although there is the potential for resolution when changing the quantification method. The potential drawback of this antibody-based method of infectious progeny evaluation to not only detect truly infectious but also dead particles, is suggested to exert a minor influence on results, since similar trends were yielded in three different experiments independent of the number of introduced bacteria and in accordance with FISH results, thereby indicating the varying infectious proportions to reflect changing numbers of infectious particles over time and hence EB-dynamics rather than random uptake of non-infectious or dead endosymbionts by host cells.

4.1.4 Comparison of the *P. amoebophila* cycle with cycles of chlamydial relatives

As demonstrated in this work by FISH and in previous studies by ultrastructural analysis (Collingro *et al*., 2005a; Fritsche *et al*., 2000), *P. amoebophila* in *Acanthamoeba* sp. occurs mainly in single-cell inclusions. Dividing RBs might be a temporary exception as inferred from DAPI-stained cell pairs that were detected between 24 and 72 hpi during synchronized infections in this study. This characteristic is clearly in contrast to the type of existence of closely related as well as less closely related chlamydiae: the sister species *P. naegleriophila* is described to occur as single cells or group of cells in the cytoplasm of its original host *Naegleria* sp. (Michel *et al*., 2000); the sister genus *Neochlamydia* also seems to lack surrounding vacuoles (Horn *et al*., 2000), while *Parachlamydia* – the second sister genus – is mostly present in vacuoles containing multiple bacteria during replication in *Acanthamoeba polyphaga* and *Acanthamoeba* sp. UWC1 (Collingro *et al*., 2005b; Greub and Raoult, 2002), as well as in *A. castellanii* Neff as indicated by the observation of distinctive cauliflower-like structures which were described in this work; other *Chlamydia*-like bacteria such as *Criblamydia*, *Waddlia* and *Simkania* were reported to occur as single or numerous grouped cells within vacuoles in amoebae and cell lines of higher eukaryotes (Chua *et al*., 2005; Goy *et al*., 2008; Kahane *et al*., 2001; Kahane *et al*., 2002; Michel *et al*., 2004; Thomas *et al*., 2006). Similarly, the clinically relevant *Chlamydia* and *Chlamydophila* were described to accumulate within large vacuoles in human-derived host cells. Therefore, *P. amoebophila* is the only known chlamydial species that mainly occurs in single cell inclusions.

Assuming that the developmental cycle of *Parachlamydia* sp. presented in this work is representative for chosen conditions, the cycles of the two members of *Parachlamydiaceae* – *Parachlamydia* sp. and *P. amoebophila* – can be compared, especially because the infection conditions were similar. Besides, the *Parachlamydia* cycle has already been partially

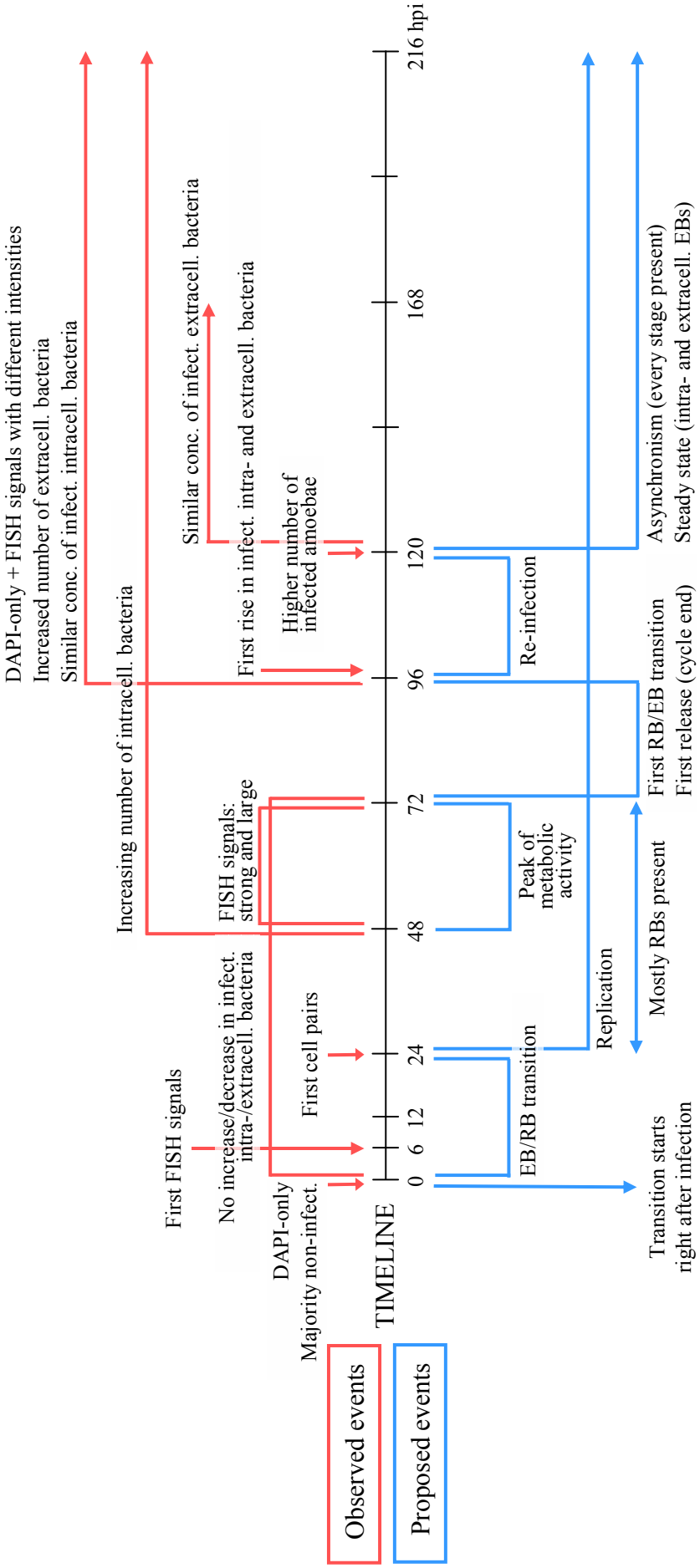

Figure 19. Timeline of observed (red) and proposed events (blue) during 9 days (216 hours post infection, hpi) of a synchronized infection (MOI 10) of *Acanthamoeba* sp. with *P. amoebophila* in complex medium. Infect., infectious. Intracell., intracellular. Extracell., extracellular. Conc., concentration.

characterized by ultrastructural analysis (Greub and Raoult, 2002) – although notably under conditions substantially different from conditions in this study – therefore representing an obvious point of reference when close phylogenetic relationship is considered. However, since the synchronized *Parachlamydia* infection was unintentionally obtained and therefore performed only once and assessed by only an order-specific FISH probe combined with DAPI staining of mixed performance, drawn conclusions have to be considered carefully.

Nevertheless, the developmental cycle of *Parachlamydia* sp. as monitored in this work suggests a timeline of major events similar to *P. amoebophila*, perhaps partly due to similar conditions, namely the same host, MOI and experimental procedure. More precisely, replication of *Parachlamydia* sp. seems to be ongoing 24 hpi as indicated by beginning accumulation of bacterial FISH signals and the enlarged square-shaped FISH signals that are in contrast to the small-sized and coccoid FISH signals clearly observable 96 and 120 hpi. Further replication is suggested by growing clusters of bacteria 48 and 72 hpi that indicate an increase of inclusion size from about 24 hpi to 72 hpi. Since amoebal host cells are packed with bacterial FISH signals 72 hpi, the majority of intracellular bacteria is believed to exist as RBs, provided that the detection of FISH probes is indicative for metabolic activity therefore allowing for a rough differentiation of EBs and RBs as discussed earlier. However, the small number of bacterial FISH signals 0 hpi compared to the theoretical MOI 10 and the increased number of FISH-detected bacteria 24 hpi indicates differential detection of chlamydial forms by FISH probes similar to observations for *P. amoebophila*. Release of bacteria seems to start between 72 and 96 hpi, since an elevated number of extracellular coccoid forms as well as intracellular DAPI-only signals suggesting the presence of metabolic inactive forms (mature EBs) are present 96 hpi. Moreover, the common dispersed nature of bacteria in contrast to the previous distinctive cluster structure together with the not clearly delimited amoebal boundaries indicate host cell lysis to occur around this time point and also 120 hpi thereby facilitating release of bacteria. In summary, *Parachlamydia* sp. seems to transform to RBs within about 24 hpi, replicates between 24 and 72 hpi and finally first exits the amoebae between 72 and 96 hpi, thereby clearly following a similar timeline as *P. amoebophila*. However, different from *P. amoebophila*, *Parachlamydia* sp. in *A. castellanii* Neff forms multiple larger inclusions and possibly elicits host cell lysis as an exit mechanism under given conditions.

A different time course was previously proposed for *Parachlamydia acanthamoeba* strain Hall's coccus in *Acanthamoeba polyphaga*. Briefly, RBs were reported to dominate 8 hpi, whereas 36 hpi EBs made up more than half of the intracellular chlamydial forms, thereby possibly indicating first RB-to-EB transition to occur earlier in the cycle than observed in this work. Also,

release through host cell lysis or expelled bacteria-containing vesicles 144 hpi in PYG medium and lysis between 3 and 5 days post infection in PAS buffer was reported in that study (Greub and Raoult, 2002). Importantly, results for the two early time points were obtained when performing the infection in PAS buffer, at 32°C and MOI 2. Also, a different amoebal species, a defined parachlamydial strain as well as a different method of assignment of chlamydial forms – namely transmission electron microscopy – were used, so that comparison to *P. amoebophila* and the unknown parachlamydial strain acquired in this work is difficult. It can be reported however, that the type of inclusions and an exit mechanism that involves host cell lysis is confirmed by the study, therefore underlining these two differences to *P. amoebophila* and generally the power of FISH to study chlamydial development. The differences to the parachlamydial cycle observed in this work could be due to different conditions and/or the description of events either based on ultrastructural classification of chlamydial forms (Greub and Raoult, 2002) or morphology visualized by FISH (this work).

As already indicated in chapter 4.1.2, *P. amoebophila* seems to be the only characterized chlamydial organism that does not primarily destroy its host cells and at the same time readily replicates and spreads between host cells when compared to other well-characterized chlamydial developmental cycles which have been conducted under standard conditions for respective chlamydiae. The mode of release for the *Chlamydia*-like organism *Simkania negevensis* in *Acanthamoeba* sp. has not yet been determined, but according to previous studies (Kahane *et al*., 2001) either non-replicative existence or very slow spread of infection without apparent lysis of amoebae is indicated. Therefore, *S. negevensis* represents the only chlamydial organism other than *P. amoebophila* that is possibly non-parasitic for amoebal host cells, but possibly different from *P. amoebophila* persists rather than actively exploits the host cell for maximal replication. In contrast, data from other chlamydiae such as *Waddlia chondrophila*, *Neochlamydia hartmanellae* as well as *Chlamydiaceae*, clearly suggest death of host cells to be a major outcome of infection independent from the host cell type, either due to apoptosis or lysis of host cells.

The *P. amoebophila* cycle length of 3 to 4 days, the length being defined as the period of time from infection to first release, corresponds to the length of a *C. pneumoniae* cycle, where host cell lysis and thereby release of progeny takes place 84 hpi (Wolf *et al*., 2000) and consistently the first substantial rise in extracellular EBs occurs between 72 and 96 hpi (Mäurer *et al*., 2007), similar to the observed increase of infectious extracellular *P. amoebophila*. Interestingly however, re-differentiation to EBs, as inferred from ultrastructure as well as from quantification of EB progeny, is reported to start earlier for *C. pneumoniae*, namely from 48 hpi in contrast to

the proposed time point of 72 hpi for *P. amoebophila*. Therefore, less time between the start of the re-differentiation process and the release of mature EBs is suggested to elapse for *P. amoebophila*, which could be due to a quicker re-differentiation of *P. amoebophila* RBs to mature EBs. This possible delay of *C. pneumoniae* release could be also speculated to occur due to its inclusion morphology: Multiple large inclusions are thought to contain chlamydial forms of different stages because of asynchronized re-differentiation to EBs from 48 hpi (Wolf *et al*., 2000). In order to account for release of mostly mature EBs, inclusions would have to gradually accumulate transformed forms and at the peak of EB number eventually exit by host cell lysis or individually by extrusion (Hybiske and Stephens, 2008). In contrast, *P. amoebophila* could release mature EBs individually and stepwise, starting when first mature EBs appear, since they occur in single-cell inclusions. A period of 2 days between start of re-differentiation to EBs and release was also indicated for *C. trachomatis*, whose developmental cycle is shorter, namely 2-3 days, so that re-differentiation starts about 24 hpi (Nicholson et al., 2003).

4.2 Infection under iron deprivation

Since members of *Chlamydiaceae* could be observed to exist in a state different from elementary and reticulate bodies in *in vitro* studies, the question whether *Chlamydia*-like organisms such as *P. amoebophila* are able to develop these so-called persistent forms that as part of an alternative phase of the developmental cycle, was started to being addressed in this work. Iron deprivation as a persistence-trigger was selected for three reasons. First, exposure of *P. amoebophila*-infected amoebae to different antibiotics – namely ampicillin, tetracycline, rifampicin, erythromycin and chloramphenicol – did not have any detectable morphological effects on the endosymbionts (personal communication, Eva Heinz) and was therefore considered to be suboptimal as a trigger. Notably, treatment of *C. trachomatis* and *C. psittaci* infected host cells with penicillin G has been shown to cause the formation of aberrantly large chlamydial forms (Lambden *et al*., 2006; Matsumoto and Manire, 1970), which were able to recover upon removal of penicillin (Matsumoto and Manire, 1970). Second, iron is considered to be an essential nutrient for most organisms including intracellular bacterial pathogens (Schaible and Kaufmann, 2004) and as such is crucial for heme proteins (e.g. cytochromes), non-heme proteins (iron-sulfur proteins) and iron-activated enzymes (e.g. ribonucleotide reductase), whereby deprivation is expected to evoke environmental stress which would possibly cause the entry into a persistent state. Third, iron deprivation conducted by chelation of intracellular iron has been shown to cause persistence of *Chlamydiaceae* in cell culture studies. Hallmarks of iron-deprived

chlamydiae were described to be decreased infectivity, predominance of RBs at late time points post infection, presence of irregularly shaped RBs and smaller inclusions (Hogan *et al*., 2004).

4.2.1 The viability assay

PI staining and subsequent microscopic differentiation between PI-stained, dead and unstained, viable amoebae was the method of choice to evaluate viability of host cells during iron deprivation by exposure to the iron chelator deferoxamine mesylate (DAM), since PI is known to quickly and reliably stain dead cells based on a loss of membrane integrity. Due to the absence of protocols for examination of amoebal viability by PI staining in literature, a PI staining procedure that would facilitate reproducible and plausible numbers of dead cells had to be developed. Notably, different procedures were tested and compared under favourable growth conditions, where high proportions of viable cells were expected.

The failure of pre-treated cells to show unstained cells is obvious, since fixatives such as methanol and ethanol permeabilize and kill cells thereby allowing for diffusion of PI into the cells and eventually binding to nucleic acids. Therefore, fixation prior to PI exposure could not be used to differentiate viable and dead cells, but might be useful as a counterstaining in combination with immunofluorescence or FISH. Also, mounting of PI-stained cells with anti-fading media did not facilitate differentiation, possibly due to toxic components that caused cell death either quickly as observed for Mowiol or gradually for Citiflour and Vectashield/DAPI, as indicated by high numbers of dead cells but not 100% right after mounting.

Consequently, 1x PBS buffer was chosen since it allowed for non-restricted viability and a low fluorescent background. However, only the PI staining in buffer combined with microscopically accessible chambers ensured high viability of reproducible quality, since desiccation of amoebae was prevented. The use of one chamber for the entire viability assay – the temporary cultivation, PI staining and evaluation – potentionally avoided loss of stressed cells that could have burst during mechanical stress caused by transfer of cells. Alternatively, evaluation of viability could have been accomplished by flow cytometry, although this approach would have probably needed a double staining combining PI and a live stain such as calcein AM to reliably determine viability. Instead, the combination of PI staining and distinctive morphology of dead amoebae facilitated confirmation of PI-based results in this work.

4.2.2 Modified PYG medium facilitates iron deprivation experiments

Infected amoebae could not be maintained in DGM-21A defined medium for *Acanthamoeba* sp., which was developed for uninfected amoebae (Schuster, 2002). The presence of endosymbionts

therefore possibly causes a lack of yet undefined nutrients for the host. Iron depletion experiments in defined medium without the iron source ferrous sulfate were thought to enforce an effect on *P. amoebophila*, since the host is believed to readily endure and buffer shortage of nutrients as inferred from long-term maintenance of unfed amoebal cultures.

In fact, severe iron chelation by DAM in regular complex amoebal medium (PYG medium) that contains yeast extract as well as ferrous ammonium sulfate as iron sources, could not generate a lack of iron that was sufficient to impair viability of uninfected and asynchronously infected amoebae. It was expected though, that truly iron-deprived organisms would exhibit an increased number of dead cells. Therefore, iron chelation in regular PYG medium was considered to be unable to generate an intracellular iron-depleted environment that would eventually lead to iron deprivation of endosymbionts. However, this conclusion was not confirmed by studies on chlamydial morphology.

In contrast, PYG medium that lacked ferrous ammonium sulfate combined with severe iron chelation allowed for effects on amoebal viability, whereby iron deprivation experiments were further conducted in this modified PYG medium. Interestingly, the sole remaining iron source yeast extract purchased from Oxoid Ltd. was found to contain about 52 parts per million (ppm) of iron (http://www.oxoid.com), which corresponds to 1.86 µM iron being externally available for organisms when cultivated in modified PYG. This iron concentration is much lower than the additional 180 µM iron available in the presence of ferrous ammonium sulphate, whereby chelation of extracellular free iron by DAM – which is reported to occur in an equimolar manner (Keberle, 1964) – could consume too much DAM to efficiently deplete intra-amoebal iron pools.

4.2.3 The proper deferoxamine mesylate (DAM) concentration for iron deprivation experiments

Viability of host cells under different concentrations of DAM was determined prior to evaluation of possible phenotypic effects on the endosymbionts, since toxic effects of DAM on amoebae that were assumed to be reflected in viability, could have indirectly caused a bacterial stress response instead of a desired direct effect induced by an iron-depleted intra-amoebal environment. The optimal DAM concentration for iron deprivation experiments was therefore considered to be the highest concentration that did not harm the uninfected hosts – the degree of influence being measured as percentage of viable cells (viability). Ideally, asynchronously infected amoebae would show decreased viability which would presumably be due to a depleted amoebal iron pool rather than a toxic effect of DAM on amoebae, since uninfected counterparts

were not stressed upon exposure to the same DAM concentration. An increased requirement for iron as a result of heavily infected amoebae could be the reason for diminished viability.
The DAM concentration that actually fulfilled the stated expectations was determined to be 250 µM, whereby effects on endosymbionts were examined primarily for synchronously infected amoebae exposed to this DAM concentration. Although viability of uninfected amoebae exposed to 250 µM DAM was significantly different from the non-exposed control, the difference was considered biologically irrelevant since the percentage of dead amoebae for 250 µM DAM did not exceed 5% - a value that is believed to represent the upper limit of normal cell death in an amoebal population as inferred from numerous viability experiments. However, DAM concentrations below 250 µM (25-180 µM DAM) were thought to potentially cause similar effects on endosymbionts, since in each case more DAM than external iron was added.
DAM concentrations higher than 250 µM were observed to result in clearly increased numbers of dead uninfected and asynchronously infected cells, which suggests either cell death due to unmanageable iron deprivation – increased by the presence of nutrient-exploiting endosymbionts – or toxic effects of DAM independent from iron deprivation.
Adverse effects of DAM occur at different concentrations depending on the cell type: While human macrophages seem to be highly tolerant to DAM (2.5 mM DAM; Newman *et al*., 1994), human monocytes and HEp-2 cells were reported to be rather sensitive (< 35 µM DAM; Al-Younes *et al*., 2001; Byrd and Horwitz, 1989). No viable cells could be detected when the free-living amoeba *Naegleria fowleri* was exposed to 1.5 mM DAM for 4 days or 3 mM for 2 days (Newsome and Wilhelm, 1983). Therefore, *Acanthamoeba* sp. seems to be rather tolerant compared to other cell types, since even 1000 µM DAM caused cell death of only about half of the amoebal population after a 5 day exposure. However, as exposure to 250 µM DAM marks the boundary of normal viability and the first biologically important decrease in viability was observed for 500 µM DAM, the appearance of adverse effects on *Acanthamoeba* sp. can be stated to occur from 250 µM.
Interestingly, synchronously infected amoebae behaved like uninfected amoebae for the DAM concentrations tested, which could be explained by the smaller bacterial load after infection, as a lower number of intracellular bacteria require a smaller amount of amoebal iron.

4.2.4 First hint for a protochlamydial stage different from established forms

The appearance of enlarged intracellular forms of *P. amoebophila* under carefully determined iron-depriving conditions was shown by three different methods of visualization, namely DAPI staining, immunofluorescence and FISH. Signal characteristics allow for speculations about the

nature of aberrant bodies: Observed homogeneous and unstructured DAPI, FISH and Hsp60 signals suggest the enlarged bodies to represent individual but expanded endosymbionts, since for each method intracellular components that are evenly dispersed throughout a cell's cytoplasm are detected. If the bodies would consist of multiple accumulated bacteria, at least DAPI and FISH signals were expected to appear as smaller, sharp-cut clusters of cocci as was possible to be resolved for clusters of *Parachlamydia* sp., although possibly different metabolic characteristics of iron-deprived endosymbionts could cause the targets of DAPI and FISH probes to be scattered and less abundant, so that resolution of multiple spatially close bacteria might not have been possible. However, due to the frequently observed large ring-shaped immunofluorescence signals when anti-*P. amoebophila* antibody was used, the presence of single, enlarged chlamydial forms can be supported, because the antibody was raised against the outer membrane of *P. amoebophila* (Eva Heinz, paper in preparation). This observation could be further confirmed by electron microscopy. The inconsistent presence of additional, mostly weak FISH signals for aberrant forms indicates a lower ribosome content that could be caused by a lower metabolic activity of these forms, which was also observed by transcriptional profiling for persistent *Chlamydiaceae* (Gérard *et al*., 2002; Mäurer *et al*., 2007).

Phenotypic effects of iron deprivation on *Chlamydiaceae* always involve the presence of smaller inclusions containing fewer bacteria thereby indicating restricted growth of iron-deprived chlamydiae (Al-Younes *et al*., 2001; Freidank *et al*., 2001; Mäurer *et al*., 2007; Raulston, 1997). Due to the formation of single-cell inclusions in the case of *P. amoebophila*, the protochlamydial equivalent would be the presence of fewer endosymbionts per amoeba at a late time point post infection. In fact, clearly less densely packed amoebae harbouring affected endosymbionts were frequently observed 120 hpi and post exposure – a time point that, under favourable conditions, implies completion of the cycle including replication. The simultaneous presence of heavily infected amoebae indicates that normal chlamydial growth was still possible, maybe due to differences in amoebal iron pools. Taken together, *P. amoebophila* could share this response to depletion of iron with its pathogenic relatives.

Conflicting reports about the size of RBs under iron deprivation can be found in the literature. While most studies observed regular-sized but occasionally irregularly shaped RBs for *Chlamydiaceae*, enlarged chlamydial forms were reported for *C. psittaci* (Goellner *et al*., 2006) and *S. negevensis* (Kahane *et al*., 2007). Therefore, enlarged forms could be characteristic for some iron-deprived chlamydial species including *P. amoebophila*. As a consequence, single-cell inclusions of *P. amoebophila* are expected to expand, which would be a different outcome than

the smaller inclusions reported for *Chlamydiaceae*, although only caused by the unique inclusion morphology.

Since *P. amoebophila* exhibits morphological features that are similar to observations for chlamydial relatives under iron deprivation, the aberrantly-sized bodies observed in this study might represent persistent forms, or more generally phrased a chlamydial stage at least morphologically different from EBs and RBs in response to adverse growth conditions. However, due to the lack of data validating the hallmarks of persistence, the existence of a persistence-like state and consequently an alternative life cycle can not yet be proposed for *P. amoebophila*. Future work will have to show loss of infectivity as well as reversibility of effects in order to confirm persistence for this *Chlamydia*-like organism.

4.3 Conclusion

In this work, distinctive chlamydial events during the developmental cycle of *P. amoebophila* in *Acanthamoeba* sp. were confirmed and chronologically defined, and therefore facilitate future studies that rely on knowledge about the life cycle of this *Chlamydia*-like organism, as for example gene and protein expression studies. More precisely, EB-to-RB transition and re-differentiation, start of replication, end of the cycle and entry into the asynchronous phase could be monitored. Surprisingly, analysis of the cycle by FISH allowed for remarkably numerous observations and provided valuable information based on different metabolic activities of chlamydial stages. Moreover, obtained data about the developmental cycle provided the basis for speculations about host-endosymbiont dynamics and mode of release. In addition to the established developmental events during favourable growth conditions, protochlamydial forms of altered morphology were detected under iron-deprived conditions. These forms were found to share morphological features of aberrant bodies that have been described for the pathogenic relatives, so that first evidence for a developmental stage different from regular chlamydial forms was presented for *P. amoebophila*.

5 List of Abbreviations

16S rDNA	small subunit ribosomal RNA-encoding gene of prokaryotes
%	percentage
°C	degree celcius
µ	micro (10^{-6})
16S rRNA	small subunit ribosomal RNA of prokaryotes
5'-3'	direction: 5' end to 3' end
A.	*Acanthamoeba*
A260, A280	absorbance at 260, 280 nm
ABC	ATP-binding cassette
ADP	adenosine diphosphate
ANOVA	analysis of variance
ATP	adenosine-5'-triphosphate
ave.	average
B.	*Balamuthia*
bidest.	bidestillatus (double destilled)
bp	base pairs
BSA	bovine serum albumin
c	centi (10^{-2})
C.	*Chlamydia* or *Chlamydophila*
CADD	chlamydial protein associating with death domains
Cand.	*Candidatus*
CBs	crescent bodies
CCD	charge-coupled device
CI	confidence interval
CPAF	chlamydia protease/proteasome-like activity factor
CT	*Chlamydia trachomatis*
*Ct*NTT	nucleotide transporter of *C. trachomatis*
CTP	cytidine triphosphate
Cy3	indocarbocyanine
D.	*Dictyostelium*
DAM	deferoxamine mesylate
DAPI	4',6-diamidino-2-phenylindole
days pi	days post infection
$_{dd}H_2O$	double distilled and filtered water
ddNTPs	dideoxynucleotides
DIC	differential interference contrast
DNA	deoxyribonucleic acid
dNTP	deoxyribonucleotide triphosphate

dTMP	thymidine 5'-monophosphate
dTTP	2'-deoxythymidine 5'-triphosphate
dUTP	2'-deoxyuridine 5'-triphosphate
EB(s)	elementary bodies
EDTA	ethylenediaminetetraacetic acid
EMP	Embden-Meyerhof-Parnas
est.	estimation
$EtOH_{abs.}$	ethanol absolute
FBPs	F-box containing proteins
Fe	iron
Fig.	figure
FISH	fluorescence *in situ* hybridization
FITC	fluorescein isothiocyanate
FLUOS	fluorescein N-hydroxysuccinimidester
g	gram
GCIP	Grap2 cyclin D-interacting protein
GTP	guanosine-5'-triphosphate
H^+	proton
HB	hybridization buffer
hpi	hours post infection
Hsp60	heat-shock protein 60
Hz	hertz
IB(s)	intermediate bodies
IF	immunofluorescence
IFN-γ	interferon-gamma
IgG	immunoglobulin
in prep.	in preparation
incl.	including
kb	kilobases
l	liter
L.	*Legionella*
Lda	lipid droplets-associated protein
LPS	lipopolysaccharides
m	milli (10^{-3}), meter
M	molar
m^2	square meter
Mb	megabases
Mg	magnesium
MHC	major histocompatibility complex
MIP	macrophage infectivity potentiator
mmHg	millimeter of mercury
mod	modified

MOI	multiplicity of infection
n	nano (10^{-9})
n.d.	not determined
Na^+	sodium ion
NAD^+	nicotinamide adenine dinucleotide (oxidized form)
NADH	reduced form of NAD^+
NADPH	reduced form of nicotinamide adenine dinucleotide phosphate
Neff	*Acanthamoeba castellanii* Neff
Neff + E25	*A. castellanii* Neff synchronously infected with *P. amoebophila*
Neff/E25	*A. castellanii* Neff asynchronously infected with *P. amoebophila*
Ø	diameter
osmol	unit of osmotic pressure
P	phosphate
p	pico (10^{-12})
P	P value
P.	*Protochlamydia*
p.a.	pro analyticum (grade of purity)
Pa	pascal
*Pam*NTT	nucleotide transporter of *P. amoebophila*
PAS	Page's amoebic saline
PBS	phosphate buffered saline
PC	*Protochlamydia amoebophila*
PCR	polymerase-chain-reaction
PFA	paraformaldehyde
Pht	phagosomal nutrient transporter
PI	propidium iodide
Pkn	protein kinase related to protein kinase N
ppm	parts per million
PRPP	phosphoribosyl pyrophosphate
PTS	phosphoenolpyruvate:phosphotransferase
PYG	peptone-yeast extract-glucose
r	radius
R.	*Rickettsia*
RB(s)	reticulate bodies
rcf	relative centrifugal force
reg	regular
RFLP	restriction fragment length polymorphism
RNA	ribonucleic acid
rRNA	ribosomal RNA
RT	room temperature
s	seconds
S.	*Simkania*

SD	standard deviation
SE	standard error of the mean
sp.	species
SPG	sucrose-phosphate-glutamate
-S-S-	disulfide bond
T3SS, T4SS	type 3/4 secretion system
Ta	annealing temperature
Tarp	translocated actin-recruiting phosphoprotein
TBE	tris/borate/EDTA
TCA	tricarboxylic acid cycle
TSY	trypticase soy broth with yeast extract
u	unit
UTP	uridine-5'-triphosphate
UV	ultraviolet
V	volt
v/v	volume to volume
vs.	versus
*Vsp*I	restriction enzyme from *Vibrio* species
w/v	weight to volume
WB	washing buffer
x	times

6 Abstract

It is known for members of the obligate intracellular *Chlamydiae* to alternate between two stages that serve different functions during the productive life cycle: infectious but metabolically inert elementary bodies (EBs) are able to survive in an extracellular environment, while fragile reticulate bodies (RBs) replicate intracellularly before bacteria are released after re-differentiation to EBs. In response to deteriorating conditions such as depletion of essential nutrients, pathogenic *Chlamydiaceae* enter a reversible stage morphologically different from EBs and RBs and known as persistent forms. In this work, the developmental cycle of an environmental representative of *Chlamydiae*, namely *Protochlamydia amoebophila* UWE25, was phenotypically characterized in *Acanthamoeba* sp. as a host. By combining fluorescence *in situ* hybridization (FISH) with the nucleic acid stain DAPI, thereby facilitating rough differentiation between EBs and RBs based on differences in metabolic activity, and quantitative analysis of infectious progeny production, distinctive developmental events during a synchronized infection were described and linked to time: first release of bacteria was determined to occur between 3 and 4 days post infection soon after first RB-to-EB transition; replication starts around 24 hours post infection (hpi) and gives rise to an increasing number of RBs which are predominantly present from 24 to 72 hpi; the cycle was observed to become asynchronous 120 hpi. Moreover, quantitative data suggest a stable rather than a parasitic host-endosymbiont relationship, that – in contrast to the related *Parachlamydia* sp. – is primarily non-lytic for its amoebal host. In addition to the well-established biphasic life cycle under favourable conditions, iron deprivation could be visualized to cause elevated levels of morphologically aberrant protochlamydial forms after 5 days of iron chelation by deferoxamine mesylate (DAM). Without having demonstrated further hallmarks of chlamydial persistence to apply to *P. amoebophila*, observed aberrant endosymbionts could represent persistent forms that promote survival under unfavourable conditions.

7 Zusammenfassung

Bakterien, die der obligat intrazellulären Familie *Chlamydiales* angehören, alternieren zwischen zwei Stadien, die verschiedene Funktionen im produktiven Lebenszyklus ausüben: Die infektiösen aber metabolisch inaktiven Elementarkörperchen (EBs) können extrazellulär überleben, während sich Retikularkörperchen (RBs) in den Wirtszellen vermehren, um nach Rückdifferenzierung zu Elementarkörperchen wieder freigesetzt zu werden. Als Reaktion auf sich verschlechternde Wachstumsbedingungen durch zum Beispiel Entzug essentieller Nährstoffe, treten die pathogenen *Chlamydiaceae* in ein reversibles Stadium ein, welches sich morphologisch von EBs und RBs unterscheidet, und als persistentes Stadium bekannt ist. In dieser Arbeit wurde der Entwicklungszyklus eines Vertreters der *Chlamydia*-ähnlichen Bakterien – nämlich *Protochlamydia amoebophila* UWE25 – in dem Wirt *Acanthamoeba* sp. phänotypisch charakterisiert. Dies wurde einerseits durch die Kombination von Fluoreszenz *in situ* Hybridisierung (FISH) mit dem Nukleinsäurefarbstoff DAPI ermöglicht, was vermutlich auf Grund unterschiedlicher metabolischer Aktivität von EBs und RBs eine grobe Differenzierung dieser zwei Formen erlaubte. Andererseits wurden die infektiösen Nachkommen eines Zyklus quantitativ erfasst, sodass letztendlich, mit Hilfe beider Ansätze, wichtige Ereignisse des Entwicklungszyklus beschrieben und zeitlich festgelegt werden konnten: So findet die erste Freisetzung von Bakterien zwischen dem dritten und vierten Tag nach der Infektion und bald nach der ersten Redifferenzierung zu EBs statt; die Replikation beginnt ungefähr 24 Stunden nach der Infektion und hat eine zunehmende Zahl von RBs zur Folge, die anschließend bis 72 Stunden nach der Infektion dominieren; 120 Stunden nach der Infektion wird der Zyklus asychron. Außerdem lassen die quantitativen Daten eine nicht-parasitische, stabile Beziehung zwischen Wirt und Endosymbiont vermuten, welche im Gegensatz zu dem Verwandten *Parachlamydia* sp. in erster Linie nicht lytisch für die Wirtsamöben zu sein scheint. Zusätzlich zu der Charakterisierung des etablierten biphasischen Lebenszyklus unter günstigen Bedingungen konnte gezeigt werden, dass der fünf-tägige Entzug von Eisen mittels des chelatbildenden Deferoxamin-Mesilats (DAM) das vermehrte Auftreten von morphologisch ungewöhnlichen protochlamydialen Formen hervorruft. Ohne weitere Kennzeichen der chlamydialen Persistenz für *P. amoebophila* demonstriert zu haben, kann jedoch über die Ausbildung von persistenten Formen dieses Organismus unter ungünstigen Bedingungen spekuliert werden.

8 References

AbdelRahman, Y.M., and Belland, R.J. (2005) The chlamydial developmental cycle. *FEMS Microbiol Rev* 29: 949.

Al-Younes, H.M., Rudel, T., Brinkmann, V., Szczepek, A.J., and Meyer, T.F. (2001) Low iron availability modulates the course of *Chlamydia pneumoniae* infection. *Cell Microbiol* 3: 427-437.

Amann, R., Springer, N., Schonhuber, W., Ludwig, W., Schmid, E.N., Muller, K.D., and Michel, R. (1997) Obligate intracellular bacterial parasites of acanthamoebae related to *Chlamydia* spp. *Appl. Environ. Microbiol.* 63: 115-121.

Amann, R.I., Binder, B.J., Olson, R.J., Chisholm, S.W., Devereux, R., and Stahl, D.A. (1990) Combination of 16S rRNA-targeted oligonucleotide probes with flow cytometry for analyzing mixed microbial populations. *Appl Environ Microbiol* 56: 1919-1925.

Angot, A., Vergunst, A., Genin, S., and Peeters, N. (2007) Exploitation of eukaryotic ubiquitin signaling pathways by effectors translocated by bacterial type III and type IV secretion systems. *PLoS Pathog* 3: e3.

Beatty, W.L., Morrison, R.P., and Byrne, G.I. (1994) Persistent chlamydiae: from cell culture to a paradigm for chlamydial pathogenesis. *Microbiol Rev* 58: 686-699.

Belland, R.J., Nelson, D.E., Virok, D., Crane, D.D., Hogan, D., Sturdevant, D. et al. (2003a) Transcriptome analysis of chlamydial growth during IFN-γ-mediated persistence and reactivation. *Proc Natl Acad Sci U S A* 100: 15971-15976.

Belland, R.J., Zhong, G., Crane, D.D., Hogan, D., Sturdevant, D., Sharma, J. et al. (2003b) Genomic transcriptional profiling of the developmental cycle of *Chlamydia trachomatis*. *Proc Natl Acad Sci U S A* 100: 8478-8483.

Birtles, R.J., Rowbotham, T.J., Storey, C., Marrie, T.J., and Raoult, D. (1997) *Chlamydia*-like obligate parasite of free-living amoebae. *Lancet* 349: 925-926.

Bovarnick, M.R., Miller, J.C., and Snyder, J.C. (1950) The influence of certain salts, amino acids, sugars, and proteins on the stability of *rickettsiae*. *J Bacteriol* 59: 509-522.

Byrd, T.F., and Horwitz, M.A. (1989) Interferon gamma-activated human monocytes downregulate transferrin receptors and inhibit the intracellular multiplication of *Legionella pneumophila* by limiting the availability of iron. *J Clin Invest* 83: 1457-1465.

Byrne, G.I., Ouellette, S.P., Wang, Z., Rao, J.P., Lu, L., Beatty, W.L., and Hudson, A.P. (2001) *Chlamydia pneumoniae* expresses genes required for DNA replication but not cytokinesis during persistent infection of HEp-2 cells. *Infect Immun* 69: 5423-5429.

Casson, N., Michel, R., Müller, K.-D., Aubert, J.D., and Greub, G. (2008) *Protochlamydia naegleriophila* as etiologic agent of pneumonia. *Emerg. Infect. Dis.* 14: 168-172.

Chellas-Géry, B., Linton, C.N., and Fields, K.A. (2007) Human GCIP interacts with CT847, a novel *Chlamydia trachomatis* type III secretion substrate, and is degraded in a tissue-culture infection model. *Cell Microbiol* 9: 2417-2430.

Chen, D.E., Podell, S., Sauer, J.D., Swanson, M.S., and Saier, M.H., Jr. (2008) The phagosomal nutrient transporter (Pht) family. *Microbiology* 154: 42-53.

Chua, P.K., Corkill, J.E., Hooi, P.S., Cheng, S.C., Winstanley, C., and Hart, C.A. (2005) Isolation of *Waddlia malaysiensis*, a novel intracellular bacterium, from fruit bat (*Eonycteris spelaea*). *Emerg Infect Dis* 11: 271-277.

Cocchiaro, J.L., Kumar, Y., Fischer, E.R., Hackstadt, T., and Valdivia, R.H. (2008) Cytoplasmic lipid droplets are translocated into the lumen of the *Chlamydia trachomatis* parasitophorous vacuole. *Proc Natl Acad Sci U S A* 105: 9379-9384.

Collingro, A., Toenshoff, E.R., Taylor, M.W., Fritsche, T.R., Wagner, M., and Horn, M. (2005a) '*Candidatus* Protochlamydia amoebophila', an endosymbiont of *Acanthamoeba* spp. *Int J Syst Evol Microbiol* 55: 1863-1866.

Collingro, A., Walochnik, J., Baranyi, C., Michel, R., Wagner, M., Horn, M., and Aspöck, H. (2004) Chlamydial endocytobionts of free-living amoebae differentially affect the growth rate of their hosts. *Eur J Protistol* 40: 57-60.

Collingro, A., Poppert, S., Heinz, E., Schmitz-Esser, S., Essig, A., Schweikert, M. et al. (2005b) Recovery of an environmental chlamydia strain from activated sludge by co-cultivation with *Acanthamoeba* sp. *Microbiology* 151: 301-309.

Conant, C.G., and Stephens, R.S. (2007) *Chlamydia* attachment to mammalian cells requires protein disulfide isomerase. *Cell Microbiol* 9: 222-232.

Corsaro, D., and Venditti, D. (2006) Diversity of the *Parachlamydiae* in the environment. *Crit Rev Microbiol* 32: 185-199.

Corsaro, D., Venditti, D., and Valassina, M. (2002) New chlamydial lineages from freshwater samples. *Microbiology* 148: 343-344.

Corsaro, D., Thomas, V., Goy, G., Venditti, D., Radek, R., and Greub, G. (2007) '*Candidatus* Rhabdochlamydia crassificans', an intracellular bacterial pathogen of the cockroach *Blatta orientalis* (Insecta: Blattodea). *Syst Appl Microbiol* 30: 221-228.

Costa, H.S., Westcot, D.M., Ullman, D.E., Rosell, R., Brown, J.K., and Johnson, M.W. (1995) Morphological variation in *Bemisia* endosymbionts. *Protoplasma* 189: 194.

Coulson, P.B., and Tyndall, R. (1978) Quantation by flow microfluorometry of total cellular DNA in Acanthamoeba. *J Histochem Cytochem* 26: 713-718.

Daims, H., Bruhl, A., Amann, R., Schleifer, K.H., and Wagner, M. (1999) The domain-specific probe EUB338 is insufficient for the detection of all Bacteria: development and evaluation of a more comprehensive probe set. *Syst Appl Microbiol* 22: 434-444.

de Bary, A. (1879) *Die Erscheinung der Symbiose*. Strassburg, Austria: Verlag von Karl J. Trubner.

Derré, I., Pypaert, M., Dautry-Varsat, A., and Agaisse, H. (2007) RNAi screen in *Drosophila* cells reveals the involvement of the Tom complex in *Chlamydia* infection. *PLoS Pathog* 3: 1446-1458.

Dilbeck, P.M., Evermann, J.F., Crawford, T.B., Ward, A.C., Leathers, C.W., Holland, C.J. et al. (1990) Isolation of a previously undescribed *Rickettsia* from an aborted bovine fetus. *J Clin Microbiol* 28: 814-816.

Draghi, A., II, Popov, V.L., Kahl, M.M., Stanton, J.B., Brown, C.C., Tsongalis, G.J. et al. (2004) Characterization of "*Candidatus* piscichlamydia salmonis" (order *Chlamydiales*), a *Chlamydia*-like bacterium associated with epitheliocystis in farmed Atlantic salmon (*Salmo salar*). *J Clin Microbiol* 42: 5286-5297.

Drobne, D., Štrus, J., Žnidaršič, N., and Zidar, P. (1999) Morphological description of bacterial infection of digestive glands in the terrestrial isopod *Porcellio scaber* (Isopoda, crustacea). *J Invertebr Pathol* 73: 113-119.

Essig, A., Heinemann, M., Simnacher, U., and Marre, R. (1997) Infection of *Acanthamoeba castellanii* by *Chlamydia pneumoniae*. *Appl Environ Microbiol* 63: 1396-1399.

Everett, K.D., Bush, R.M., and Andersen, A.A. (1999) Emended description of the order *Chlamydiales*, proposal of *Parachlamydiaceae* fam. nov. and *Simkaniaceae* fam. nov., each containing one monotypic genus, revised taxonomy of the family *Chlamydiaceae*, including a new genus and five new species, and standards for the identification of organisms. *Int J Syst Bacteriol* 49 Pt 2: 415-440.

Fields, K.A., Mead, D.J., Dooley, C.A., and Hackstadt, T. (2003) *Chlamydia trachomatis* type III secretion: evidence for a functional apparatus during early-cycle development. *Mol Microbiol* 48: 671-683.

Freidank, H.M., Billing, H., and Wiedmann-Al-Ahmad, M. (2001) Influence of iron restriction on *Chlamydia pneumoniae* and *C. trachomatis*. *J Med Microbiol* 50: 223-227.

Friedman, M.G., Dvoskin, B., and Kahane, S. (2003) Infections with the *Chlamydia*-like microorganism *Simkania negevensis*, a possible emerging pathogen. *Microbes Infect* 5: 1013-1021.

Friis, R.R. (1972) Interaction of L cells and *Chlamydia psittaci*: entry of the parasite and host responses to its development. *J Bacteriol* 110: 706-721.

Fritsche, T.R., Sobek, D., and Gautom, R.K. (1998) Enhancement of in vitro cytopathogenicity by *Acanthamoeba* spp. following acquisition of bacterial endosymbionts. *FEMS Microbiol Lett* 166: 231-236.

Fritsche, T.R., Gautom, R.K., Seyedirashti, S., Bergeron, D.L., and Lindquist, T.D. (1993) Occurrence of bacterial endosymbionts in *Acanthamoeba* spp. isolated from corneal and environmental specimens and contact lenses. *J Clin Microbiol* 31: 1122-1126.

Fritsche, T.R., Horn, M., Wagner, M., Herwig, R.P., Schleifer, K.-H., and Gautom, R.K. (2000) Phylogenetic diversity among geographically dispersed *Chlamydiales* endosymbionts recovered from clinical and environmental isolates of *Acanthamoeba* spp. *Appl. Environ. Microbiol.* 66: 2613-2619.

Gérard, H.C., Krausse-Opatz, B., Wang, Z., Rudy, D., Rao, J.P., Zeidler, H. et al. (2001) Expression of *Chlamydia trachomatis* genes encoding products required for DNA synthesis and cell division during active versus persistent infection. *Mol Microbiol* 41: 731-741.

Gérard, H.C., Freise, J., Wang, Z., Roberts, G., Rudy, D., Krauss-Opatz, B. et al. (2002) *Chlamydia trachomatis* genes whose products are related to energy metabolism are expressed differentially in active vs. persistent infection. *Microbes Infect* 4: 13-22.

Goellner, S., Schubert, E., Liebler-Tenorio, E., Hotzel, H., Saluz, H.P., and Sachse, K. (2006) Transcriptional response patterns of *Chlamydophila psittaci* in different *in vitro* models of persistent infection. *Infect Immun* 74: 4801-4808.

Goy, G., Croxatto, A., and Greub, G. (2008) *Waddlia chondrophila* enters and multiplies within human macrophages. *Microbes Infect* 10: 556-562.

Greub, G., and Raoult, D. (2002) Crescent bodies of *Parachlamydia acanthamoeba* and its life cycle within *Acanthamoeba polyphaga*: an electron micrograph study. *Appl. Environ. Microbiol.* 68: 3076-3084.

Greub, G., Mege, J.L., and Raoult, D. (2003a) *Parachlamydia acanthamoebae* enters and multiplies within human macrophages and induces their apoptosis [corrected]. *Infect Immun* 71: 5979-5985.

Greub, G., Scola, B.L., and Raoult, D. (2003b) *Parachlamydia acanthamoeba* is endosymbiotic or lytic for *Acanthamoeba polyphaga* depending on the incubation temperature. *Ann NY Acad Sci* 990: 628-634.

Greub, G., Collyn, F., Guy, L., and Roten, C.-A. (2004) A genomic island present along the bacterial chromosome of the *Parachlamydiaceae* UWE25, an obligate amoebal endosymbiont, encodes a potentially functional F-like conjugative DNA transfer system. *BMC Microbiol* 4: 48.

Haferkamp, I., Schmitz-Esser, S., Wagner, M., Neigel, N., Horn, M., and Neuhaus, H.E. (2006) Tapping the nucleotide pool of the host: novel nucleotide carrier proteins of *Protochlamydia amoebophila*. *Mol Microbiol* 60: 1534-1545.

Haider, S., Collingro, A., Walochnik, J., Wagner, M., and Horn, M. (2008) *Chlamydia*-like bacteria in respiratory samples of community-acquired pneumonia patients. *FEMS Microbiol Lett* 281: 198-202.

Harb, O.S., Gao, L.Y., and Abu Kwaik, Y. (2000) From protozoa to mammalian cells: a new paradigm in the life cycle of intracellular bacterial pathogens. *Environ Microbiol* 2: 251-265.

Harper, A., Pogson, C.I., Jones, M.L., and Pearce, J.H. (2000) Chlamydial development is adversely affected by minor changes in amino acid supply, blood plasma amino acid levels, and glucose deprivation. *Infect Immun* 68: 1457-1464.

Heinz, E., Kolarov, I., Kastner, C., Toenshoff, E.R., Wagner, M., and Horn, M. (2007) An *Acanthamoeba* sp. containing two phylogenetically different bacterial endosymbionts. *Environ Microbiol* 9: 1604-1609.

Ho, T.D., and Starnbach, M.N. (2005) The *Salmonella enterica* serovar typhimurium-encoded type III secretion systems can translocate *Chlamydia trachomatis* proteins into the cytosol of host cells. *Infect Immun* 73: 905-911.

Hogan, R.J., Mathews, S.A., Mukhopadhyay, S., Summersgill, J.T., and Timms, P. (2004) Chlamydial persistence: beyond the biphasic paradigm. *Infect Immun* 72: 1843-1855.

Horn, M. (2008) *Chlamydiae* as symbionts in eukaryotes. *Annu Rev Microbiol*.

Horn, M., and Wagner, M. (2001) Evidence for additional genus-level diversity of *Chlamydiales* in the environment. *FEMS Microbiol Lett* 204: 71.

Horn, M., and Wagner, M. (2004) Bacterial endosymbionts of free-living amoebae. *J Euk Microbiol* 51: 509-514.

Horn, M., Wagner, M., Muller, K.-D., Schmid, E.N., Fritsche, T.R., Schleifer, K.-H., and Michel, R. (2000) *Neochlamydia hartmannellae* gen. nov., sp. nov. (*Parachlamydiaceae*), an endoparasite of the amoeba *Hartmannella vermiformis*. *Microbiology* 146: 1231-1239.

Horn, M., Collingro, A., Schmitz-Esser, S., Beier, C.L., Purkhold, U., Fartmann, B. et al. (2004) Illuminating the evolutionary history of *Chlamydiae*. *Science* 304: 728-730.

Hueck, C.J. (1998) Type III protein secretion systems in bacterial pathogens of animals and plants. *Microbiol Mol Biol Rev* 62: 379-433.

Hybiske, K., and Stephens, R.S. (2007) Mechanisms of host cell exit by the intracellular bacterium *Chlamydia*. *Proc Natl Acad Sci U S A* 104: 11430-11435.

Hybiske, K., and Stephens, R.S. (2008) Exit strategies of intracellular pathogens. *Nat Rev Microbiol* 6: 99-110.

Iliffe-Lee, E.R., and McClarty, G. (1999) Glucose metabolism in *Chlamydia trachomatis*: the 'energy parasite' hypothesis revisited. *Mol Microbiol* 33: 177-187.

Israelsson, O. (2007) Chlamydial symbionts in the enigmatic *Xenoturbella* (Deuterostomia). *J Invertebr Pathol* 96: 213-220.

Jacobs, A. (1977) Low molecular weight intracellular iron transport compounds. *Blood* 50: 433-439.

Jager, B.V., and Stamm, W.P. (1972) Brain abscesses caused by free-living amoeba probably of the genus *Hartmannella* in a patient with Hodgkin's disease. *Lancet* 2: 1343-1345.

Kahane, S., and Friedman, M.G. (1992) Reversibility of heat shock in *Chlamydia trachomatis*. *FEMS Microbiol Lett* 76: 25-30.

Kahane, S., Kimmel, N., and Friedman, M.G. (2002) The growth cycle of *Simkania negevensis*. *Microbiology* 148: 735-742.

Kahane, S., Dvoskin, B., and Friedman, M.G. (2008) The role of monocyte/macrophages as vehicles of dissemination of *Simkania negevensis*: an *in vitro* simulation model. *FEMS Immunol Med Microbiol* 52: 219-227.

Kahane, S., Everett, K.D., Kimmel, N., and Friedman, M.G. (1999) *Simkania negevensis* strain ZT: growth, antigenic and genome characteristics. *Int. J. Syst. Bacteriol.* 2: 815-820.

Kahane, S., Dvoskin, B., Mathias, M., and Friedman, M.G. (2001) Infection of *Acanthamoeba polyphaga* with *Simkania negevensis* and *S. negevensis* Survival within Amoebal Cysts. *Appl. Environ. Microbiol.* 67: 4789-4795.

Kahane, S., Fruchter, D., Dvoskin, B., and Friedman, M.G. (2007) Versatility of *Simkania negevensis* infection in vitro and induction of host cell inflammatory cytokine response. *J Infect* 55: e13.

Kahane, S., Gonen, R., Sayada, C., Elion, J., and Friedman, M.G. (1993) Description and partial characterization of a new *Chlamydia*-like microorganism. *FEMS Microbiol Lett* 109: 329-333.

Karlsen, M., Nylund, A., Watanabe, K., Helvik, J.V., Nylund, S., and Plarre, H. (2008) Characterization of '*Candidatus* Clavochlamydia salmonicola': an intracellular bacterium infecting salmonid fish. *Environ Microbiol* 10: 208-218.

Keberle, H. (1964) The biochemistry of desferrioxamine and its relation to iron metabolism. *Ann N Y Acad Sci* 119: 758-768.

Koehler, L., Nettelnbreker, E., Hudson, A.P., Ott, N., Gérard, H.C., Branigan, P.J. et al. (1997) Ultrastructural and molecular analyses of the persistence of *Chlamydia trachomatis* (serovar K) in human monocytes. *Microb Pathog* 22: 133-142.

Kostanjšek, R., Štrus, J., Drobne, D., and Avguštin, G. (2004) '*Candidatus* Rhabdochlamydia porcellionis', an intracellular bacterium from the hepatopancreas of the terrestrial isopod *Porcellio scaber* (Crustacea: Isopoda). *Int J Syst Evol Microbiol* 54: 543-549.

Kumar, Y., Cocchiaro, J., and Valdivia, R.H. (2006) The obligate intracellular pathogen *Chlamydia trachomatis* targets host lipid droplets. *Curr Biol* 16: 1646-1651.

Kutlin, A., Flegg, C., Stenzel, D., Reznik, T., Roblin, P.M., Mathews, S. et al. (2001) Ultrastructural study of *Chlamydia pneumoniae* in a continuous-infection model. *J Clin Microbiol* 39: 3721-3723.

Lambden, P.R., Pickett, M.A., and Clarke, I.N. (2006) The effect of penicillin on *Chlamydia trachomatis* DNA replication. *Microbiology* 152: 2573-2578.

Lane, D.J. (1991) *Nucleic acid techniques in bacterial systematics*. New York, NY: John Wiley and Sons.

Manor, E., and Sarov, I. (1986) Fate of *Chlamydia trachomatis* in human monocytes and monocyte-derived macrophages. *Infect Immun* 54: 90-95.

Matsumoto, A., and Manire, G.P. (1970) Electron microscopic observations on the effects of penicillin on the morphology of *Chlamydia psittaci*. *J Bacteriol* 101: 278-285.

Mäurer, A.P., Mehlitz, A., Mollenkopf, H.J., and Meyer, T.F. (2007) Gene expression profiles of *Chlamydophila pneumoniae* during the developmental cycle and iron depletion-mediated persistence. *PLoS Pathog* 3: e83.

McClarty, G. (1999) *Chlamydia*: American Society for Microbiology, Washington, DC.

Michel, R., Hauröder-Philippczyk, B., Müller, K.D., and Weishaar, I. (1994) Acanthamoeba from human nasal mucosa infected with an obligate intracellular parasite. *Eur J Protistol* 30: 104-110.

Michel, R., Müller, K.D., Hauröder, B., and Zöller, L. (2000) A coccoid bacterial parasite of *Naegleria* sp. (Schizopyrenida: Vahlkampfiidae) inhibits cyst formation of its host but not transformation to the flagellate stage. *Acta Protozool* 39: 199-207.

Michel, R., Steinert, M., Zöller, L., Hauröder, B., and Henning, K. (2004) Free-living amoebae may serve as hosts for the *Chlamydia*-like bacterium *Waddlia chondrophila* isolated from an aborted bovine foetus. *Acta Protozool* 43: 37-42.

Michel, R., Müller, K.-D., Zöller, L., Walochnik, J., Hartmann, M., and Schmid, E.-N. (2005) Free-living amoebae serve as a host for the *Chlamydia*-like bacterium *Simkania negevensis*. *Acta Protozool* 44: 113-121.

Motulsky, H. (1995) *Intuitive Biostatistics*: Oxford University Press, USA.

Naginton, J., Watson, P.G., Playfair, T.J., McGill, J., Jones, B.R., and Steele, A.D. (1974) Amoebic infection of the eye. *Lancet* 2: 1537-1540.

Neeper, I.D., Patton, D.L., and Kuo, C.C. (1990) Cinematographic observations of growth cycles of *Chlamydia trachomatis* in primary cultures of human amniotic cells. *Infect Immun* 58: 2042-2047.

Neff, L., Daher, S., Muzzin, P., Spenato, U., Gülaçar, F., Gabay, C., and Bas, S. (2007) Molecular characterization and subcellular localization of macrophage infectivity potentiator, a *Chlamydia trachomatis* lipoprotein. *J Bacteriol* 189: 4739-4748.

Neff, R.J. (1957) Purification, axenic cultivation, and description of a soil amoeba, *Acanthamoeba* sp. *J Protozool* 4: 176-182.

Newman, S.L., Gootee, L., Brunner, G., and Deepe, G.S., Jr. (1994) Chloroquine induces human macrophage killing of *Histoplasma capsulatum* by limiting the availability of intracellular iron and is therapeutic in a murine model of histoplasmosis. *J Clin Invest* 93: 1422-1429.

Newsome, A.L., and Wilhelm, W.E. (1983) Inhibition of *Naegleria fowleri* by microbial iron-chelating agents: ecological implications. *Appl Environ Microbiol* 45: 665-668.

Nicholson, T.L., Olinger, L., Chong, K., Schoolnik, G., and Stephens, R.S. (2003) Global stage-specific gene regulation during the developmental cycle of *Chlamydia trachomatis*. *J Bacteriol* 185: 3179-3189.

Ogata, H., La Scola, B., Audic, S., Renesto, P., Blanc, G., Robert, C. et al. (2006) Genome sequence of *Rickettsia bellii* illuminates the role of amoebae in gene exchanges between intracellular pathogens. *PLoS Genet* 2: e76.

Ojcius, D.M., Souque, P., Perfettini, J.-L., and Dautry-Varsat, A. (1998) Apoptosis of epithelial cells and macrophages due to infection with the obligate intracellular pathogen *Chlamydia psittaci*. *J Immunol* 161: 4220 - 4226.

Pagnier, I., Raoult, D., and La Scola, B. (2008) Isolation and identification of amoeba-resisting bacteria from water in human environment by using an *Acanthamoeba polyphaga* co-culture procedure. *Environ Microbiol* 10: 1135-1144.

Pantoja, L.G., Miller, R.D., Ramirez, J.A., Molestina, R.E., and Summersgill, J.T. (2001) Characterization of *Chlamydia pneumoniae* persistence in HEp-2 cells treated with gamma interferon. *Infect Immun* 69: 7927-7932.

Poppert, S., Essig, A., Marre, R., Wagner, M., and Horn, M. (2002) Detection and differentiation of chlamydiae by fluorescence in situ hybridization. *Appl Environ Microbiol* 68: 4081-4089.

Raulston, J.E. (1997) Response of *Chlamydia trachomatis* serovar E to iron restriction in vitro and evidence for iron-regulated chlamydial proteins. *Infect Immun* 65: 4539-4547.

Rurangirwa, F.R., Dilbeck, P.M., Crawford, T.B., McGuire, T.C., and McElwain, T.F. (1999) Analysis of the 16S rRNA gene of micro-organism WSU 86-1044 from an aborted bovine foetus reveals that it is a member of the order *Chlamydiales*: proposal of *Waddliaceae* fam. nov., *Waddlia chondrophila* gen. nov., sp. nov. *Int J Syst Bacteriol* 49 Pt 2: 577-581.

Salim, O., Skilton, R.J., Lambden, P.R., Fane, B.A., and Clarke, I.N. (2008) Behind the chlamydial cloak: The replication cycle of chlamydiaphage Chp2, revealed. *Virology* 377: 440-445.

Schaible, U.E., and Kaufmann, S.H. (2004) Iron and microbial infection. *Nat Rev Microbiol* 2: 946-953.

Schmitz-Esser, S., Linka, N., Collingro, A., Beier, C.L., Neuhaus, H.E., Wagner, M., and Horn, M. (2004) ATP/ADP translocases: a common feature of obligate intracellular amoebal symbionts related to *Chlamydiae* and *Rickettsiae*. *J Bacteriol* 186: 683-691.

Schuster, F.L. (2002) Cultivation of pathogenic and opportunistic free-living amebas. *Clin Microbiol Rev* 15: 342-354.

Subtil, A., Delevoye, C., Balañá, M.E., Tastevin, L., Perrinet, S., and Dautry-Varsat, A. (2005) A directed screen for chlamydial proteins secreted by a type III mechanism identifies a translocated protein and numerous other new candidates. *Mol Microbiol* 56: 1636-1647.

Thao, M.L., Baumann, L., Hess, J.M., Falk, B.W., Ng, J.C., Gullan, P.J., and Baumann, P. (2003) Phylogenetic evidence for two new insect-associated *Chlamydia* of the family *Simkaniaceae*. *Curr Microbiol* 47: 46-50.

Thomas, V., Casson, N., and Greub, G. (2006) *Criblamydia sequanensis*, a new intracellular *Chlamydiales* isolated from Seine river water using amoebal co-culture. *Environ Microbiol* 8: 2125-2135.

Trentmann, O., Horn, M., van Scheltinga, A.C., Neuhaus, H.E., and Haferkamp, I. (2007) Enlightening energy parasitism by analysis of an ATP/ADP transporter from *Chlamydiae*. *PLoS Biol* 5: e231.

Wolf, K., Fischer, E., and Hackstadt, T. (2000) Ultrastructural analysis of developmental events in *Chlamydia pneumoniae*-infected cells. *Infect Immun* 68: 2379-2385.

Wyrick, P.B., and Brownridge, E.A. (1978) Growth of *Chlamydia psittaci* in macrophages. *Infect Immun* 19: 1054-1060.

Yuan, Y., Lyng, K., Zhang, Y.X., Rockey, D.D., and Morrison, R.P. (1992) Monoclonal antibodies define genus-specific, species-specific, and cross-reactive epitopes of the chlamydial 60-kilodalton heat shock protein (hsp60): specific immunodetection and purification of chlamydial hsp60. *Infect Immun* 60: 2288-2296.

9 Acknowledgements

I want to thank Matthias Horn for his warm-hearted wisdom and subtle guidance, Michi Wagner for having created an inspiring research atmosphere, my immediate advisor Susi Haider, Silvia Knab and Barbara Sixt for research discussions and friendship, and the whole DOME crew for providing a witty and supportive environment.

I also want to express my appreciation for all the people who facilitated my diploma thesis by taking care of my daughter Luisa: Dennis Johnson, Monika and Lonnie Johnson; my sisters Johanna and Teresia König. Luisa, may this work be more beneficial than unhealthy for your future.

My deepest appreciation goes to my parents, who supported me unconditionally, and David Berry for his love and intellectual contribution.

10 Curriculum vitae

Lena König

Personal data

Date of birth	June 3rd, 1981
Place of birth	Grambach bei Graz, Austria
Nationality	Austrian

Education

1988-1992	Öffentliche Volksschule "Waldschule", Dr.-Schober-Straße 1, 1130 Vienna, Austria
1992-2000	Bundesrealgymnasium, Linzer Straße 146, 1140 Vienna, Austria
2000-2003	Studies in biology at the University of Vienna
Since 2003	Branch of study: microbiology/genetics, diploma thesis at the Department of Microbial Ecology (2007-2008), University of Vienna